NONLINEAR AND SWITCHED SYSTEMS: GEOMETRIC MOTION PLANNING, NON-MONOTONIC LYAPUNOV FUNCTIONS AND INPUT-TO-STATE STABILITY

BY

SHENYU LIU

DISSERTATION

Submitted in partial fulfillment of the requirements
for the degree of Doctor of Philosophy in Electrical and Computer Engineering
in the Graduate College of the
University of Illinois at Urbana-Champaign, 2020

Urbana, Illinois

Doctoral Committee:

Professor Daniel Liberzon, Chair
Associate Professor Mohamed-Ali Belabbas
Professor Vadim Zharnitsky
Professor Yuliy Baryshnikov

ABSTRACT

Both synthesis of control strategy for motion planning and analysis of stability of nonlinear and switched systems have been researched in this work. In terms of control strategy, we propose a novel approach to the long-standing problem of motion planning for nonholonomic systems. The admissible motion is obtained by properly assigning "length" to the motion trajectories which penalizes them in the inadmissible directions, and "deforming" them in order to minimize the "length" via solving a set of parabolic partial differential equations. Several variations of the fundamental motion planning problem are also considered in this work. In terms of stability analysis, we have studied two approaches related to non-monotonic Lyapunov functions. More explicitly, the techniques of "almost Lyapunov" functions and higher order derivatives of Lyapunov functions – which were used to study the stability of autonomous nonlinear systems in the literature – are generalized to nonlinear systems with inputs. Under some mild assumptions, the nonlinear systems can be proven to be input-to-state stable using these techniques of non-monotonic Lyapunov functions. In addition, the methodology used in the derivation can also be used to show the equivalence between several stability properties of state-dependent switched systems.

ACKNOWLEDGMENTS

This project would not have been possible without the support of many people. Many thanks to my advisers, Professor Daniel Liberzon and Professor Mohamed-Ali Belabbas, who read my numerous revisions and helped make some sense of the confusion. Also thanks to my committee members, Professor Vadim Zharnitsky and Professor Yuliy Baryshnikov, who offered guidance and support. Thanks to the editorial services, Department of Electrical and Computer Engineering, for their great help with my writing and compiling the dissertation. And finally, thanks to my parents, and numerous friends who endured this long process with me, always offering support and love.

TABLE OF CONTENTS

LIST OF FIGURES

CHAPTER 1

INTRODUCTION

In the author's perspective, most engineering control problems can be described with two phases: The first phase is to design and propose some pre-computed, offline control strategy or profile, obeying which certain goals can be achieved by the system when there is no disturbance. The second phase is then to incorporate an online control regulator so that even in the presence of disturbance, the aforementioned control strategy can still be followed by the system with a certain level of stability. This work illustrates what the author has thought and achieved in both phases.

In terms of synthesis of control, motion planning has been one of the most widely studied problems in the literature (see, e.g., [1],[2],[3],[4]). From path planning of unmanned vehicle to locomotion designing of moving robots, lots of motion planning methods have been developed (see, e.g., [5],[6],[7],[8],[9],[10], etc.). Chapter 2 focuses on the particular motion problem in which the dynamics of the system on which we intend to perform motion planning is given as first-order differential equations that are affine in controls. When the system is driftless, it is related to the geometrical problem of finding sub-Riemannian geodesic [11]. Sufficient condition for controllability exists [12] (and hence feasible trajectories exist which connect any initial state to goal state) and arbitrary curves can be tracked by the system approximately using oscillatory inputs [13]. However, in the presence of a drift term in the dynamics of the system, controllability is unclear, let alone how the system should be steered in order to reach its goal state. To tackle this problem, in this work a novel approach is proposed for solving the motion planning problem for non-holonomic systems with drift. In this approach, an arbitrary curve of states between initial state and goal state is first sketched and then deformed into a curve via solving a set of PDEs. Along with the deformation, the value of an energy functional evaluated on the curve is minimized. Controls are subsequently

extracted from that energy minimizing curve and they generate an admissible path for the non-holonomic system. It is theoretically proven that under some mild assumptions on the system, the non-holonomic system can reach a destination arbitrarily close to the goal state prescribed earlier along the admissible path resulting from the algorithm. In addition to the fundamental motion planning problem, several variants including control affine system with drift, holonomic constraints, state and input constraints, indefinite boundary conditions and free terminal time are also studied in this work. The algorithm is illustrated on many canonical motion planning problems and they show great potential of this geometrical motion planning approach. This chapter is a summary of the work that the author did in [14], [15], [16], [17] and [18].

In terms of analysis of control, asymptotic stability of nonlinear systems is typically shown through Lyapunov's direct method (see, e.g., [19]). Despite the elegance of the theory, Lyapunov's direct method is in general difficult to apply in practice, due to the strict requirement that the Lyapunov function and its time derivative need to be opposite sign definite. The relaxation of the negative definiteness constraint on the time derivative of the Lyapunov function leads to the study of non-monotonic Lyapunov functions, and under some additional mild assumptions researchers have been using non-monotonic Lyapunov functions to still show stability of nonlinear systems (see, e.g., [20],[21], [22], [23], etc.). Chapter 3 reviews former stability results for autonomous systems which were derived via non-monotonic Lyapunov functions and then generalizes them to stability results for nonlinear systems with inputs. We first propose the concept of almost Lyapunov functions – which do not have negative time derivative everywhere but rather on the complement of some "bad sets" – for autonomous nonlinear systems. Local and global stability results are given in this case, provided that the "bad sets" are sufficiently small. The definition of almost Lyapunov functions is then generalized to nonlinear systems with inputs, in which case the well-known input-to-state stability can be guaranteed again when the "bad sets" are sufficiently small. On the other hand, the known approach of showing asymptotic stability for autonomous nonlinear systems via studying the higher order derivatives of the Lyapunov functions is also generalized to the study of input-to-state stability for time-varying systems with inputs. By properly defining the higher order derivatives of Lyapunov functions in

the presence of inputs, the author proves that as long as there is a negative definite linear combination of those higher order derivatives with non-negative coefficients, the system is input-to-state stable. This chapter is a summary of the work that the author did in [24], [25], [26] and [27].

Lastly, in Chapter 4 of this dissertation, several stability related properties are studied for state-dependent switched systems [28]. In particular, the gap between global stability plus asymptotic gain and input-to-state stability for state-dependent switched systems has been researched. While uniformity in convergence is always guaranteed for systems with Lipschitz vector field and a globally asymptotically stable origin [29], this is not the case for a state-dependent switched system as its vector field may not even be continuous at the switch guards. A direct consequence is that global stability plus asymptotic gain does not necessarily imply input-to-state stability, which is shown by a counterexample in this work. Several regularity assumptions including a transversality assumption for the vector field on the switch guards are proposed in order to draw the equivalence, and it is summarized as a theorem. The proof of the theorem consists of a bypass via the corresponding auxiliary system which takes in a bounded disturbance and showing that it is globally uniformly asymptotically stable. As a byproduct, the property of continuous dependence of solutions on initial conditions for state-dependent systems under the same assumptions can be concluded. This problem is also studied by the author in [30].

CHAPTER 2

MOTION PLANNING FOR NON-HOLONOMIC SYSTEM VIA GEOMETRICAL APPROACH

Given a control system

$$\dot{x} = f(x, u) \tag{2.1}$$

evolving on a differentiable manifold M and two points $x_i, x_f \in M$, the *motion planning problem* in time $T > 0$ is to find a control $u^*(t)$ that *steers* the system from x_i to x_f in T units of time, i.e. so that the solution $x^*(t)$ of Eq. (2.1) with $u = u^*$ and $x^*(0) = x_i$ yields $x^*(T) = x_f$. Due to its ubiquity in control applications ranging from robotics to autonomous wheeled vehicles, motion planning has been widely studied (see, e.g., [1],[2],[3],[4]) and a host of methods have been developed. One of the early control papers in which the issue of motion planning for non-holonomic systems was clearly addressed is [11], where motion planning is stated as a sub-Riemannian geodesic problem. For a more recent survey of this line of work, we refer to the recent monograph [12]. Another common approach to non-holonomic motion planning is based on the use of sinusoidal driving signals; the basic relation underlying these methods is the system approximation

$$\dot{x} = \lim_{\omega \to \infty} \left(\sqrt{\omega} \sin(\omega t) f_1(x) + \sqrt{\omega} \cos(\omega t) f_2(x) \right) \Leftrightarrow \dot{x} = [f_1, f_2](x)$$

where $[f_1, f_2]$ is the *Lie bracket* [31] of the vector fields f_1, f_2. See for example [13] and the very recent [32] for work on how oscillations can be used for orientation control in $SO(3)$. This idea is also used in derivative-free optimization [33],[34]. Indeed, this insight is at the basis of the work of Brockett [35], Murray et al. [36] and Laferriere and Sussman [37]. Furthermore, interesting recent work shows that some special functions – which can be thought of as generalizations of harmonic functions – play a distinguished role in solving under-actuated control problems [38].

Amongst the methods not relying explicitly on Lie brackets computations, we mention the LQR-tree method [6], in which the authors solve motion planning problems by building a sparse tree of LQR stabilized trajectories, and for which the basin of attraction is verified to be large enough using sum-of-square techniques. Sum-of-squares for stability region verification was also used for trajectory planning [39]. In the recent work [10], the authors address motion planning of hybrid systems using motion primitives and focus on prehensile manipulation tasks; and in [5] the author deals with vehicle control using motion primitives. For control and verification of hybrid systems in general, we refer to [40], and for a recent survey of motion planning for self-driving vehicles in urban environments, we refer to [9]. Motion planning for scenarios with multiple contact points, which fall under the category of hybrid dynamics, have also been investigated in [41]. Other interesting ways to obtain feasible trajectories for given problems and dynamics include random sampling-based [7], graph-based [42] and optimization-based approaches [8].

The major difficulties that can arise in motion planning problems are:

1. the nonholonomic character of the dynamics,

2. the presence of a drift term, and

3. the presence of constraints on the inputs/states.

From a theoretical point of view, the Chow-Rashevski theorem provides us with conditions under which a driftless non-holonomic system is controllable (see [12]), but in the latter two cases, no equivalent result is known: the general case of controllability of non-linear systems with drift is still a largely open problem. Nevertheless, for some specific nonlinear systems with drift, motion planning or control algorithms are given in [43],[44],[45].

In this work we propose a new geometrical approach for motion planning, which differs from all the aforementioned methods in the literature. The novelty of the work lies in an extension of the so-called *geometric heat flow* (see [46] for its use in motion planning) to encompass dynamics with constraints and drift. The method works by "deforming" an arbitrary path between x_i and x_f into an almost feasible trajectory for the system, from which we can extract the controls u^* that drive the system from x_i to x_f approximately.

2.1 Basic problem formulation

Let $M = \mathbb{R}^n$ and refer to M as the configuration space. Note that M can more generally be a C^2-differentiable manifold. Consider the *affine in the control* dynamics given by

$$\dot{x} = F_d(x) + F(x)u \tag{2.2}$$

where, for all $x \in \mathbb{R}^n$, $F_d(x) \in \mathbb{R}^n$ is a vector representing the drift dynamics when in state x; $F(x) = \{f_1, \cdots, f_m\} \in \mathbb{R}^{n \times m}$, where the columns $f_1, \cdots f_m$ are the admissible control directions and $u = \{u_1, \cdots, u_m\}^\top \in \mathbb{R}^m$ are the inputs. In order for x to be a solution of (2.2), we must have $\dot{x} \in F_d(x) + \operatorname{span} F(x)$, as illustrated in Fig. 2.1.

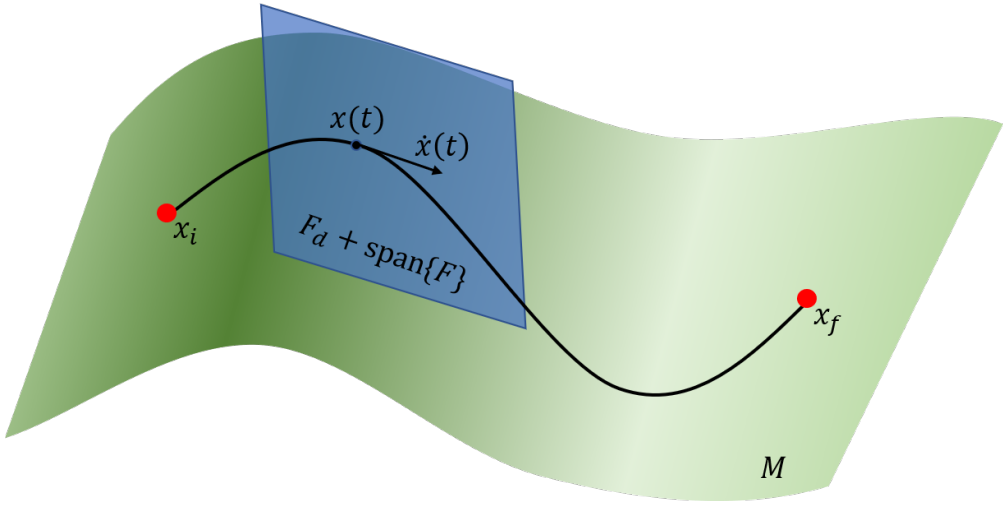

Figure 2.1: Illustration of motion planning problem.

We make the following *assumption*:

Assumption 2.1. *Both $F_d(x), F(x)$ are assumed to be at least C^2, Lipschitz with constants L_1, L_2 respectively, and we assume that $F(x)$ is of constant rank almost everywhere in $\mathbb{R}^n$.*

This is a typical regularity assumption for most practical systems. Moreover, this assumption can be weakened at the expense of longer analysis. We focus here on the case $n \geq m$, that is, on potentially *under-actuated* dynamics.

Recall that $x_i, x_f \in M$ are the desired initial and final states respectively, and $T > 0$ is a fixed time allowed to perform the motion. The set of **admissible controls** is $\mathcal{U} :=$

$L^2([0,T] \to \mathbb{R}^m)$, that is, square integrable functions defined over the interval $[0,T]$. We set

$$\mathcal{X} := \{x(\cdot) \in AC([0,T] \to \mathbb{R}^n) : x(0) = x_i, x(T) = x_f\},$$

the space of *absolutely continuous* $\mathbb{R}^n$-valued functions with start- and end-values x_i and x_f respectively. We call any $x(\cdot) \in \mathcal{X}$ an **admissible solution** if there exists $u \in \mathcal{U}$ so that the generalized derivative $\dot{x}(t)$ of $x(\cdot)$ satisfies (2.2). Denote by $\mathcal{X}^* \subseteq \mathcal{X}$ the set of admissible solutions. Our *motion planning problem* (from x_i to x_f with time T) is hence to find some $x \in \mathcal{X}^*$, and it is *feasible* if and only if $\mathcal{X}^* \neq \emptyset$. All open sets in $\mathcal{X}$ are with respect to the natural norm $\|x\|_{AC} := \int_0^T (|x(t)| + |\dot{x}(t)|)\, dt$.

We additionally introduce the space of *continuous controls* $\mathcal{U}' := C^0([0,T] \to \mathbb{R}^m)$, to which correspond differentiable trajectories $\mathcal{X}' := \{x(\cdot) \in C^1([0,T] \to \mathbb{R}^n) : x(0) = x_i, x(T) = x_f\}$. It is well-known that $\mathcal{U}'$ is a dense subspace in $\mathcal{U}$ with respect to the L_2 norm and that $\mathcal{X}'$ is a dense subspace in $\mathcal{X}$ with respect to the $\|\cdot\|_{AC}$ norm. Working over $\mathcal{X}'$ instead of $\mathcal{X}$ allows us to "smoothly deform" a curve, a term which is more rigorously defined later.

2.1.1 Controllability

Before we try to find a solution to the motion planning problem, a good question we should ask ourselves is whether such trajectories of motions exist. A sufficient condition is given in the literature (see, e.g., [12]) when the system is driftless, that is, when $F_d \equiv 0$, in which case (2.2) becomes

$$\dot{x} = F(x)u. \tag{2.3}$$

As briefly mentioned in Chapter 1, a fundamental operation on vector fields when studying the reachable space of a system is the Lie bracket of two vector fields, defined as

$$[f_i, f_j](x) = \frac{\partial f_i}{\partial x}|_x f_j(x) - \frac{\partial f_j}{\partial x}|_x f_i(x).$$

A *distribution* $\Delta(x)$ is a vector subspace of $\mathbb{R}^n$ or, in general, of T_xM, which depends on x.

We say that a vector field f belongs to $\Delta(x)$ if $f(x) \in \Delta(x)$. Note that $f \in \Delta(x_1)$ does not imply that $f \in \Delta(x_2)$ for $x_2 \neq x_1$. Given the system (2.3), we define the distribution

$$\Delta_0(x) = \operatorname{span} F(x). \tag{2.4}$$

This distribution represents the space of infinitesimal motions the system can perform when in state x. A key difference between linear and nonlinear systems is that the reachable space of (2.3) from x_0 is the same as the reachable space of the system

$$\dot{x} = \sum_{i=1}^{m} f_i(x)u_i + \sum_{i \neq j} [f_i, f_j](x)u_{ij}, \tag{2.5}$$

where the additional control directions $[f_i, f_j]$ can be approximately achieved by infinitesimal motions in the directions of $f_i, f_j, -f_i, -f_j$ sequentially. On the other hand, when at state x, the space of available directions of motion for system (2.5) is given by the distribution

$$\begin{aligned} \Delta_1(x) &= \operatorname{span}\{f_1, \ldots, f_m, [f_1, f_2], \ldots, [f_{m-1}, f_m]\} \\ &= \Delta_0 \oplus \operatorname{span}\{[f_i, f_j] \mid f_i, f_j \in \Delta_0(x)\}. \end{aligned}$$

Using this construction iteratively, we see that the distributions

$$\Delta_i(x) := \Delta_{i-1}(x) \oplus \operatorname{span}\{[f_1, f_2](x) \mid f_1, f_2 \in \Delta_{i-1}(x)\} \tag{2.6}$$

are key to understanding the reachable space of the system (2.3). The precise relationship is given by Chow's theorem:

Theorem 2.1 (Chow - Rashevskii)**.** *Consider the control system* (2.3) *and the associated distribution* (2.4)*. If*

$$\lim_{i \to \infty} \Delta_i(x) = \mathbb{R}^n$$

for all $x \in \mathbb{R}^n$*, then the system* (2.3) *is controllable.*

Although some sufficient conditions such as *small-time local controllability* or *small-time local accessibility* (see, e.g., [47],[48]) exist, they are either too strong or not generic; the

controllability of non-holonomic systems with drift is still unclear in general. In this work we are more interested in finding one solution, provided that the motion planning problem is feasible.

2.1.2 Riemannian geometry

A *Riemannian metric* on M is a family of positive-definite inner products

$$g_x(\cdot,\cdot) : T_xM \times T_xM \to \mathbb{R}, \quad x \in M.$$

In this way the curve parameterized by $s \in [0,1]$ has length

$$L(x) := \int_0^1 \sqrt{g_x(\dot{x},\dot{x})}ds. \tag{2.7}$$

Since $M = \mathbb{R}^d$ in our problem, we can define

$$g_x(\dot{x},\dot{x}) := \dot{x}^T G(x)\dot{x}. \tag{2.8}$$

where the matrix $G(x)$ is symmetric, positive definite for all $x \in \mathbb{R}^n$, which is called the *Riemannian metric tensor*. When $G \equiv I$, we recover the usual Euclidean length. It is not hard to check that $L(x)$ is independent of the curve parameterization and therefore length is indeed well defined on the path. The Riemannian distance stemming from the Riemannian metric is then:

$$d(x_i, x_f) := \inf_{x\in\mathcal{X}} L(x), \tag{2.9}$$

where we recall $\mathcal{X}$ is the set of all absolutely continuous functions with $x(0) = x_i, x(T) = x_f$. If this infimum is achievable for some $x^* \in \mathcal{X}$, then x^* is called a *geodesic* between x_i and x_f on M.

Nevertheless, the square root in (2.7) makes analysis difficult. The next lemma shows that when minimizer of (2.9) exists, it can be equivalently found by the minimizer of the

energy functional

$$E(x) = \int_0^1 g_x(\dot{x}, \dot{x}) ds \tag{2.10}$$

Lemma 2.1. *If $x^* \in \mathcal{X}$ is a minimizer of $E(x)$, $g_{x^*(t)}(\dot{x}^*(t), \dot{x}^*(t))$ is constant for all $t \in [0, 1]$. In addition, x^* is also a minimizer of $L(x)$.*

Proof. By Cauchy-Schwarz inequality, for any $x \in \mathcal{X}$,

$$L(x)^2 = \left(\int_0^1 \sqrt{g_x(\dot{x}, \dot{x})} dt \right)^2 \leq \int_0^1 1^2 dt \int_0^1 g_x(\dot{x}, \dot{x}) dt = E(x).$$

The middle equality is achieved if and only if $g_x(\dot{x}, \dot{x})$ is a constant. Thus Let $\bar{x} \in \mathcal{X}$ be a minimizer of $L(x)$ with constant $g_{\bar{x}}(\dot{\bar{x}}, \dot{\bar{x}})$. Then

$$E(\bar{x}) = L(\bar{x})^2 \leq L(x^*)^2 \leq E(x^*) \leq E(\bar{x}).$$

Thus all the inequalities must be equalities, which means $L(x^*) = L(\bar{x})$, that is, x^* is a minimizer of $L(x)$ as well and $L(x^*)^2 = E(x^*)$, that is, $g_{x^*}(\dot{x}^*, \dot{x}^*)$ is constant. □

The Riemannian metric is suitable for the motion planning problem of driftless systems, as studied in our first work [14]. Tailored to systems with drift, we will instead use the modified map

$$g_x(\dot{x}, \dot{x}) := (\dot{x} - F_d(x))^T G(x)(\dot{x} - F_d(x)). \tag{2.11}$$

By its definition g_x is no longer an inner product (*e.g.*, $g_x(0, 0) \neq 0$); we unofficially call it *affine Riemannian metric* and consequently the length and energy defined in (2.7),(2.10) will be termed *affine length* and *affine energy* with this new g_x (the latter term is also written as $\mathcal{A}$, sometimes called "action functional"). Lemma 2.1 still holds because its proof is not changed. With that being said, we will later use the word "length" or phrase "length minimizing" ambiguously when we are actually referring to "energy" or "energy minimizing".

Encoding non-holonomic dynamics To encode the non-holonomic dynamics into the affine Riemannian metric, we define

$$G(x) = (\bar{F}(x)^{-1})^\top D \bar{F}(x)^{-1}, \tag{2.12}$$

where $D = \text{diag}(\underbrace{\lambda, \cdots, \lambda}_{n-m}, \underbrace{1, \cdots, 1}_{m})$ for some large $\lambda > 0$, $\bar{F}(x) = (F_c(x)|F(x)) \in \mathbb{R}^{n \times n}$ so that it is full rank. Such $F_c(x)$ matrix can be obtained, e.g., via the Gram-Schmidt process. Note that the column space of $F_c(x)$ contains all the undesirable directions of motion and λ penalizes the component of a curve in these directions.

To intuitively understand the connection between curve length and the dynamics of the system, consider an arbitrary curve x, with $\dot{x} = F_d(x) + F(x)u + F_c(x)v$. For simplicity we assume the matrix $F(x) = (F_c(x)|F(x))$ is orthonormal. Plug this x into the action functional (2.10) we have

$$\begin{aligned}
\mathcal{A}(x) &= \int_0^T (\dot{x} - F_d(x))^T G(x)(\dot{x} - F_d(x))ds \\
&= \int_0^T (\dot{x} - F_d(x))^T \bar{F}(x) D \bar{F}(x)^\top (\dot{x} - F_d(x))ds \\
&= \int_0^T (F(x)u + F_c(x)v)^\top \bar{F}(x) D \bar{F}(x)^\top (F(x)u + F_c(x)v)ds \\
&= \int_0^T |u|^2 + \lambda |v|^2 ds.
\end{aligned}$$

For admissible curves, $v \equiv 0$ and hence the action functional yields the energy, which is independent of λ. For inadmissible curves, the component in span $F_c(x)$ is scaled by λ. Because λ is very large, consequently the length is also very large. By minimizing the length of a curve, we are in fact minimizing the component of the motion that is in the undesirable directions. In other words, the curve with minimal length is approximately an admissible solution to our motion planning problem.

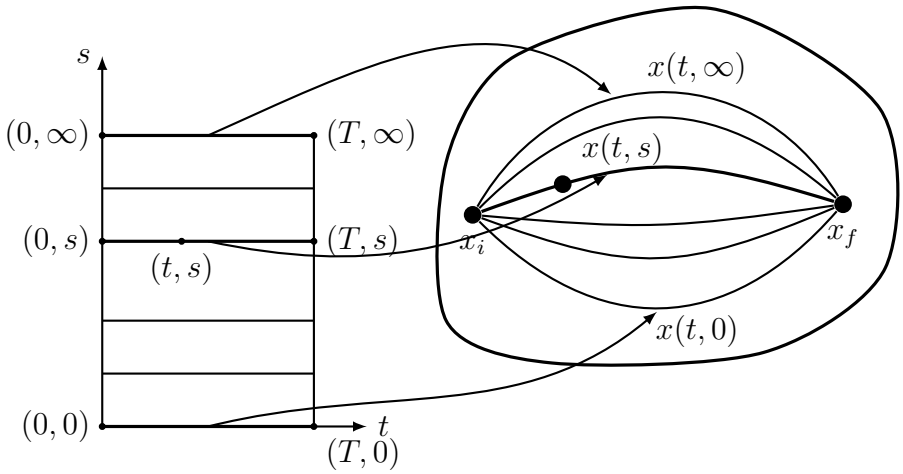

Figure 2.2: Homotopy of trajectories joining x_i to x_f in M.

2.1.3 Affine geometric heat flow

As mentioned in Section 2.1.2, we rely on "deforming" curves in order to minimize the length for solving the motion planning problem. The "deformation" is realized by *homotopies*. In other words, we use $x(t,s) : [0,T] \times [0, s_{\max})$ where the variable s is the homotopy parameter and for each s fixed, $x(\cdot, s) \in \mathcal{X}'$. See Fig. 2.2 for an illustration of the homotopy.

Geometric heat flow For the Reimannian metric $G(x)$ introduced earlier, we denote by ∇ the **Levi-Civita** connection of $G(x)$ as in [49], and by $\nabla_f g$ the covariant derivative of the vector field g along the vector field f. Recall that if $a(t) = \sum_{k=1}^{n} a_k(t) e^k$, where $a_i(t)$ are real numbers and e^k basis vectors, is a vector field along a curve $x(t)$, and g is a vector field defined in a neighborhood of $x(t)$, then $\nabla_a g := \frac{da}{dt} + \sum_{i,j,k} \Gamma_{ij}^k a_i g_j e^k$, where

$$\Gamma_{jk}^i(x) := \frac{1}{2} \sum_l G^{il} \left(\frac{\partial G_{lj}}{\partial x_k} + \frac{\partial G_{lk}}{\partial x_j} - \frac{\partial G_{jk}}{\partial x_l} \right) \tag{2.13}$$

are the *Chirstoffel symbols* of G.

The so-called *geometric heat flow* (GHF) is a parabolic partial differential equation, which evolves a curve with fixed end-points toward a curve of minimal length: namely, given

a Riemannian metric and an associated Levi-Civita connection ∇, the GHF is the PDE

$$\frac{\partial x(t,s)}{\partial s} = \nabla_{\dot{x}(t,s)} \dot{x}(t,s), \tag{2.14}$$

where $\dot{x}(t,s) := \frac{\partial x(t,s)}{\partial t}$. Note the GHF is a parabolic PDE, so in order to solve it we need *boundary conditions*

$$x(0,s) = x_i, x(T,s) = x_f \quad \forall s \geq 0 \tag{2.15}$$

and *initial condition*

$$x(\cdot,0) = v(\cdot) \in \mathcal{X}'. \tag{2.16}$$

We refer the reader to [49] for a proof that this PDE yields a curve of minimal length. For applications of this flow to motion planning problems, and some illustrations of its solutions, we refer to [14], [15].

Affine geometric heat flow With a slight abuse of notation, we define for $G(x) \in \mathbb{R}^{n\times n}$, $f, g \in \mathbb{R}^n$

$$\left[f \left(\frac{\partial G}{\partial x} \right) g \right] := \begin{pmatrix} f^\top \frac{\partial G}{\partial x_1} g \\ \vdots \\ f^\top \frac{\partial G}{\partial x_n} g \end{pmatrix} \in \mathbb{R}^n;$$

i.e. $\left[f \left(\frac{\partial G}{\partial x} \right) g \right]$ is the vector in $\mathbb{R}^n$ with ith entry $f^\top \frac{\partial G}{\partial x_i} g$, where $\frac{\partial G}{\partial x_i}$ is the $n \times n$ matrix with kl entry $\frac{\partial G_{kl}}{\partial x_i}$. We furthermore use the notation

$$(f \cdot G) := \left(\sum_{l=1}^{n} f_l \frac{\partial G_{ij}}{\partial x_l} \right)_{ij} \in \mathbb{R}^{n\times n}. \tag{2.17}$$

Taking inspiration from the GHF, in [16] we introduce what we term the *affine geometric heat flow* (AGHF):

$$\frac{\partial x(t,s)}{\partial s} = \nabla_{\dot{x}(t,s)} \left(\dot{x}(t,s) - F_d(x(t,s)) \right) + r(x(t,s)), \tag{2.18}$$

where

$$r(x(t,s)) = G^{-1}\left(\left(\frac{\partial F_d}{\partial x}\right)^{\top} G(\dot{x} - F_d) + \frac{1}{2}\left[(\dot{x} - F_d)\left(\frac{\partial G}{\partial x}\right) F_d\right]\right).$$

The AGHF (2.18) comprises two terms with different objectives: the first term can be thought of as minimizing the length of the curve, and the second term as insuring that the resulting trajectory is feasible for a system with drift vector field $F_d(x)$. In more detail, the first term is the covariant derivative of $\dot{x}(t,s) - F_d(x)$ in the direction $\dot{x}(t,s)$. To understand the origin of this term, recall that $\nabla_{\dot{x}}\dot{x}$ is the acceleration vector of the curve. Because the curve $x(t,s)$ is parametrized by length (i.e. $\|\dot{x}\| = 1$), for all s, updating the curve in the direction of its acceleration decreases its curvature. This can be thought of as the reason why the GHF minimizes length of the curve. In the AGHF, we replaced the term $\dot{x}$ by $\dot{x} - F_d(x(t,s))$; hence we subtracted from the tangent vector to the curve at $x(t,s)$ the drift vector field at that point. This term thus *"minimizes the length" of the resulting curve* discounting the effect of the drift term. The idea behind this term is that since the drift vector field cannot be altered by the controls, it should not influence the computation of the curvature.

The role of the second term is to align the direction of the curve at x with the drift vector field at that point. To argue for this, we will describe how this term moves a point $x(t,s)$ of the solution curve at iteration s to a point $x(t, s+\delta s)$ for a small increment δs. Denote by $\langle v, w\rangle$ the inner product of $v, w \in T_xM$, and consider the function

$$P : TM \to \mathbb{R} : (x,v) \mapsto \langle v - F_d(x), F_d(x)\rangle = \langle v, F_d(x)\rangle - \langle F_d(x), F_d(x)\rangle .$$

This function takes an element from the tangent bundle (x,v), with $x \in M$ and $v \in T_xM$ to yield the inner product of v with $F_d(x)$ minus $\langle F_d(x), F_d(x)\rangle$. We will assume that v is fixed, and consider $P_v : M \to \mathbb{R} : P_v(x) := P(x,v)$. The function clearly reaches its maximal value when $F_d(x)$ is aligned with v. Hence, the gradient flow of this function seen as a function from $M \to \mathbb{R}$ will tend to align $F_d(x)$ with v. Now one can show that the term $r(x(t,s))$ defined above is the *gradient of the function* $P_{\dot{x}}(x) : M \to \mathbb{R}$ for the Riemannian metric G: the effect of this term is thus to move the curve (i.e. move $x(t, s+\delta s)$) so that $F_d(x(t, s+\delta s))$

is more aligned with $\dot{x}(t,s)$. Said otherwise, this term deforms the curve so that $F_d(x)$ is more aligned with $\dot{x}(t,s)$.

We highlight that the flow can only update $x(t,s)$, and not $\dot{x}(t,s)$, and thus we move $x(t,s)$ in search of $F_d(x(t,s))$ more aligned with $\dot{x}(t,s)$.

On the convergence of AGHF The AGHF is a set of nonlinear PDEs, thus the existence of a solution is not guaranteed as a priori even for short time. The next lemma not only provides a convergence guarantee for our AGHF, it also shows that indeed the length of the curve is minimized along the deformation.

Lemma 2.2. *Let $x^*(t)$ be a steady-state solution of the AGHF (2.18), that is,*

$$\nabla_{\dot{x}^*(t)} \left(\dot{x}^*(t) - F_d(x^*(t))\right) + r(x^*(t)) = 0. \tag{2.19}$$

Then $x^*(t)$ is an extremal curve of the action functional

$$\mathcal{A}(x(\cdot)) := \frac{1}{2}\int_0^T (\dot{x} - F_d(x))^\top G(x)(\dot{x} - F_d(x))dt. \tag{2.20}$$

Furthermore, $\mathcal{A}$ decreases along the solutions of the AGHF; i.e. if $x(t,s)$ is such a solution, then $\frac{d}{ds}\mathcal{A}(x(\cdot,s)) \leq 0$, and equality holds only if $x(\cdot,s)$ is an extremal curve for $\mathcal{A}$.

Proof. To prove the first part in Lemma 2.2, it suffices to show that the steady-state solution of the AGHF satisfies the Euler-Lagrange equation

$$\frac{d}{dt}\frac{\partial L}{\partial \dot{x}} - \frac{\partial L}{\partial x} = 0, \tag{2.21}$$

where the Lagrangian is given by

$$L(x,\dot{x}) = \frac{1}{2}g_x(\dot{x},\dot{x}) = \frac{1}{2}(\dot{x} - F_d(x))^\top G(x)(\dot{x} - F_d(x)). \tag{2.22}$$

To this end, write $f := F_d$ and $L = \frac{1}{2}(\dot{x}_i - f_i)G_{ij}(\dot{x}_j - f_j)$, where we adopt the Einstein

convention of summing over repeated indices. We have

$$\begin{aligned}
\frac{\partial L}{\partial x_k} &= -\frac{\partial f_i}{\partial x_k} G_{ij}(\dot{x}_j - f_j) + \frac{1}{2}(\dot{x}_i - f_i)\frac{\partial G_{ij}}{\partial x_k}(\dot{x}_j - f_j), \\
\frac{\partial L}{\partial \dot{x}_k} &= (\dot{x}_i - f_i)G_{ik}, \\
\frac{d}{dt}\frac{\partial L}{\partial \dot{x}_k} &= (\ddot{x}_i - \frac{\partial f_i}{\partial x_l}\dot{x}_l)G_{ik} + (\dot{x}_i - f_i)\frac{\partial G_{ik}}{\partial x_l}\dot{x}_l.
\end{aligned}$$

The Euler-Lagrange equations (2.21) can be written, after some rearrangements and using the notation introduced earlier, as

$$\begin{aligned}
0 &= \frac{d}{dt}\frac{\partial L}{\partial \dot{x}} - \frac{\partial L}{\partial x} \\
&= (\dot{x} \cdot G)(\dot{x} - f) + G(\ddot{x} - \frac{\partial f}{\partial x}\dot{x}) + \left(\frac{\partial f}{\partial x}\right)^{\top} G(\dot{x} - f) - \frac{1}{2}\left[(\dot{x} - f)\left(\frac{\partial G}{\partial x}\right)(\dot{x} - f)\right].
\end{aligned}$$

After some algebraic computations, we obtain that

$$0 = \frac{d}{dt}\frac{\partial L}{\partial \dot{x}} - \frac{\partial L}{\partial x} = G(x)\Big(\nabla_{\dot{x}}\left(\dot{x} - F_d(x)\right) + r(x)\Big). \tag{2.23}$$

By definition (2.12), G is positive definite so (2.21) holds if and only if (2.19) holds, which completes the proof for the first part. Next we show that (2.18) is a gradient descent of the action functional (2.20). First from (2.23) we see that (2.18) is equivalent to the PDE

$$G(x)\frac{\partial x}{\partial s} = \left(\frac{d}{dt}\frac{\partial L}{\partial \dot{x}} - \frac{\partial L}{\partial x}\right). \tag{2.24}$$

Secondly, by first order approximation we have

$$x(t, s + \delta) = x(t, s) + \delta\frac{\partial x}{\partial s}(t, s) + o(\delta).$$

Plugging it into the first-order variation of L, we have

$$\begin{aligned}\mathcal{A}(x(\cdot, s+\delta)) &= \int_0^T L(x(t, s+\delta), x_t(t, s+\delta))dt \\ &= \int_0^T L(x(t,s), x_t(t,s)) + (\delta\frac{\partial x}{\partial s}(t,s) + o(\delta))^\top \frac{\partial L}{\partial x} \\ &\quad + \left(\frac{d}{dt}(\delta\frac{\partial x}{\partial s}(t,s) + o(\delta))\right)^\top \frac{\partial L}{\partial x_t} + o(\delta)dt \\ &= \mathcal{A}(x(\cdot,s)) + \delta\int_0^T \frac{\partial x}{\partial s}(t,s)^\top \frac{\partial L}{\partial x} + x_{ts}(t,s)^\top \frac{\partial L}{\partial x_t}dt + o(\delta),\end{aligned}$$

where all $o(\delta)$ terms are collected together. Use integration by parts for the $x_{ts}(t,s)^\top \frac{\partial L}{\partial x_t}$ term, we have

$$\begin{aligned}&\mathcal{A}(x(\cdot, s+\delta)) \\ &\qquad = \mathcal{A}(x(\cdot,s)) + \delta\left(\frac{\partial x(t,s)}{\partial s}^\top \frac{\partial L}{\partial \dot{x}}\bigg|_0^T + \int_0^T \frac{\partial x(t,s)}{\partial s}^\top \left(\frac{\partial L}{\partial x} - \frac{d}{dt}\frac{\partial L}{\partial \dot{x}}\right)dt\right) + o(\delta).\end{aligned}$$

The evaluated term $\frac{\partial x}{\partial s}^\top \frac{\partial L}{\partial \dot{x}}\Big|_0^T$ vanishes because of the boundary conditions (2.15). Taking the limit $\delta \to 0$ and plugging (2.24) in,

$$\begin{aligned}\frac{d\mathcal{A}(x(\cdot,s))}{ds} &= \lim_{\delta\to 0}\frac{\mathcal{A}(x(\cdot,s+\delta)) - \mathcal{A}(x(\cdot,s))}{\delta} \\ &= \int_0^T \frac{\partial x(t,s)}{\partial s}^\top \left(\frac{\partial L}{\partial x} - \frac{d}{dt}\frac{\partial L}{\partial x_t}\right)dt = -\int_0^T \frac{\partial x(t,s)}{\partial s}^\top G(x)\frac{\partial x(t,s)}{\partial s}dt.\end{aligned}$$

Again because G is positive definite, $\frac{d\mathcal{A}(x(\cdot,s))}{ds} \le 0$ and equality holds if and only if $\frac{\partial x}{\partial s} = 0$ almost everywhere, i.e., $x(\cdot,s)$ is an extremal curve for $\mathcal{A}$. □

2.2 Results for motion planning

2.2.1 Algorithm

The algorithm consists of the following steps:

1. Encode system dynamics into the Riemannian metric G.

2. Solve the AGHF (2.18) with boundary conditions (2.15) and initial condition (2.16).

3. Evaluate
$$u(t) := F(x(t, s_{\max}))^{\dagger}(\dot{x}(t, s_{\max}) - F_d(x(t, s_{\max})). \tag{2.25}$$

The control $u(t)$ obtained in (2.25) yields, when integrating (2.2), a trajectory $\tilde{x}(t)$, which is our solution to the motion planning problem. We call it *integrated path*.

We make several remarks here. Firstly in Step 1 the complementary matrix F_c does not depend on the drift F_d and neither is there an orthogonality requirement between F and F_c, which gives much freedom in the construction of F_c and hence in many cases one can choose $\bar{F} = (F_c|F)$; consequently the Riemannian metric tensor G will have a relatively simple expression. Secondly, in Step 2 while solving the AGHF, the initial condition can be an arbitrary curve in the set $\mathcal{X}'$; in other words, there are no non-holonomic constraints imposed on the initial curve; as long as it is smooth and connects x_i to x_f, it can be used to solve our AGHF. However, whether our algorithm yields a "good" solution to the motion planning problem depends on the choice of initial curve, which is inherently related to the controllability of the system and feasibility of the problem, and thus as mentioned earlier, is still an open problem. Lastly, our algorithm does not find an element in $\mathcal{X}^*$; it only finds an approximation to such element. In addition, the accuracy of the approximation depends on the value of λ used in the construction of G. The second and last remarks will be further addressed in Section 2.2.2.

2.2.2 Theoretical guarantee of the results

As mentioned in Section 2.2.1, our algorithm only finds an approximation of an admissible solution to the motion planning problem. More precisely, our algorithm solves the following *relaxed motion planning problem*:

Relaxed motion planning problem Given $x_i, x_f \in \mathbb{R}^n, T > 0, \epsilon > 0$, find $u \in \mathcal{U}$ (potentially $u \in \mathcal{U}'$) such that the corresponding solution of (2.2) with initial condition

$x(0) = x_i$ satisfies $|x(T) - x_f| \leq \epsilon$.

The next theorem provides a theoretical guarantee for our algorithm.

Theorem 2.2. *Consider the system* (2.2) *and let* $x_i, x_f \in \mathbb{R}^n$. *Assume that the motion planning problem from* x_i *to* x_f *is feasible (i.e.* $\mathcal{X}^*$ *is non-empty) and that Assumption 2.1 is met. Then there exists* $C > 0$ *such that for any* $\lambda > 0$, *there exists an open set* $\Omega_\lambda \subseteq \mathcal{X}'$ *(with respect to* $\|\cdot\|_{AC}$*) so that as long as the initial curve* $v \in \Omega_\lambda$, *the integrated path* $\tilde{x}(t)$ *from our algorithm with sufficiently large* $s_{\max}$ *has the property that*

$$|\tilde{x}(T) - x_f| \leq \sqrt{\frac{3TMC}{\lambda}} \exp\left(\frac{3T}{2}(L_2^2 T + L_1^2 C)\right). \tag{2.26}$$

Proof. Since the motion planning problem is feasible, there exists $x^*(\cdot) \in \mathcal{X}^*$ so we have $\dot{x}^* = F_d(x^*) + F(x^*)u^*$ for some $u^*(\cdot) \in \mathcal{U}$. Plug this x^* into (2.22) and we have $L(x^*(t), \dot{x}^*(t)) = |u^*(t)|^2$. Pick $C > \mathcal{A}(x^*) = \int_0^T |u^*(t)|^2 dt$. Note that C is independent of λ. Denote $\Omega_\lambda^{\mathrm{AC}} := \{x \in \mathcal{X} : V(x) < C\}$. $\Omega_\lambda^{\mathrm{AC}}$ is not empty because it at least contains x^*; in addition, because $\mathcal{A}$ is continuous over $\mathcal{X}$ with respect to $\|\cdot\|_{AC}$, $\Omega_\lambda^{\mathrm{AC}}$ is open. Since $\mathcal{X}'$ is dense in $\mathcal{X}$, $\Omega'_\lambda := \Omega_\lambda^{\mathrm{AC}} \cap \mathcal{X}'$ is open as well. From Lemma 2.2 we know that $\mathcal{A}(x(\cdot, s))$ is non-increasing so Ω'_λ is invariant. Let Ω_λ be the region of attraction to Ω'_λ; that is, $\Omega'_\lambda \subset \Omega_\lambda \subset \mathcal{X}'$ and all AGHF solutions $x(\cdot, s)$ derived from (2.18) with any initial condition $v \in \Omega_\lambda$ will converge to the invariant set Ω'_λ when s increases. Consequently when $s_{\max}$ is sufficiently large, $\mathcal{A}(x(\cdot, s_{\max})) \leq C$.

Define the curve $x(t) := x(t, s_{\max})$ and for each $t \in [0, T]$ let $u(t) \in \mathbb{R}^m, u_c(t) \in \mathbb{R}^{n-m}$ be given by

$$\begin{pmatrix} u_c(t) \\ u(t) \end{pmatrix} = \bar{F}(x(t))^{-1}(\dot{x}(t) - F_d(x(t))). \tag{2.27}$$

Plug it into (2.22) and we have

$$C \geq \mathcal{A}(x) = \int_0^T L(x(t), \dot{x}(t))dt = \int_0^T |u(t)|^2 + \lambda |u_c(t)|^2 dt.$$

$$\Rightarrow \int_0^T |u(t)|^2 dt \leq C, \quad \int_0^T |u_c(t)|^2 dt \leq \frac{C}{\lambda}. \tag{2.28}$$

Comparing (2.27) with (2.25), we see that the extracted control is exactly u; in other words, the integrated path is given by

$$\tilde{x}(0) = x_i, \quad \dot{\tilde{x}} = F_d(\tilde{x}) + F(\tilde{x})u.$$

Define the error $e(t) := x(t) - \tilde{x}(t)$. Then

$$e(0) = 0, \ \dot{e} = (F_d(x) - F_d(\tilde{x})) + (F(x) - F(\tilde{x}))u + F_c(x)u_c.$$

Therefore we have

$$e(t) = \int_0^t (F_d(x(\tau)) - F_d(\tilde{x}(\tau))) + (F(x(\tau)) - F(\tilde{x}(\tau)))u(\tau) + F_c(x(\tau))u_c(\tau)d\tau.$$

Squaring the norm of $e(t)$ and applying Cauchy-Schwartz inequality,

$$|e(t)|^2 \leq t \int_0^t (|F_d(x(\tau)) - F_d(\tilde{x}(\tau))| + |(F(x(\tau)) - F(\tilde{x}(\tau)))u(\tau)| + |F_c(x(\tau))u_c(\tau)|)^2 d\tau.$$

Using power mean inequality, the square of the sum of three terms inside integral is no larger than three times the sum of the square of each individual,

$$|e(t)|^2 \leq 3t \int_0^t |F_d(x(\tau)) - F_d(\tilde{x}(\tau))|^2 + |(F(x(\tau)) - F(\tilde{x}(\tau)))u(\tau)|^2 + |F_c(x(\tau))u_c(\tau)|^2 d\tau.$$

Owing to the fact that F_d, F are globally Lipschitz and F_c is globally bounded, we conclude that

$$|e(t)|^2 \leq 3t \int_0^t (L_2^2 + L_1^2|u(\tau)|^2)|e(\tau)|^2 d\tau + 3t \int_0^t M|u_c(\tau)|^2 d\tau.$$

Next, by Grönwall inequality and the fact that $3t \int_0^t (L_2^2 + L_1^2|u(\tau)|^2)|e(\tau)|^2 d\tau$ is a non-decreasing function of t,

$$|e(t)|^2 \leq \left(3t \int_0^t M|u_c(\tau)|^2 d\tau\right) \exp\left(3t \int_0^t (L_2^2 + L_1^2|u(\tau)|^2) d\tau\right).$$

Finally, substituting in the inequalities from (2.28), we conclude that

$$|e(t)|^2 \leq \frac{3tMC}{\lambda} \exp\big(3t(L_2^2 t + L_1^2 C)\big).$$

Thus $|\tilde{x}(T) - x_f| = |e(T)| \leq \sqrt{\frac{3TMC}{\lambda}} \exp\big(\frac{3T}{2}(L_2^2 T + L_1^2 C)\big)$ as was to be proved. □

Discussion The bound (2.26) in Theorem 2.2 quantifies the trade-off between the size of the parameter λ, and the quality of the controlled obtained, where quality is measured according to how close to the desired final state the control drives the system. By picking λ sufficiently large, the relaxed motion planning problem is solved. However large λ prolongs computation time; there is a trade-off between accuracy and efficiency of our algorithm.

The uniform convergence of e to 0 shown in the proof as λ goes to infinity also suggests that the limit curve $x^* := \lim_{\lambda\to\infty} \tilde{x}$ may be an element in $\mathcal{X}^*$. This problem subsumes the question of smoothness of sub-Riemannian geodesics [50]. From a theoretical point of view we are also interested in the question whether the steady state solutions $x(\cdot, \infty)$ of our AGHF will converge, and what topological space the limit will be in if they converge. This remains a challenge as of this writing, as we are only capable to show C^1 convergence so the limit is C^0. More efforts can be devoted in this research direction.

Lastly, our algorithm will only work when the motion planning problem is feasible and the initial curve $v \in \Omega_\lambda$, where Ω_λ is implicit in general. This makes our algorithm vulnerable not only because Ω_λ might be bounded and "small", but also because it depends on the penalty λ and hence an arbitrarily chosen $v \in \mathcal{X}$ may not work. Nevertheless, we will see in the examples of Section 2.2.3 that an arbitrary choice of initial condition very often yields a convergent solution.

2.2.3 Examples

Non-holonomic integrator The dynamics of non-holonomic integrator is given by

$$\begin{pmatrix} \dot{x} \\ \dot{y} \\ \dot{z} \end{pmatrix} = \underbrace{\begin{pmatrix} 1 \\ 0 \\ -y \end{pmatrix}}_{f_1} u_1 + \underbrace{\begin{pmatrix} 0 \\ 1 \\ x \end{pmatrix}}_{f_2} u_2. \tag{2.29}$$

This is a driftless system. Define $f_3 = \frac{1}{2}[f_1, f_2] = \begin{pmatrix} 0 & 0 & 1 \end{pmatrix}^\top$ and we see span $f_1, f_2, f_3 = \mathbb{R}^3$ for all $x \in \mathbb{R}^3$. Hence the system (2.29) is controllable by Theorem 2.1. As a result $\bar{F}(x) = \begin{pmatrix} f_1, f_2, f_3 \end{pmatrix}$ and we can find $G(x)$ by (2.12):

$$G(x) = \begin{pmatrix} \lambda y^2 + 1 & -\lambda xy & \lambda y \\ -\lambda xy & \lambda x^2 + 1 & -\lambda x \\ \lambda y & -\lambda x & \lambda \end{pmatrix}.$$

Then using the formula (2.13) we can compute

$$\Gamma^1_{:,:} = \begin{pmatrix} 0 & ny & 0 \\ ny & -2nx & n \\ 0 & n & 0 \end{pmatrix}, \Gamma^2_{:,:} = \begin{pmatrix} -2ny & nx & -n \\ nx & 0 & 0 \\ -n & 0 & 0 \end{pmatrix}, \Gamma^3_{:,:} = \begin{pmatrix} -2nxy & nx^2 - ny^2 & -nx \\ nx^2 - ny^2 & 2nxy & -ny \\ -nx & -ny & 0 \end{pmatrix}.$$

In addition since the system is driftless, we only need to solve the GHF (2.14); the details are omitted here.

We tested our algorithm for the classical problem with $x_i = (0, 0, 0)^\top, x_f = (0, 0, 1)^\top$, and the result is shown in Fig 2.3. While the light blue curve represents the initial curve v, the red curve is the AGHF solution $x(\cdot, s_{\max})$ and the black curve is the integrated path from our algorithm. Note that in this case we cannot simply pick the initial curve v to be the straight line between x_i, x_f as it is in fact a local extremal (saddle point) of (2.20) because of the symmetry. Instead we use the initial curve $v(t) = (0.1 \sin(2\pi t), 0, t)^\top$, with $\lambda = 100, s_{\max} = 3$. We observe that the integrated path from our algorithm is very close to

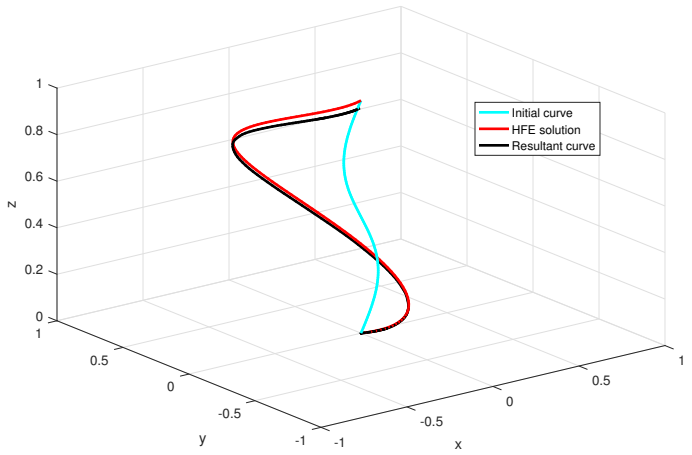

Figure 2.3: AGHF algorithm applied on a non-holonomic integrator.

the AGHF solution $x(\cdot, s_{\max})$ and both of them are of helix-shape. While the AGHF solution connects x_i, x_f, it is not admissible; on the other hand, the integrated path is admissible by its construction, but it does not connect x_f but terminates in a small neighborhood of x_f instead. It indeed is a solution to the relaxed motion planning problem.

Unicycle The next example is the canonical planar unicycle or rolling coin as depicted in Fig. 2.4. The unicycle is a 3 degree of freedom system with configuration variables (q_x, q_y), describing the position of the center of the wheel, and θ describing the orientation of the wheel with respect to the x-axis. We treat the work space as $\mathbb{R}^3$ rather than $\mathbb{R}^2 \times S^1$ but keep in mind that the two are different. The kinematics is given by the differential equations

$$\underbrace{\begin{pmatrix} \dot{q}_x \\ \dot{q}_y \\ \dot{\theta} \end{pmatrix}}_{\dot{x}} = \underbrace{\begin{pmatrix} \cos\theta \\ \sin\theta \\ 0 \end{pmatrix}}_{f_1} u_1 + \underbrace{\begin{pmatrix} 0 \\ 0 \\ 1 \end{pmatrix}}_{f_2} u_2. \tag{2.30}$$

The two inputs, u_1, u_2, can be treated as its linear and steering velocity, respectively. Again we first verify that the system is controllable. Since the rank of $\Delta_0(x) = \text{span}\{f_1(x), f_2(x)\}$

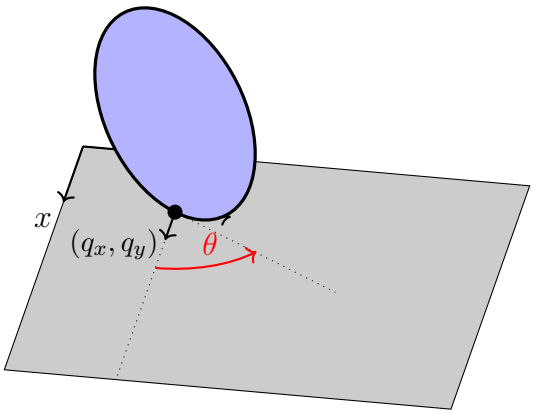

Figure 2.4: Planar unicycle or rolling coin model.

is 2 everywhere, we need to evaluate $\Delta_1(x)$. To this end, we compute the Lie bracket

$$[f_1, f_2](x) = \begin{pmatrix} 0 & 0 & -\sin(\theta) \\ 0 & 0 & \cos(\theta) \\ 0 & 0 & 0 \end{pmatrix} f_2 - 0 = \begin{pmatrix} -\sin(\theta) \\ \cos(\theta) \\ 0 \end{pmatrix}.$$

It is easy to see that $\Delta_1(x) = \text{span}\{f_1(x), f_2(x), [f_1, f_2](x)\}$ is of rank 3 everywhere, and thus by Theorem 2.1, the unicycle is controllable. Our method is guaranteed to apply. Setting $f_3(x) := [f_1, f_2](x) = \begin{pmatrix} -\sin(\theta) & \cos(\theta) & 0 \end{pmatrix}^\top$ and $\bar{F}(x) = (f_1(x)\ f_2(x)\ f_3(x))$, a short calculation by (2.12) yields:

$$G = \begin{pmatrix} (\lambda - 1)\sin^2(\theta) + 1 & -\frac{\sin(2\theta)(\lambda-1)}{2} & 0 \\ -\frac{\sin(2\theta)(\lambda-1)}{2} & (\lambda - 1)\cos^2(\theta) + 1 & 0 \\ 0 & 0 & 1 \end{pmatrix}.$$

Again this system is driftless so we only need to consider the GHF (2.14). We now use our method to solve the following problem: transfer a unicycle from position $x_i = (0, 0, 0)^\top$ to $x_f = (0, 1, 0)^\top$, which is also called the *parallel parking* problem. We show the result in Fig. 2.5 with $\lambda = 200$ and initial condition $v(t) = (\sin(\pi t), t, 0)^\top$. The 3D configuration plot is on the left while the 2D projected view is on the right. As in Fig. 2.3, the light blue curve represents the initial curve v, the red curve is the AGHF solution $x(\cdot, s_{\max})$ and the black curve is the integrated path from our algorithm. The reason we do not use a straight line as

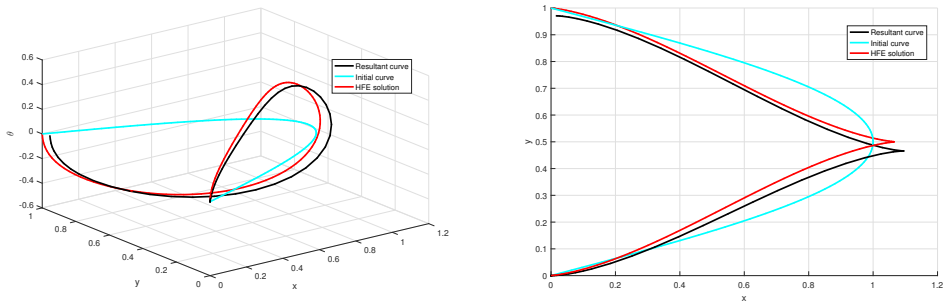

Figure 2.5: Parallel parking of a unicycle scenario 1.

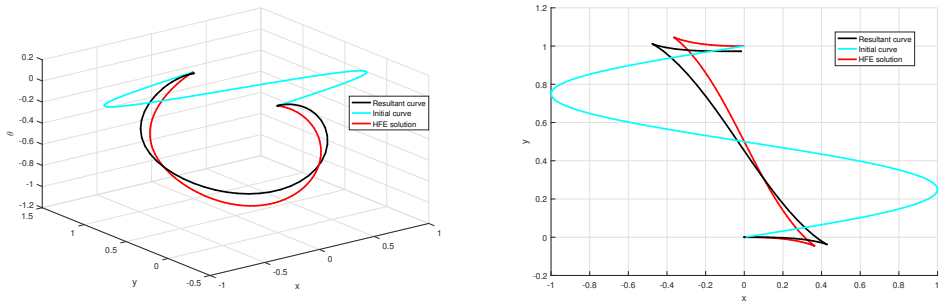

Figure 2.6: Parallel parking of a unicycle scenario 2.

the initial curve is the same as in the case of the non-holonomic integrator. It can be seen that when $s_{\max} = 2$, the solution is in a V-shape which is almost one of the practical parallel parking strategies.

It is also observed that when the initial curve is defined to be $v(t) = (\sin(2\pi t), t, 0)^\top$ instead, the limiting curve will approach a Z-shaped path, which is shown in Fig. 2.6. Note that this "parallel parking" strategy is also practical, but belongs to a different *homotopy group* than the one above.

Unicycle with constant linear velocity While we still focus on the unicycle model (2.30), we constrain it with unit linear velocity. This is similar to the model of *Dubins car* [51], except that we do not have constraints on the steering velocity. In this case we

have $u_1 \equiv 1$ and hence (2.30) becomes

$$\underbrace{\begin{pmatrix} \dot{q}_x \\ \dot{q}_y \\ \dot{\theta} \end{pmatrix}}_{\dot{x}} = \underbrace{\begin{pmatrix} \cos\theta \\ \sin\theta \\ 0 \end{pmatrix}}_{F_d} + \underbrace{\begin{pmatrix} 0 \\ 0 \\ 1 \end{pmatrix}}_{F} u, \tag{2.31}$$

where the first control direction vector is now the drift. Note that in this case even when $u = 0$, $\dot{x} \neq 0$. Intuitively the system is semi-controllable in the sense that as long as $\sqrt{((q_x)_i - (q_x)_f)^2 + ((q_y)_i - (q_y)_f)^2} < T$, the system is controllable (by steering at the beginning and ending so that the orientation is aligned with the direction pointing from $((q_x)_i, (q_y)_i)^\top$ to $((q_x)_f, (q_y)_f)^\top$ in the middle of time). Following our method, we pick $F_c = \begin{pmatrix} 1 & 0 \\ 0 & 0 \\ 0 & 1 \end{pmatrix}$ so that $\bar{F}$ is the identity matrix. Hence according to (2.12) we have $G = \mathrm{diag}(\lambda, \lambda, 1)$. The corresponding Lagrangian (2.22) is

$$L(x, \dot{x}) = \lambda(\dot{q}_x - \cos(\theta))^2 + \lambda(\dot{q}_y - \sin(\theta))^2 + \dot{\theta}^2.$$

We still examine our algorithm on the parallel parking problem with $x_i = (0, 0, 0)^\top, x_f = (0, 1, 0)^\top$. With $\lambda = 1000, T = 5$, we obtain the results shown in Fig. 2.7. The first row contains paths in the 3D configuration space while the bottom row is the corresponding (q_x, q_y)-plane projected views. The unicycle follows the black solid curve and moves from the position with the lightest blue color to positions with darker blue colors gradually, with its orientation and magnitude of linear velocity at each snapshot indicated by the red arrow. We see that the initial sketch of straight line $x(t, 0) = v(t) = (0, t, 0)^\top$ in Fig. 2.7a and Fig. 2.7d cannot be followed by the unicycle as such a path violates the non-slip constraints and does not follow the drift dynamics. Fig. 2.7b and Fig. 2.7e show the curve $x(t, s)$ with $s = 10$. Fig. 2.7c and Fig. 2.7f show $x(t, s_{\max})$ with $s_{\max} = 500$. The integrated trajectory (cyan dotted line) generated by using the extracted control (as in Step 4) is very close to $x(t, s_{\max})$ and drives the unicycle close to x_f with very high precision. As a comparison, the

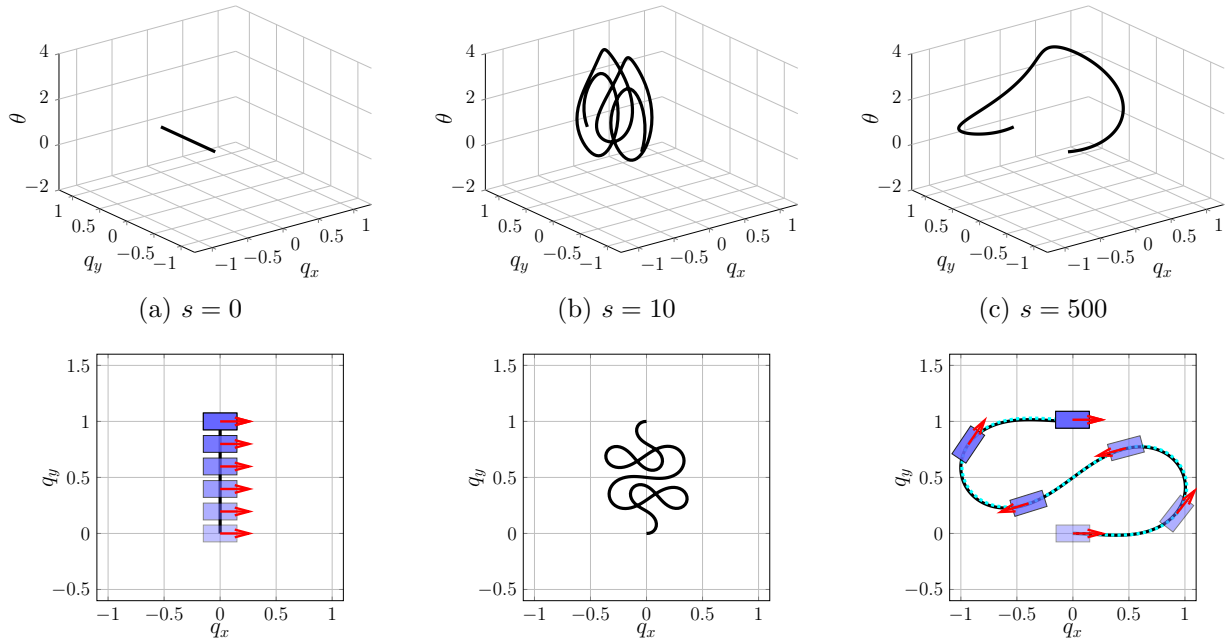

(a) $s = 0$ (b) $s = 10$ (c) $s = 500$

(d) (e) (f)

Figure 2.7: Parallel parking of a unicycle with constant linear velocity.

integrated S-shaped path is very different from the V-shaped or Z-shaped paths which we derived in the previous example for the general planar unicycle (2.30). This is reasonable since in the those cases the unicycle has to move backwards, which is not allowed for a unicycle with constant linear velocity.

Dynamic unicycle We now consider the unicycle with inertia; the acceleration of the unicycle is proportional to the applied torque following Newton's second law. To model this system in the form of (2.2), we add two states to the unicycle configuration: u_1 and u_2, representing the linear and angular velocity. Acting on the accelerations $\dot{u}_1, \dot{u}_2$, the controls

v_1, v_2 are a force and a torque, respectively.

$$\underbrace{\begin{pmatrix} \dot{q}_x \\ \dot{q}_y \\ \dot{\theta} \\ \dot{u}_1 \\ \dot{u}_2 \end{pmatrix}}_{\dot{x}} = \underbrace{\begin{pmatrix} u_1 \cos\theta \\ u_1 \sin\theta \\ u_2 \\ 0 \\ 0 \end{pmatrix}}_{F_d} + \underbrace{\begin{pmatrix} 0 & 0 \\ 0 & 0 \\ 0 & 0 \\ 1 & 0 \\ 0 & 1 \end{pmatrix}}_{F} \underbrace{\begin{pmatrix} v_1 \\ v_2 \end{pmatrix}}_{v} \tag{2.32}$$

Similar to the previous case, we can take $\bar{F}$ to be the identity matrix and $G = \mathrm{diag}(\lambda, \lambda, \lambda, 1, 1)$. Consequently,

$$L(x, \dot{x}) = \lambda \left((\dot{q}_x - u_1 \cos(\theta))^2 + (\dot{q}_y - u_1 \sin(\theta))^2 + (\dot{\theta} - u_2)^2 \right) + \dot{u}_1^2 + \dot{u}_2^2.$$

We set the boundary condition to $x_i = (0, 0, 0, 0, 0)^\top$ and $x_f = (0, -1, 0, 0, 0)^\top$. The boundary values for u_1 and u_2 are 0, meaning the unicycle starts and ends with 0 velocities. We use a partial sinusoid $v(t) = (\sin(2\pi t), -t, 0, 0, 0)$ as the initial sketch $x(t, 0)$, shown in Fig. 2.8a and Fig. 2.8d. Following the remaining steps of the algorithm with $\lambda = 50000, T = 1$, the results are shown in Fig. 2.8. The unicycle cannot follow the initial curve as seen in Fig. 2.8d. The AGHF yields the curve $x(t, s_{\max})$ shown in Fig. 2.8f (black solid line). Extracting the control, we obtain a trajectory (cyan dotted line) that is almost identical. This example is very similar to the parallel parking example of the planar unicycle; nevertheless the controls extracted from our algorithm in this case are the accelerations rather than velocities.

Car The last example we will consider in this subsection is the car depicted in Fig. 2.9. Similar to the unicycle, a car on the plane is described by its position and orientation ($(q_x, q_y) \in \mathbb{R}^2$ and $\phi \in S^1$ respectively), with an extra state $\theta \in S^1$ representing the angle of its front wheels with respect to the current orientation. Its dynamics is modeled according

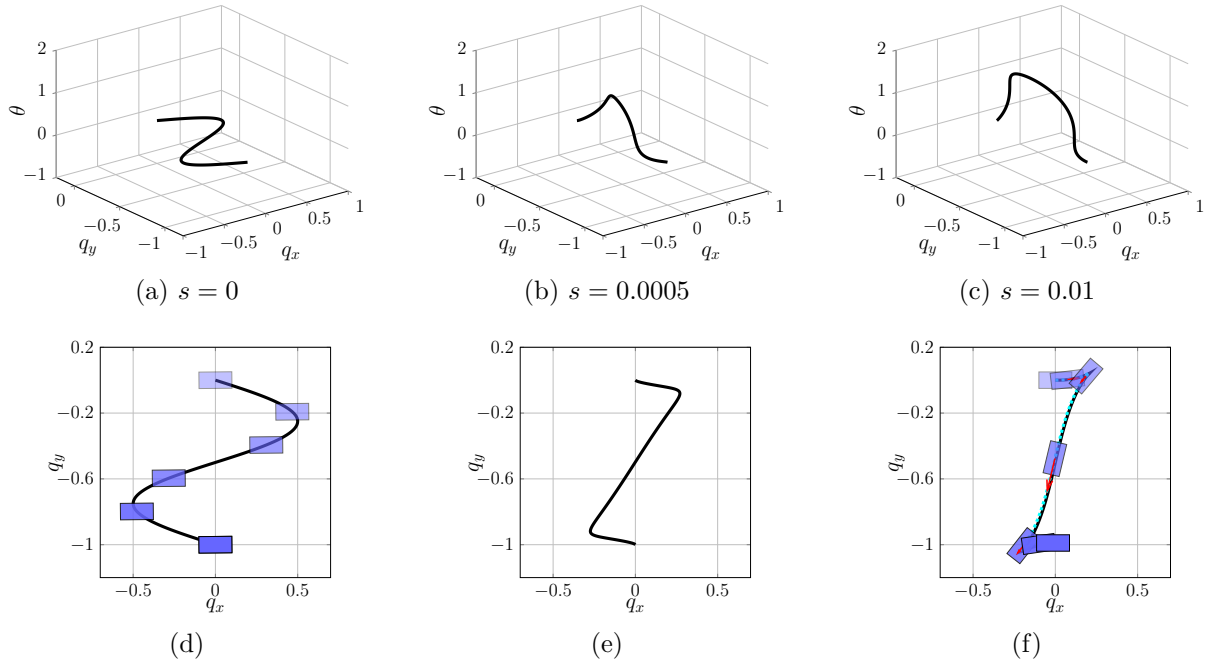

(a) $s = 0$ (b) $s = 0.0005$ (c) $s = 0.01$

(d) (e) (f)

Figure 2.8: Parallel parking of a dynamic unicycle.

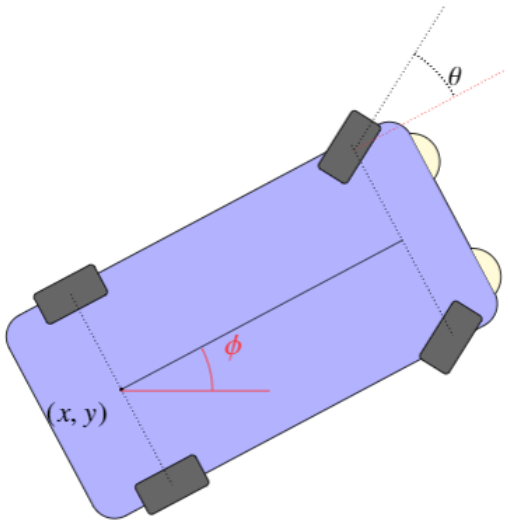

Figure 2.9: A car model.

to

$$\begin{pmatrix} \dot{x} \\ \dot{y} \\ \dot{\theta} \\ \dot{\phi} \end{pmatrix} = u_1 \underbrace{\begin{pmatrix} \cos\phi \\ \sin\phi \\ 0 \\ \frac{1}{d}\sin\theta \end{pmatrix}}_{f_1} + u_2 \underbrace{\begin{pmatrix} 0 \\ 0 \\ 1 \\ 0 \end{pmatrix}}_{f_2}, \tag{2.33}$$

where d is the *wheelbase*, the distance between the front and rear axles of a vehicle. We left the verification of controllability of the car as an exercise for readers. On the other hand, it is not hard to find that by defining $f_3 = (0, 0, 1, 0)^\top$, $f_4 = (0, 0, 0, 1)^\top$, we can construct $\bar{F}(x) = (f_1, f_2, f_3, f_4)$ which is full rank. Thus via (2.12) $G(x)$ is computed to be

$$\begin{aligned}
G_{11} &= \frac{c+1}{d^2}\sin^2\theta\cos^2\phi + (c-1)\sin^2\phi + 1, \\
G_{22} &= \frac{c+1}{d^2}\sin^2\theta\sin^2\phi - (c-1)\sin^2\phi + c, \\
G_{33} &= 1, \\
G_{44} &= c, \\
G_{12} &= G_{21} = \frac{c+1}{d^2}\sin^2\theta\sin\phi\cos\phi - (c-1)\sin\phi\cos\phi, \\
G_{14} &= G_{41} = -\frac{c}{d}\sin\theta\cos\phi, \\
G_{24} &= G_{42} = -\frac{c}{d}\sin\theta\sin\phi, \\
G_{13} &= G_{31} = G_{23} = G_{32} = G_{34} = G_{43} = 0.
\end{aligned}$$

Note that the physical nature of the car is very similar to the unicycle, and hence we expect that the "parallel parking" of a car will be analogous to that of unicycle. This is indeed reflected in our simulation and hence not repeated here. However, unlike the unicycle which has 0 wheelbase and can turn without moving, a car has to move back and forth in order to turn around. Indeed our algorithm results in an "economical" 180° turn-around strategy with just 3 moves. Since the configuration space in this case is 4-dimensional, we only show the xy-plane motion planning and the corresponding control in Fig. 2.10.

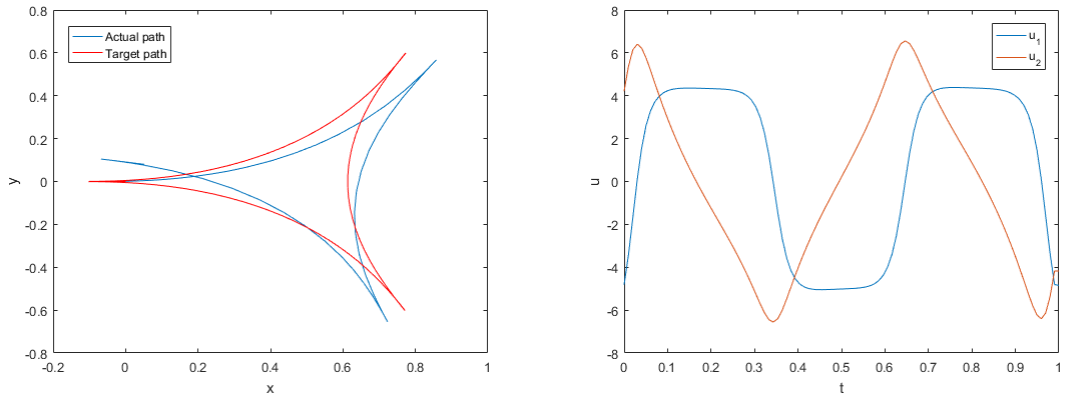

Figure 2.10: 180° turn motion planning of a car and the corresponding controls.

2.3 Extensions of the method

2.3.1 Holonomic constraints and non-holonomic constraints

Constraints imposed by the system dynamics (2.2) are called non-holonomic constraints since they are confining the time derivative of the states; on the other hand, constraints such as

$$q_i(x) = 0, \quad i = 1, 2, \cdots, k \tag{2.34}$$

are called holonomic constraints as they are directly confining the states. In Section 2.2 we have concluded the algorithm of motion planning in the presence of non-holonomic constraints. In this subsection we provide an alternative view of holonomic constraints and draw some connections between non-holonomic constraints and holonomic constraints so that they can be integrated into our algorithm at the same time.

To this end, write $Q(x) = 0$ as the matrix form of (2.34) and assume Q is a k-dimensional vector valued, differentiable function. Differentiate on both sides, we have

$$H(x)\dot{x} = 0, \tag{2.35}$$

where for each $x \in \mathbb{R}^n$, $H(x) \in \mathbb{R}^{k\times n}$ is the Jacobian of Q evaluated at x. For simplicity we assume H is of full rank k. Our motion planning in the presence of both holonomic con-

straints and non-holonomic constraints, in view of (2.2) and (2.35), is hence mathematically formulated as

$$\dot{x} = F_d(x) + F(x)u,$$
$$H(x)\dot{x} = 0.$$

Plugging the first row into the second, we have

$$H(x)F_d(x) + H(x)F(x)u = 0. \tag{2.36}$$

For each fixed x, (2.36) is a non-homogenous matrix equation, and a solution exists if and only if $H(x)F_d(x) \in \operatorname{span} H(x)F(x)$. Note that HF has dimension $k \times m$, and by Sylvester's rank inequality we have

$$k + m - n \leq \operatorname{Rank}(HF) \leq k \wedge m.$$

In addition because $\operatorname{Rank}(HF) + \operatorname{Nullity}(HF) = k \vee m$, we conclude $|k - m| \leq l := \operatorname{Nullity}(HF) \leq n - (k \wedge m)$. When a solution exists, the general expression of the solution of u in (2.36) has the form

$$u = u_1 + u_2,$$

where u_1 is a specific solution to (2.36), for example, $u_1 = (H(x)F(x))^\dagger H(x)F_d(x)$ where † represents the pseudo-inverse and $u_2 \in \ker H(x)F(x)$. Let $A(x) = \{a_1(x), \cdots, a_l(x)\}$ be the basis of $\ker H(x)F(x)$. Then we have $u = (H(x)F(x))^\dagger H(x)F_d(x) + A(x)v$ for some $v \in \mathbb{R}^l$. Plugging it into (2.2), we have

$$\dot{x} = \Big(I + (H(x)F(x))^\dagger H(x)\Big)F_d(x) + F(x)A(x)v := \tilde{F}_d(x) + \tilde{F}(x)v, \tag{2.37}$$

where $\tilde{F}_d(x) = \Big(I + (H(x)F(x))^\dagger H(x)\Big)F_d(x)$ and $\tilde{F}(x) = F(x)A(x)$. Therefore the motion planning problem with both non-holonomic and holonomic constraints becomes the one with only non-holonomic constraints; the only difference is that the drift term and admissible control direction matrix are changed. As a result, our AGHF algorithm can still be applied while only the first step needs to be modified; to be more precise, we now need to find the complement matrix of $\tilde{F}$ instead of F, and we have $\bar{F} = (\tilde{F}_c|\tilde{F})$.

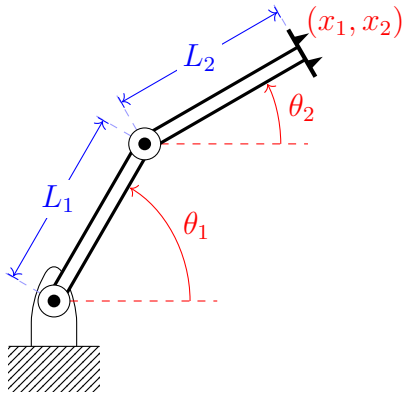

Figure 2.11: Two-link articulated arm.

Case study: the two-link manipulator In this example we consider a two-link manipulator in the plane, see Fig. 2.11. The working space, in terms of the position of the tool tip (x_1, x_2), is a subset of $\mathbb{R}^2$. The configuration space when the joint angles are also taken into account can be treated as a subset of $\mathbb{R}^4$. As a result, the two-link articulated arm can be described as a system with 4 degrees of freedom and 2 holonomic constraints relating the position (x_1, x_2) of the tip to the joint angles θ_1, θ_2 by the following equations:

$$\begin{cases} q_1(x) = L_1 \cos(\theta_1) + L_2 \cos(\theta_2) - x_1 = 0, \\ q_2(x) = L_1 \sin(\theta_1) + L_2 \sin(\theta_2) - x_2 = 0. \end{cases} \tag{2.38}$$

Taking differential of the two constraints, we find $H(x) = \begin{pmatrix} -1 & 0 & -L_1 \sin\theta_1 & -L_2 \sin\theta_2 \\ 0 & -1 & L_1 \cos\theta_1 & L_2 \cos\theta_2 \end{pmatrix}$. Note that in this model there are no non-holonomic constraints; in other words, $F_d(x) \equiv 0, F(x) \equiv I$ and hence $\tilde{F}_d(x) \equiv 0, \tilde{F}(x) = (H(x)^\top)^\perp$. Thus when $L_1 = L_2 = 1$, we have $\tilde{F}_c(x) = \begin{pmatrix} 1 & 0 \\ 0 & 1 \\ \sin\theta_1 & -\cos\theta_1 \\ \sin\theta_2 & -\cos\theta_2 \end{pmatrix}$ and we find $\tilde{F}(x) = \begin{pmatrix} -\sin\theta_1 & -\sin\theta_2 \\ \cos\theta_1 & \cos\theta_2 \\ 1 & 0 \\ 0 & 1 \end{pmatrix}$. Because $\bar{F} = (\tilde{F}_c | \tilde{F})$ is orthonormal,

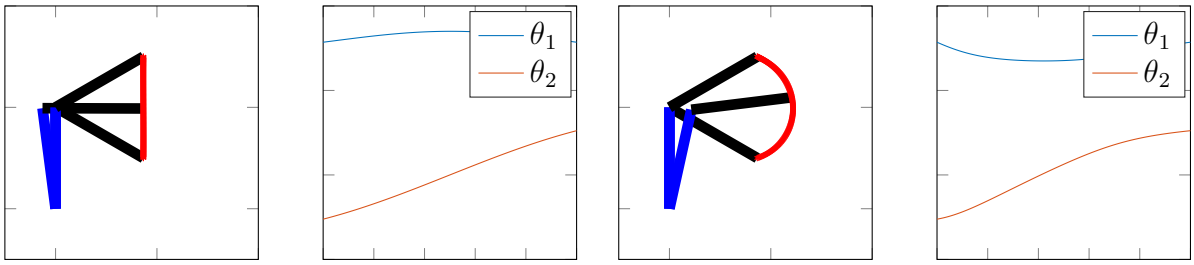

(a) Vertical motion illustration (b) Joint angles for vertical motion (c) Circular motion illustration (d) Joint angles for circular motion

Figure 2.12: Vertical motion and circular motion of the two-link articulated arm.

$$G = \bar{F}\,\mathrm{diag}([\lambda\,\lambda\,1\,1])\bar{F}^\top$$
$$= \begin{pmatrix} \sin^2\theta_1 + \sin^2\theta_2 + \lambda & -\frac{\sin 2\theta_1}{2} - \frac{\sin 2\theta_2}{2} & (\lambda-1)\sin\theta_1 & (\lambda-1)\sin\theta_2 \\ -\frac{\sin 2\theta_1}{2} - \frac{\sin 2\theta_2}{2} & \cos^2\theta_1 + \cos^2\theta_2 + \lambda & -(\lambda-1)\cos\theta_1 & -(\lambda-1)\cos\theta_2 \\ (\lambda-1)\sin\theta_1 & -(\lambda-1)\cos\theta_1 & \lambda+1 & \lambda\cos(\theta_1-\theta_2) \\ (\lambda-1)\sin\theta_2 & -\cos\theta_2\,\lambda - 1 & \lambda\,\cos\theta_1 - \theta_2 & \lambda+1 \end{pmatrix}.$$

Our goal is to plan the motion of the tip of the arm, from an initial state $x(0) = x_i = (\sqrt{2}/2, 1-\sqrt{2}/2, \pi/2, -\pi/4)^\top$ to a final state $x(1) = x_f = (\sqrt{2}/2, 1+\sqrt{2}/2, \pi/2, \pi/4)^\top$. We furthermore require the motion to follow a *straight line* given by $x_1 = constant$. The resulting motion planning problem thus contains, in addition to the two holonomic constraints relating the tip of the arm to the angles given in Eq. (2.38), the constraint $q_3(x) = x_1 - c = 0$ and the corresponding constrained direction is $\frac{\partial q_3}{\partial x} = (1,0,0,0)^\top$. Given these constraints, we implement the three steps of the AGHF algorithm and show the results in Fig. 2.12a. We then replaced the constraint of vertical motion by asking that the tip follows an arc of a circle. The corresponding holonomic constraint is $q_4(x) = (x_1 - x_{1c})^2 + (x_2 - x_{2c})^2 - r^2 = 0$ for some constants x_{1c}, x_{2c}, r. The differential of this constraint is easily evaluated. We show in Fig. 2.12c the result obtained. Note that this illustrates the use of our method to solve *inverse kinematic problems* numerically.

2.3.2 State constraints and input constraints

State constraints Firstly, we describe state constraints or obstacles as $\Omega \subset \mathbb{R}^n$ in the configuration space via function $r : M \to \mathbb{R}$ according to

$$\Omega := \{x \in M : r(x) \leq 0\}.$$

The boundary of an obstacle is thus $\partial\Omega = \{x \in M : r(x) = 0\}$. We encode state constraints into our Riemannian metric via a *barrier function* $b(x)$ with the following properties:

1. $b(x)$ is positive and differentiable for all $x \in M \backslash \Omega$.
2. $b(x) \to \infty$ as $x \to \partial\Omega$.
3. $b(x) = 1$ when x is far away from Ω.

Barrier functions are a common practice in the optimization literature (see, e.g., [52]). The idea is that we would like $b(x)$ to be large when x is in the vicinity of Ω, and to become infinite if $x \in \partial\Omega$. Thus instead of (2.12) we set

$$G(x) = b(x)(\bar{F}(x)^{-1})^\top D\bar{F}(x)^{-1}, \tag{2.39}$$

that is, we multiply the right-hand side of (2.12) by $b(x)$ when defining G. As a result, we see that the length of a path that is in the vicinity of an obstacle is much larger than the length of a path which steers well-clear of the obstacle, where quantifying "well-clear" of course depends on the choice of $b(x)$ and how quickly it decays near the boundary of the obstacle. In the case when obstacles are balls, that is, $\Omega = \cup_{i=1}^{l}\{x \in \mathbb{R}^n : |x - c_i| \leq r_i\}$ where l is the total number of balls, one candidate of such $b(x)$ function will be a modification of the penalty function from avoidance control [53]:

$$b(x) = 1 + \sum_{i=1}^{l} \left(\min\left\{0, \frac{|x - c_i|^2 - R_i^2}{|x - c_i|^2 - r_i^2}\right\}\right)^2, \tag{2.40}$$

where R_i is such that $r_i < R_i$ for all $i = 1, 2, \cdots, l$, and R_i can be thought of as a *radius of detection* of the obstacle, in the sense that outside this radius, the obstacle does not affect

the metric. Note that $b(x)$ defined in (2.40) satisfies the 3 properties mentioned earlier. In addition, one can cover any obstacles with balls and use the above barrier function as a default approach. The derivative of b is also not hard to compute. In case the obstacle is a single ball with center c and radius r and radius of detection R, the derivative of $b(x)$ can be easily computed:

$$\frac{db(x)}{dx} = \begin{cases} 0 & \text{if } |x-c| \geq R \text{ or } |x-c| < r, \\ \frac{4(R^2-r^2)(|x-c|^2-R^2)}{(|x-c|^2-r^2)^3}(x-c) & \text{if } r < |x-c| < R, \\ \text{not defined} & \text{if } |x-c| = r. \end{cases} \tag{2.41}$$

It can be generalized to multiple ball obstacles by taking sum of derivatives and intersection of conditions.

In terms of the algorithm, in addition to the modified Riemannian metric tensor $b(x)G(x)$ we should use instead, we also need to pay some attention to the choice of initial curve v while solving the AGHF. While the non-holonomic constraints do not need to be satisfied along v, the state constraints have to be satisfied. This is because $b(x)$ approaches infinity when x approaches to $\partial\Omega$, and it is not defined on $\partial\Omega$. Hence the Riemannian metric is not well defined if v crosses the obstacles Ω.

Case study: unicycle/car with state constraints We now apply this method on the unicycle model (2.30) or car model (2.33) with different state constraints. We first pick two point obstacles located at $(-0.7, 0), (0.7, 0)$ in the xy-plane. The motion planning problem is formulated as follows: We desire to transfer the unicycle from $x_i = (-1, 0, 0)^\top$ to $x_f = (1, 0, 0)^\top$ in 1 unit of time, while avoiding the two point obstacles mentioned above. Provided these constraints, we sketch an arbitrary initial curve $v(t)$ that connects x_i and x_f and avoids the obstacles. We opted simply for a sinusoidal curve in xy-plane and kept $\theta \equiv 0$, as shown in Fig. 2.13a, with the red dots representing the two obstacles and the blue curve representing v. The unicycle certainly cannot follow this initial curve, as the motion direction is not aligned with the unicycle orientation. In Figs. 2.13b to 2.13d, we show the gradual deformation of the curve by the AGHF in the xy-plane as s increases. In the final step $s = 4$, the curve becomes almost admissible and we see that the unicycle can basically

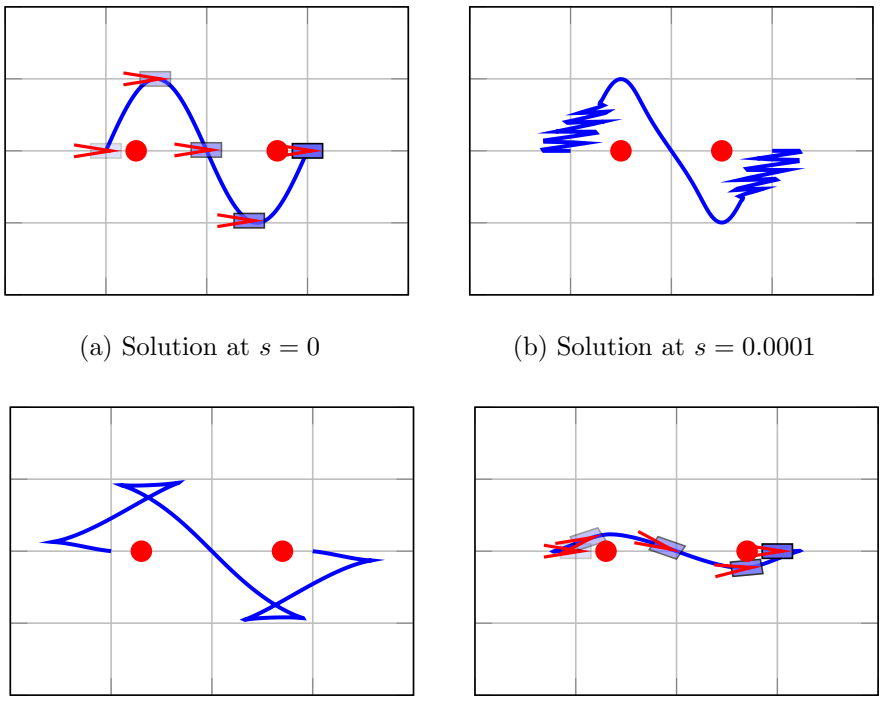

(a) Solution at $s = 0$

(b) Solution at $s = 0.0001$

(c) Solution at $s = 0.01$

(d) Solution at $s = 4$

Figure 2.13: motion planning for a unicycle avoiding two point obstacles.

follow such trajectory to reach x_f. It is worth noting that because the obstacles are very close to the initial and final states, the unicycle has to move backward first in order to have more room to maneuver around said obstacles. Similarly, it overshoots the second obstacles before backing up and parking at its final destination.

Similar to ball obstacles as described in (2.40), the barrier function for wall obstacles is also algebraically simple. We now illustrate our method for planning the motion of a car (2.33) within limited spaces. Without more mathematics, our first experiment is still a 180° turn. Without any obstacles and using the initial curve as shown in Fig. 2.14a which is clearly not admissible, we recover the old triple point turning result in Section 2.2.3 and we repeat it here in Fig. 2.14b. This corresponds to the most efficient way of 180° turning of a car in practice, assuming there are no other spatial obstacles. If in addition, we impose additional parallel curbs, which are encoded in the barrier function $b(x)$ as described earlier, the constrained space the car can move in results in additional back-and-forth as seen in Fig. 2.14c. The narrower the street, the more back-and-forth needed.

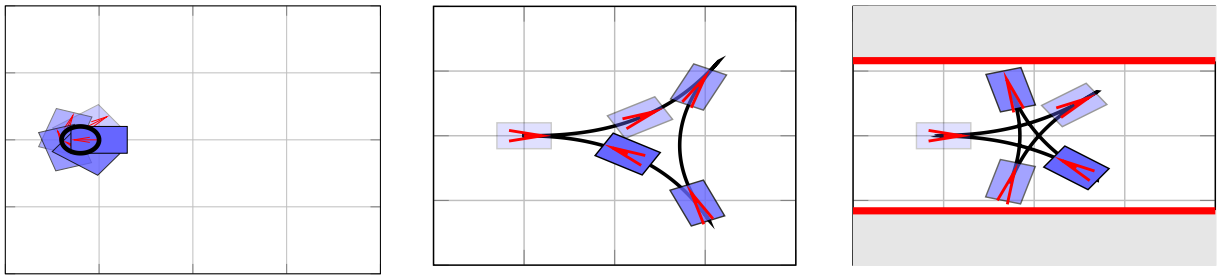

(a) Initial sketch (b) Free 3 points turning (c) 5 points turning between walls

Figure 2.14: Car 180° turn experiment.

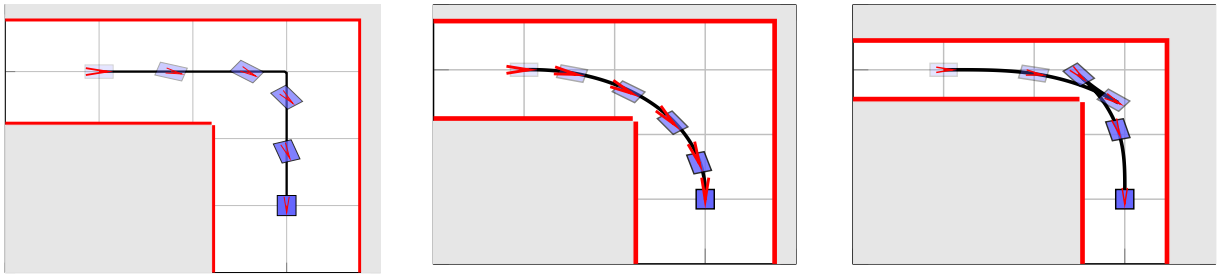

(a) Initial sketch (b) Turn in a wide street corner (c) Back-forth behavior at narrow street corner

Figure 2.15: Car turning in a street corner experiment.

We conclude the discussion with the case of a car turning in a narrow street corner. The initial curve is simply an L-shaped curve in xy-plane with ϕ linear with respect to t and $\theta \equiv 0$, as illustrated in Fig. 2.15a. With the curbs modeled as obstacles, our method generates the relatively "optimal" path for this corner turn. Interestingly enough, the car is able to perform the turn in one shot if the street is relatively wide as shown in Fig. 2.15b, or may need extra maneuvering if the street is narrow, as shown in Fig. 2.15c. We emphasize that both simulations are performed with the same initial curve provided in Fig. 2.15a. The only difference is the street width. Whether one shot or two is automatically determined by the solution of AGHF without any further specification. Finally, we note that in addition to the curb of the streets which are modeled as obstacles in the xy-plane, we could also put limits on the steering angle θ as an obstacle.

Case study: simultaneous multi-vehicle motion planning Suppose there are l unicycles and each of them has its own state $x_i = (x_{i,1}, x_{i,2}, \theta_i)^\top$ and the dynamics as in (2.30) for some input $u_{i,1}, u_{i,2}$. The system of multi-vehicle has total dimension of $3l$. If we denote the total state as $x^\top = (x_1^\top, \cdots x_l^\top)$, the overall dynamics is

$$\dot{x} = \mathrm{diag}(F_1(x_1), \cdots, F_l(x_l))u := F(x)u,$$

where $F_i = \begin{pmatrix} \cos\theta_i & 0 \\ \sin\theta_i & 0 \\ 0 & 1 \end{pmatrix}$ and $u = (u_{1,1}, u_{1,2} \cdots u_{l,1}, u_{l,2})^\top$. While planning the path for all l vehicles, they are also supposed to avoid collision with each other. Collision between the i, j-th vehicles is avoided if

$$(x_{i1} - x_{j1})^2 + (x_{j2} - x_{j2})^2 \geq r_c^2, \tag{2.42}$$

where r_c is a safety radius guaranteeing collision-free space between two vehicles. Thus the (2.40)-like barrier function induced from (2.42) is

$$b_c(x) = 1 + \sum_{i \neq j} \left(\min \left\{ 0, \frac{(x_{i1} - x_{j1})^2 + (x_{j2} - x_{j2})^2 - R^2}{(x_{i1} - x_{j1})^2 + (x_{j2} - x_{j2})^2 - r_c^2} \right\} \right)^2 .$$

Similarly if two vehicles are too close, $b_c(x)$ becomes large and the metric at this state of vehicles is large. As an example, we show that 2 vehicles can be motion planned simultaneously using our methods. In the first case two unicycles are initially at states $(0, 1, 0)^\top, (0, -1, 0)^\top$, that is, parked at $(0, 1), (0, -1)$ in the xy-plane while both facing east. The task is to swap the position of the two unicycles. The initial sketch is a circle passing through the two unicycles, shown in Fig. 2.16a – clearly these two curves are inadmissible since the orientation vectors of the unicycles are not tangent to the curves. After running our algorithm, the initial sketch deforms into the two V-shaped paths as in Fig. 2.16b; now the two unicycles are able to perform the swap of positions along such paths.

While readers might think this scenario differs little from motion planning for single vehicle and hence is less challenging, the next scenario is more interesting and shows the power of our algorithm in multi-vehicle motion planning. In this case one unicycle is supposed to move from $(-1, 0, \pi/2)^\top$ to $(1, 0, \pi/2)^\top$ while the other is supposed to move from $(0, -1, 0)^\top$ to $(0, 1, 0)^\top$. Note that because of symmetry, the optimal path for each individual vehicle will intersect with the other. Nevertheless, by picking exaggerated initial curves that do not intersect with each other as shown in Fig. 2.16c, our algorithm gives reasonable admissible paths for the two vehicles. The result in Fig. 2.16d graphically seems to be intersected paths; however the vehicles pass the intersection at different times and so collision is avoided.

As a remark, if we perform motion planning for each individual vehicle first while treating the other vehicles as obstacles, the avoidance problem becomes dynamic in the sense that now the obstacles are moving with respect to time. On the other hand, avoidance of collision between vehicles and avoidance of static obstacles are processed in the same way in our method.

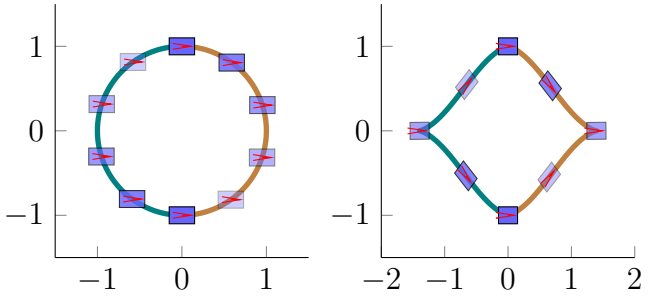

(a) Case 1 initial curve (b) Case 1 final curve

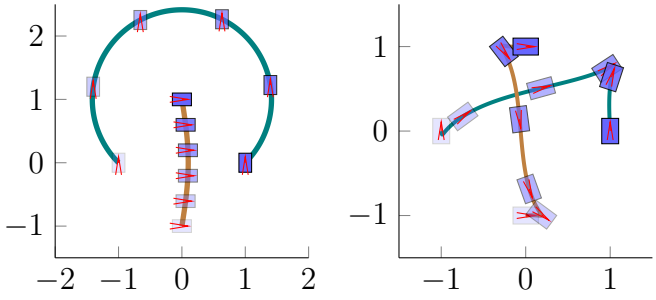

(c) Case 2 initial curve (d) Case 2 final curve

Figure 2.16: Two vehicles simulation.

Input constraints Previously we have shown that constraints in states can be handled by multiplying the inner product matrix $G(x)$ by an appropriately defined barrier function $b(x)$. Now we show that being able to overcome state constraints and drift allows us to handle input constraints, i.e., systems of the type

$$\begin{aligned} \dot{x} &= f(x,u) \\ l(x(t),u(t)) &\geq 0, \quad \forall t \in [0,T], \end{aligned} \tag{2.43}$$

with l being a differentiable function, at the expanse of using controls that are differentiable almost everywhere. For example, common constraints such as magnitude bounds on the controls $|u| \leq u^{\max}$, for a given $u^{\max}$, can be implemented by setting $l(u) = u^{\max} - |u| \geq 0$.

Defining $\dot{u} = v$ and also *augmented state* $y = \begin{pmatrix} x \\ u \end{pmatrix} \in \mathbb{R}^{n+m}$, then we can set

$$\dot{y} = \begin{pmatrix} \dot{x} \\ \dot{u} \end{pmatrix} = \underbrace{\begin{pmatrix} f(x,u) \\ 0 \end{pmatrix}}_{F_d} + \underbrace{\begin{pmatrix} 0 \\ I_{m\times m} \end{pmatrix}}_{F} v, \tag{2.44}$$

which is a system with affine control and drift, similar to (2.2).

To implement the constraints on the controls u, we choose a barrier function, e.g. $b(y) := 1 + \frac{1}{l(x,u)}$, and similar to (2.39) we have

$$G(y) := b(y)(\bar{F}(y)^{-1})^\top D\bar{F}(y)^{-1}.$$

Note that if we pick $F_c = \begin{pmatrix} 0 & I_{n\times n} \end{pmatrix}^\top$, we will simply have $\bar{F} = (F_c|F) = I_{(n+m)\times(n+m)}$. Thus $G(y) = b(y)D$. In addition, (2.22) gives

$$L(y,\dot{y}) = b(y)(\dot{y} - F_d(y))^\top G(y)(\dot{y} - F_d(y)) = b(y)(\lambda|\dot{x} - f(x,u)|^2 + |\dot{u}|^2).$$

We can argue that the AGHF will yield an admissible control meeting the constraints as follows: When a curve $y(t)$ is close to the boundary of obstacles defined by the l, l is close to 0 and thus $b(y)$ and L are large. Since the AGHF minimizes $\mathcal{A} = \int_0^T L dt$, the curve will be deformed away from the obstacles and hence u will meet the input constraints. The rest of our algorithm for motion planning is not changed, except that in Step 2, since u_i's are now states of the augmented system, initial conditions and boundary conditions need to be provided. Those values are not specified in the problem and can arbitrary; however, the initial curve and boundary values do need to satisfy the constraints on inputs and be compatible with each other.

As a remark, it is observed that although this technique seems to work for any nonlinear systems of the form (2.43), Ω_λ in Theorem 2.2 might be extremely small. As a result, deriving an admissible path from any arbitrary initial curve is not always guaranteed. To emphasize this point, consider the case when the system is driftless, affine in control and satisfies the

condition in Theorem 2.1. Such a system is always controllable when the control input is unconstrained. Nevertheless, when formulated in the form of (2.44), the augmented system has drift, in which case the reachable space of the system becomes unclear and admissible path may even not exist. Nevertheless, state augmentation does work on the next example of planar kinematic unicycle with constrained inputs.

Case study: unicycle with constrained inputs We return to the original kinematics planar unicycle (2.30), and we impose magnitude bound on either the linear or steering velocity. As we have discussed earlier, the first step for handling input constraints is to perform a dynamical extension and include a barrier function. We use here the barrier function

$$b(x) = \frac{1}{(u_i^{\max})^2 - {u_i}^2}, \quad i = 1 \text{ or } 2$$

for the constraint in linear velocity or steering velocity, respectively. In addition, after state augmentation we recover the dynamic unicycle model of (2.32). Because u_1 and u_2 are now the states, initial sketches of them are needed. The boundary values and initial sketch in the previous unconstrained dynamic unicycle example with $u_1 = u_2 \equiv 0$ satisfy the input constraints and thus they are used to solve (2.18). The remaining steps are similar. The two cases of constrained linear velocity with $u_1^{\max} = 2$ and constrained steering velocity with $u_2^{\max} = \frac{\pi}{2}$ individually are shown in Fig. 2.17. Fig. 2.17a and Fig. 2.17b are the xy-plane projected views, where the solid dark curves are the AGHF solution $x(\cdot, s_m ax)$ and cyan dotted curves are the integrated paths. Our motion planning algorithm tells us that the unicycle should follow the cyan dotted curves and move from the lightest color position to the darker ones gradually. Fig. 2.17a and Fig. 2.17d are the extracted controls, where the red dashed lines represent the bounds on the magnitude of inputs.

We observe in Fig. 2.17a that when the linear velocity is constrained, the integrated path tends to align with the straight line connecting x_i, x_f. A compensation for this is that more effort is put into steering in the beginning and ending of the trip (with peak value of $|u_2|$ larger than 5 as seen in Fig. 2.17c) in order to quickly adjust the orientation. This can be understood as follows: Since the total traveling time is fixed ($T = 1$), constrained

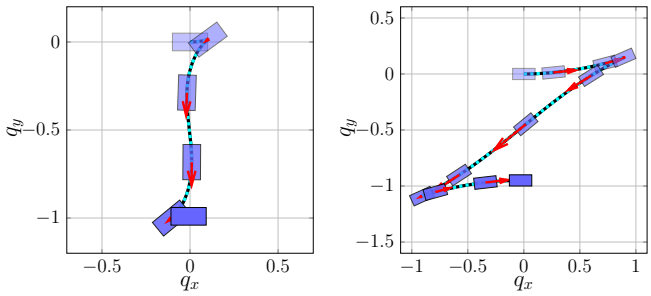

(a) Trajectory for bounded linear velocity

(b) Trajectory for bounded steering velocity

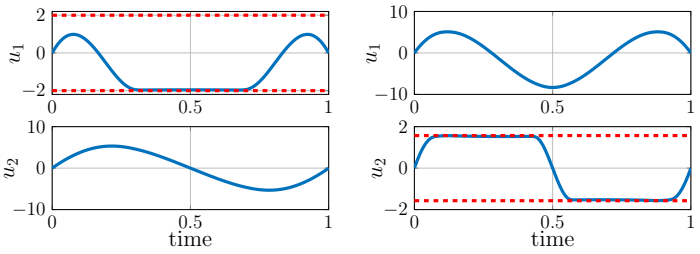

(c) Input profile for bounded linear velocity

(d) Input profile for bounded steering velocity

Figure 2.17: Parallel parking of a unicycle with input constraints.

linear velocity means little freedom in the 2D shape of the path, but it has to be close to the straight line (otherwise the unicycle will not be able to get to the target in time). On the other hand, when steering velocity is constrained, we have a distorted Z-shaped path as shown in Fig. 2.17b. The most significant difference is that the 2 acute angles on the path are much smaller, resulting from the fact that steering velocity has to be small. The total length of the 2D path is much longer, and to compensate for that linear velocity is also larger (with peak value of $|u_1|$ larger than 5 as seen in Fig. 2.17d).

It is observed that for most $t \in [0, T]$, the constrained inputs almost meet their boundary values (however the constrained inputs will never reach their boundary values due to the soft barrier function $b(x)$); this is close to a bang-bang control strategy, which is very often the optimal control strategy for most control problems with bounded inputs. Nevertheless, with finite λ, our integrated path is always C^1 so the control is always continuous; thus, we will never derive a true piece-wise continuous bang-bang control switching between boundary values. It remains an interesting yet challenging question whether the limit of solutions when λ goes to infinity is the "true" optimal path of minimal sub-Riemannian length.

2.3.3 Indefinite boundary conditions

For physical systems with no external inputs, the momentum conservation imposes implicit constraints to the system. A direct consequence of that requires those conserved quantities to be the same for the initial and finial configuration of the system. In other words, the solution of motion planning may not exist for any pair of $x_i, x_f \in M$. For some $\Omega_i, \Omega_f \subseteq M$ which are the subset of admissible initial and final states, we would rather treat the motion planning problem "solved" as long as an admissible curve connecting x_i, x_f is found such that x_i, x_f $x_i \in \Omega_i$. This discussion leads to the concept of *indefinite boundary conditions*. Another situation where indefinite boundary conditions are preferred is the case when the "optimal" final/initial states need to be determined in addition to the motion planning problem. For example, while the final joint angles are predetermined for the motion planning problem for a robot made of linkages to perform a somersault as in [54], [55], there are no constraints on the final velocities of the joints if "landing with impact" is allowed. Meanwhile, if the final configuration is fully fixed for the same somersault problem, we have freedom in designing the initial configuration for achieving an "optimal" somersault and hence it should not be fixed prior to the motion planning problem.

To formulate indefinite boundary conditions, let $S_{bc} \subset S := \{1, \cdots, d\} \times \{0, T\}$. For some given $x^{bc}(i,t) \in \mathbb{R}^n, (i,t) \in S_{bc}$,

$$x_i(t,s) = x^{bc}(i,t) \quad \forall (i,t) \in S_{bc}, s \geq 0. \tag{2.45}$$

In other words, we only fix some of the boundary states while leaving the rest free. We allow the case that $S_{bc} = \emptyset$, meaning that there are no boundary conditions at all. On the other hand when $S_{bc} = S$, we recover the fully constrained boundary conditions. Recall that in order to solve the AGHF (2.18), we still need an initial curve (2.16); this time the initial curve v also only needs to satisfy indefinite boundary conditions in the sense that

$$v \in \mathcal{X}'' := \{x \in \mathcal{X} : x_i(t) = x^{bc}(i,t) \quad \forall (i,t) \in S_{bc}\}.$$

Note that when S_{bc} is a proper subset of S, algebraically (2.45) does not provide enough

boundary conditions to solve (2.18). Nevertheless, because the steady-state solution of AGHF is an extremal of the functional (2.53), it should also give 0 variation with respect to perturbations in the free boundary states; In other words, we should also have

$$\frac{\partial L}{\partial (x_i)_t}(x(t,s),\dot{x}(t,s)) = 0 \quad \forall (i,t) \in S \backslash S_{bc}, s \geq 0. \tag{2.46}$$

Equation (2.46) together with (2.45) are the new boundary conditions we will use for solving the AGHF equation (2.18) for the indefinite boundary conditions case. Modifying the proof for Lemma 2.2 in the sense that we still have $x_s^\top \frac{\partial L}{\partial x_t} = 0$ for both $t = 0, T$ and all $s \geq 0$ after the integration by parts step because of our new boundary conditions (2.45), (2.46), we come up with the following lemma:

Lemma 2.3. *Let $x(t,s)$ be a solution to the AGHF* (2.18) *with an initial condition* (2.16) *and boundary conditions* (2.45), (2.46). *Then $\frac{\partial \mathcal{A}(x(\cdot,s))}{\partial s} \leq 0$, and it is* 0 *if and only if* (2.18) *is satisfied on the curve $x(\cdot, s)$.*

As a remark, similar arguments also hold if we require the indefinite boundary states to be not fully free but only in some subsets of $\mathbb{R}^n$. In other words, if the motion planning problem needs to satisfy the boundary condition that

$$x_i \in \Omega_i := \{x \in \mathbb{R}^n : \phi_j^i(x) = 0, j = 1, \cdots, n^i\},$$
$$x_f \in \Omega_f := \{x \in \mathbb{R}^n : \phi_k^f(x) = 0, k = 1, \cdots, n^f\},$$

then all we need are some transversality conditions that $\frac{\partial L}{\partial x_t}(x(0,s), x_t(0,s))$ is a linear combination of $\nabla \phi_j^i$'s and $\frac{\partial L}{\partial x_t}(x(T,s), x_t(T,s))$ is a linear combination of $\nabla \phi_k^f$'s in the non-degenerate case. For more information on transversality conditions for optimization, see, e.g., [56]. For how the AGHF with indefinite boundary conditions is used for planning mid-air somersault motion of a three-link robot, see [17].

2.3.4 Free terminal time

This subsection is a brief summary of the work [18]. For a driftless affine system, if $u(\cdot) : [0,1] \to \mathbb{R}^m$ gives an admissible path satisfying the boundary condition $x(0) = x_i, x(1) = x_f$, then $\frac{1}{T}u\left(\frac{t}{T}\right)$ gives a time scaled admissible path with $x'(0) = x_i, x'(T) = x_f$. In other words, there is no need to consider the terminal time T other than 1 since it can always be done by scaling the inputs. However, when there are input constraints or in the presence of the drift term, such scaling is no longer true and hence the minimization of $\mathcal{A}$ in (2.20) as studied in Lemma 2.2 or Lemma 2.3 should be with respect to T as well. In addition, unlike the driftless case, the reachable space of an affine system with drift or constrained inputs is somehow related to the terminal time T. For example, the unicycle with unit linear velocity can only reach planar positions within the ball of radius T at time T. Thus we cannot simply just fix a random T prior to minimizing $\mathcal{A}$, in which case solutions may even not exist. This leads to the study of free terminal time.

Compared with the case of fixed terminal time, free terminal time in the view of maximum principle means that the Hamiltonian is identically 0 along the optimal trajectory. That information is not helpful in our case, as our analysis does not rely on the costates or Hamiltonian. Instead, while we still consider functions defined over a fixed domain $[0,1]$, the way to tackle free terminal time is to augment a new state $\tau \in \mathbb{R}$ to the system, which is the true time variable that starts from $\tau(0) = 0$ and $\tau(1) = T$ yet to be determined. There is also an additional constraint on the function $\tau(\cdot)$ that it needs to be strictly increasing, in which case the inverse function τ^{-1} exists and we can recover the control as a function of the true time from $u(\cdot)$ by $u^\dagger(t) = u(\tau^{-1}(t))$. For smooth $\tau(\cdot)$, this monotonicity constraint can be resolved by deploying our earlier technique on constrained inputs by treating the derivative of τ as another extra state, or simply by defining $\dot{\tau}(t) = a(t)^2$, $\dot{a}(t) = u_0(t)$ where u_0 is the additional input to the twice-augmented system. Note that since τ is the true time, $\frac{dx}{d\tau}$ should obey the true system dynamics (2.2) instead of $\frac{dx}{dt}$. Thus using chain rule, we have

$\dot{x} := \frac{dx}{dt} = \frac{dx}{d\tau}\frac{d\tau}{dt} = h(x)a^2 + F(x)a^2u$. In summary, denoting the augmented state

$$x' = \begin{pmatrix} x \\ \tau \\ a \end{pmatrix}, \tag{2.47}$$

we have

$$\dot{x}' = \begin{pmatrix} \dot{x} \\ \dot{\tau} \\ \dot{a} \end{pmatrix} = \underbrace{\begin{pmatrix} h(x)a^2 \\ a^2 \\ 0 \end{pmatrix}}_{h'(x')} + \underbrace{\begin{pmatrix} F(x)a & 0 \\ 0 & 0 \\ 0 & 1 \end{pmatrix}}_{F'(x')} \begin{pmatrix} au \\ u_0 \end{pmatrix}. \tag{2.48}$$

By this augmentation we have new drift term h' and new admissible control direction matrix F'. The reason we take one a out from F' and multiply it to the control u will be explained later when we discuss the total energy consumption of the planned path. In addition, by observation we see that if the inadmissible control direction matrix is constructed by

$$F_c'(x') := \begin{pmatrix} F_c(x) & 0 \\ 0 & 1 \\ 0 & 0 \end{pmatrix} \tag{2.49}$$

then $\bar{F}' = (F_c' \ F')$ is full rank if $\bar{F} = (F_c \ F)$ is full rank as we needed earlier. Because the dimension of the system (2.48) is now $n+2$, D', G', L' should all be defined accordingly. There are also some small tweaks on the boundary conditions. With indefinite boundary conditions (2.45), (2.46) as mentioned earlier, we also have a new boundary condition on τ because true time also starts at 0:

$$\tau(0, s) = 0 \quad \forall s \geq 0. \tag{2.50}$$

We do not have any constraints on $\tau(1, s), a(0, s), a(1, s)$; nevertheless, according to the

previous discussion on indefinite boundary conditions we should have some other constraints

$$\begin{aligned}
&\frac{\partial L}{\partial \tau_t}(\bar{x}(1,s),\bar{x}_t(1,s),1)=0,\\
&\frac{\partial L}{\partial a_t}(\bar{x}(0,s),\bar{x}_t(0,s),0)=0,\\
&\frac{\partial L}{\partial a_t}(\bar{x}(1,s),\bar{x}_t(1,s),1)=0
\end{aligned} \tag{2.51}$$

for all $s \geq 0$. The algorithm is slightly different from the algorithm in Section 2.2.1 in this case, especially for the control extraction part. We summarize it as follows:

1. Augment the states as in (2.47). Encode system dynamics and constraints into the Riemannian metric G;

2. Pick some $T_g > 0, a_g^i, a_g^f \in \mathbb{R}$ as the initial guess for $T, a(0), a(1)$. Let $z' \in C^1([0,1] \to \mathbb{R}^{n+2})$ be an initial curve such that $z_i'(t) = x^{bc}(i,t)$ for all $(i,t) \in S_{bc}$, $z_{n+1}'(0) = 0, z_{n+1}'(1) = T_g, z_{n+2}'(0) = a_g^i, z_{n+2}'(1) = a_g^f$. Solve the AGHF (2.18) with boundary conditions (2.45), (2.46), (2.50), (2.51) and initial curve z' described above. Denote the solution by $x'(t,s)$.

3. Fix $s_{\max}$ sufficiently large. Define

$$w(t) := \bar{F}'(x(t,s_{\max}))^{-1}(x_t'(t,s_{\max}) - h'(x'(t,s_{\max})).$$

   Split w so $w^\top = (v^\top \ v_0 \ u^\top \ u_0)$ such that $v \in C^0([0,1] \to \mathbb{R}^{n-m}), u \in C^0([0,1] \to \mathbb{R}^m)$, $v_0, u_0 \in C^0([0,1] \to \mathbb{R})$. Define

$$\tilde{\tau}(s) = \int_0^s a(t)^2 dt, \tag{2.52}$$

   where

$$a(t) = \int_0^t u_0(r)dr + x_{n+2}'(0,s_{\max}) = x_{n+2}'(t,s_{\max}). \tag{2.53}$$

Then $T = \tilde{\tau}(1)$ is our resultant terminal time and

$$u^\dagger(t) = \frac{u(\tilde{\tau}^{-1}(t))}{a(\tilde{\tau}^{-1}(t))}$$

is our resultant control.

Output: The integrated path $\tilde{x}^\dagger$ is obtained by integrating (2.2) with the resultant control $u^\dagger(\cdot)$ and initial value $\tilde{x}^\dagger(0) = (x_1'(0, s_{\max})\ x_2'(0, s_{\max}) \cdots x_n'(0, s_{\max}))^\top$.

Theorem 2.3. *Consider the system* (2.2) *and assume the motion planning problem with indefinite boundary conditions and free terminal time is feasible. The integrated path* $\tilde{x}^\dagger(\cdot)$ *from our algorithm with properly chosen initial curve* z' *and sufficiently large* $s_{\max}$ *has the properties that for all* $(i, 0) \in S_{bc}$,

$$\tilde{x}_i^\dagger(0) = x^{bc}(i, 0) \tag{2.54}$$

and there exists $K > 0$ *such that for all* $(i, T) \in S_{bc}$,

$$|\tilde{x}_i^\dagger(T) - x^{bc}(i, T)| \leq \frac{K}{\sqrt{\lambda}}. \tag{2.55}$$

Proof. Note that the property (2.54) is directly given by the construction. The major difference between the two algorithms is in Step 3, where a time scaling is involved in the second algorithm on free terminal time. Nevertheless, if we directly feed (u, u_0) to the system (2.48) as required by the Step 4 in the first algorithm, by the results of Theorem 2.2 we again conclude the bounds of (2.26) for all $(i, T) \in S_{bc}$, where

$$\tilde{x}(t) = \tilde{x}^\dagger(0) + \int_0^t h(\tilde{x}(s))a(s)^2 + F(\tilde{x}(s))a(s)u(s)ds$$

and a as defined in (2.53). On the other hand, the integrated path is given by

$$\tilde{x}^\dagger(t) = \tilde{x}^\dagger(0) + \int_0^t h(\tilde{x}^\dagger(r)) + F(\tilde{x}^\dagger(s))u^\dagger(r)dr = \tilde{x}^\dagger(0) + \int_0^t h(\tilde{x}^\dagger(r)) + \frac{F(\tilde{x}^\dagger(r))}{a(\tilde{\tau}^{-1}(r))}u(\tilde{\tau}^{-1}(r))dr.$$

Setting $\tilde{\tau}^{-1}(r) = s$ and noting that $\frac{dr}{ds} = \frac{d\tilde{\tau}(s)}{ds} = a(s)^2$, we see that

$$\begin{aligned}\tilde{x}^\dagger(t) &= \tilde{x}^\dagger(0) + \int_0^{\tilde{\tau}^{-1}(t)} \left(h(\tilde{x}^\dagger(\tilde{\tau}(s))) + \frac{F(\tilde{x}^\dagger(\tilde{\tau}(s)))}{a(s)} u(s) \right) a(s)^2 ds \\ &= \tilde{x}^\dagger(0) + \int_0^{\tilde{\tau}^{-1}(t)} h(\tilde{x}^\dagger(\tilde{\tau}(s)))a(s)^2 + F(\tilde{x}^\dagger(\tilde{\tau}(s)))a(s)u(s) ds.\end{aligned}$$

which implies that $\tilde{x}^\dagger(t) = \tilde{x}(\tilde{\tau}^{-1}(t))$. In particular, $\tilde{x}^\dagger(T) = \tilde{x}(1)$ and we conclude (2.55) from (2.26). □

Next we provide a heuristic argument that our resultant input is "economical". Plugging $x'(t, s_{\max})$ into L (2.22), we have

$$L(x'(t, s_{\max}), x'_t(t, s_{\max})) = w(t)^\top D w(t) = \lambda |v(t)|^2 + \lambda v_0(t)^2 + |u(t)|^2 + u_0(t)^2 \geq |u(t)|^2.$$

Thanks to Lemma 2.3 we see that the action functional $\mathcal{A} = \int_0^1 L dt$ is minimized when solving the AGHF; in other words, the L^2-norm of $u(\cdot)$ is relatively small from our algorithm. On the other hand, again by the change of variable via $\tilde{\tau}^{-1}(r) = s$, this L^2-norm is exactly the energy of the actual input:

$$E = \int_0^T |u^\dagger(r)|^2 dr = \int_0^T \frac{|u(\tilde{\tau}^{-1}(r))|^2}{a(\tilde{\tau}^{-1}(r))^2} dr = \int_0^1 |u(s)|^2 ds.$$

This in fact is not a coincidence; it is only achieved when we design the $F'(x')$ in that particular form as in (2.48) where we have shifted one a to the input. To summarize: Not only does our algorithm find an approximation to an admissible path which satisfies the indefinite boundary conditions with free terminal time, but the energy consumption of the planned path is also relatively small.

Case study: unicycle with unit linear velocity We revisit our example of unicycle with unit linear velocity (2.31). We are again interested in the parallel parking problem, but this time we set the terminal time T free. We would also like to ensure that the energy cost $E = \int_0^T u(\tau)^2 d\tau$ is small. As discussed earlier, the first step in the algorithm suggest a state

augmentation and we have

$$h'(x') = \begin{pmatrix} a^2\cos\theta \\ a^2\sin\theta \\ 0 \\ a^2 \\ 0 \end{pmatrix}, \quad \bar{F}'(x') = \begin{pmatrix} 1 & 0 & 0 & 0 & 0 \\ 0 & 1 & 0 & 0 & 0 \\ 0 & 0 & 0 & a & 0 \\ 0 & 0 & 1 & 0 & 0 \\ 0 & 0 & 0 & 0 & 1 \end{pmatrix}.$$

We pick $\lambda = 1000, T_g = 10, a_g^i = a_g^f = 1$, and let z' be the line segment connecting the boundary conditions for our algorithm. We use $s_{\max} = 1$ to extract the controls. The extracted control is shown as the black curve in Fig. 2.18a and the integrated path is shown as the black curve in Fig. 2.18b. In addition, it turns out that by our algorithm $T = 1.4072$ and for this particular input it is computed that $E = 20.5487$, shown as the red star in Fig. 2.18c. As a comparison, consider another heuristic admissible path for the unicycle system (2.31) which consists of two semicircles, as shown by the curve labelled "Heuristic" in Fig. 2.18b. Such a path has a total length of $\frac{\pi}{2}$, and hence the total traveling time is also $\frac{\pi}{2}$ because of unit velocity. By observation we see that u, or the turning rate, is equal to the curvature of the path and thus $u(t) = 4$ for the first half and $u(t) = -4$ for the second half. As a result, the total energy cost in this case is $4^2 \times \frac{\pi}{2} \approx 25.13$. Both the total time and energy costs of this heuristic path are larger than what we derived from our proposed algorithm. On the other hand, if we adopt our previous motion planning algorithm with fixed terminal time T, we are able to get a family of results for different prescribed values of T, illustrated in Fig. 2.18. Interestingly enough, this motion planning problem of constant linear velocity unicycle has no global minimal energy solution, as seen in the Fig. 2.18c where the energy plot with respect to T approaches 0 as T increases. Nevertheless, there is a local minimal energy solution, which is approximately given by our free terminal time motion planning algorithm.

Now we remark on finding the true optimal solution to this motion planning problem via

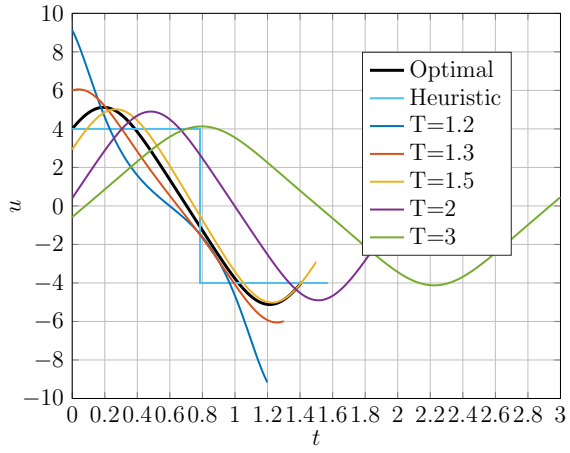

(a) u vs. t

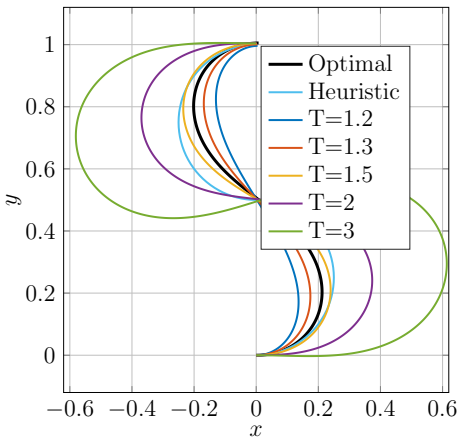

(b) Trajectory in xy-plane

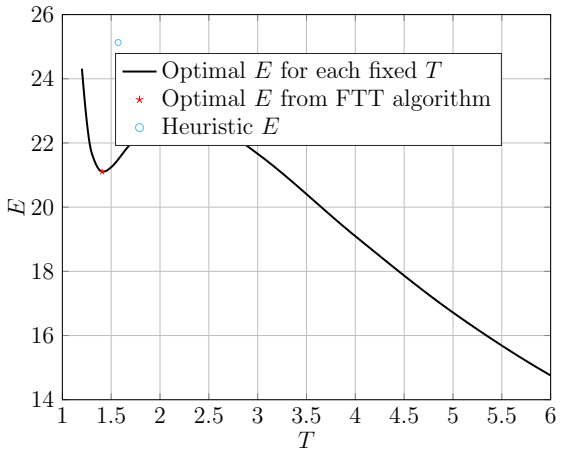

(c) E vs. T

Figure 2.18: Parallel parking of a unicycle with constant linear velocity and minimal energy cost.

maximum principle. We start by formulating the Hamiltonian as

$$H = p^\top f - L = p_1 \cos(\theta) + p_2 \sin(\theta) + p_3 u - u^2. \tag{2.56}$$

By maximum principle we have that $u = \frac{p_3}{2}$, p_1, p_2 are constants and $\dot{p}_3 = p_1 \sin(\theta) - p_2 \cos(\theta)$. In addition, since the problem has a free terminal time, we have $H \equiv 0$. While we still have boundary conditions on the states x, y, θ, we do not know the value of p_1, p_2, and neither are there are any boundary conditions for p_3. On the other hand, if we take the second derivative of θ, we see that

$$\ddot{\theta} = \frac{du}{d\theta} = \frac{1}{2}\frac{dp_3}{dt} = \frac{p_1}{2}\sin(\theta) - \frac{p_2}{2}\cos(\theta), \tag{2.57}$$

which is a second-order nonlinear ODE. While there are no general solutions for nonlinear ODEs with indefinite boundary conditions and free terminal time, the general solution of (2.57) can be expressed in terms of Jacobi elliptic functions [57], which requires quite a lot of work. It can also be seen that finding the exact optimal path via maximum principle is difficult to generalize for more complicated systems or in higher dimensions. On the contrary, in exchange for the true minimal cost and an exact expression of the optimal solution, our algorithm is quite systematic and usually gives a good approximate solution within reasonable computation time.

2.4 Discussion and future work

In this work we have proposed an innovative motion planning algorithm for dynamical systems with drift that are affine in controls. We have formulated an AGHF equation, obeying which the initial curve is deformed to a curve with locally minimal "length". Controls are extracted from this minimizer and the integrated path is derived by feeding the system with the extracted control, which gives us a solution to the motion planning problem. It was then proven that when the initial sketch is in a neighborhood of an admissible path and when the penalty is sufficiently large, the system can reach arbitrarily close to its target by following

the integrated path.

We then extended the algorithm to encode different kinds of constraints and variants. We have first shown that by applying some algebraic tricks, holonomic constraints are similar to non-holonomic constraints and they can be directly handled by our algorithm. Next by using barrier functions, state constraints can encoded to our Riemannian metric. Input constraints can be processed similar to state constraints via state augmentation. We have also shown that by modifying the boundary conditions for our AGHF, our algorithm can also handle motion planning problems when the initial state and final state are not fixed points but belong to some subsets on the manifold. Thanks to the techniques for dealing with indefinite boundary conditions, we could also solve motion planning problems with free terminal time.

Our algorithm is practiced on lots of canonical systems in different scenarios, including but not limited to non-holonomic integrators, kinematic unicycles, dynamic unicycles, cars, etc. The simulation results of all those examples have verified the feasibility of our algorithm and shown great potential of its future development.

Future work will include (1) testing our algorithm on more practical systems, (2) optimizing the algorithm structure as well as the numerical toolbox we used for solving the PDEs in order to shorten the computation time, and (3) enhancing our algorithm so that it can also handle switching of system models.

CHAPTER 3

STABILITY OF NONLINEAR SYSTEMS VIA NON-MONOTONIC LYAPUNOV FUNCTIONS

3.1 Non-monotonic Lyapunov functions

3.1.1 Literature review

For general nonlinear systems, asymptotic stability is typically shown through Lyapunov's direct method (see, e.g., [19]), which involves constructing a positive definite Lyapunov function V whose time derivative $\dot{V}$ along solutions is negative definite. Because of the opposite sign definite constraints and the fact that $\dot{V}$ is coupled to V via the system's dynamics, although the classical Lyapunov results are theoretically elegant, they have many difficulties in the application. In addition, even if this property holds for the nominal system, stability is not guaranteed when there is a perturbation because V might not necessarily decrease along solutions of the perturbed system. One natural way to address this issue is to find another Lyapunov function W for this perturbed system by perturbing V accordingly; this is known as the Zubov method [58] for which there are many recent results such as [59],[60]. On the other hand, if it is desirable to use the same candidate Lyapunov function V, one may hope to establish stability, at least in some weaker sense, if V does not increase too often or too much along perturbed solutions. This leads to the study of non-monotonic Lyapunov functions, which means the time derivative of the Lyapunov function might be positive from time to time when it is evaluated along a solution of the system. In this case there is still a chance that the system is asymptotically stable as long as V converges to 0 asymptotically with bounded overshoots.

Besides the above applications to perturbed systems, non-monotonic Lyapunov functions can be useful when computational complexity is the main difficulty. While it is straightfor-

ward to compute the derivative of an arbitrary Lyapunov function along solutions, it might be quite challenging to analytically check the sign of this derivative either for all states, or just for a region of interest. For example, in the case when both the differential equation and the Lyapunov function are polynomials of high degree, the derivative is also a polynomial and verifying stability reduces to checking whether a polynomial is negative definite. This problem is computationally hard, as it is related to Hilbert's 17th problem [61] and is an important subject of current research (see, e.g., [62],[63]). Following existing techniques, we may be able to verify that the time derivative of V is negative only in a proper subset of the region of interest, while not in the entire region. This demonstrates the need for tools that would let one conclude stability if V is only a non-monotonic function when it is evaluated along some solutions of the system.

When a general candidate Lyapunov function is constructed, the sign of its derivative along solutions can also be checked by techniques based on random sampling [64] instead of deterministic methods. This approach only requires one to verify that the derivative is negative at a sequence of states picked randomly inside the region. One can use the Chernoff bound (see, e.g., [64],[65]) to characterize the number of such sample points needed to obtain a reliable upper bound on the relative measure of points in the region of interest for which the desired inequality can possibly fail. Hence the problem is again converted into finding an non-monotonic Lyapunov function. See also [66] for some related recent work.

The idea for the study of non-monotonic V is behind the simple idea that "if over any long enough period V decreases more than it increases, then V is asymptotically decreasing". There are basically 3 different approaches to show stability via non-monotonic Lyapunov function, including the following:

- Consider the "finite step Lyapunov" function. In other words, we do not enforce V to decrease all the time along any solutions of the system; we only need the existence of a finite time T such that the change of V over time T to be negative for any solution that does not start from the equilibrium. This is studied in [20].

- Require some higher order time derivatives of V to be negative. As an illustration, if whenever $\dot{V} > 0$, we also know that "$\ddot{V}$" – the rate of the change of $\dot{V}$ – is negative,

then $\dot{V}$ will become negative again soon enough. This idea was summarized in the early paper [67] by Butz, where a linear combination of higher order derivatives of V up to order 3 was studied. The collection of higher order derivatives is also called vector Lyapunov function in [68],[69], which can be used to analyze the stability of a system. A similar idea of higher order derivatives of V for analyzing discrete time systems is studied in [21] and then this technique is practiced for fuzzy systems in [70]. Much later after Butz's work, in [71] a general result was concluded for time-varying systems that under some mild assumptions, as long as there exists a negative definite linear combination of the higher order derivatives of V and the coefficients form a Hurwitz polynomial, then the system is globally uniformly asymptotically stable. The result is derived by repeatedly applying the comparison principle for first-order differential relations. In [23] the same authors argued that in fact Hurwitzness is not needed; as long as the coefficients are non-negative, the same results can be concluded.

- Another approach is to bound the region Ω in the state space where V does not decrease fast enough, as studied in [72], [27] via the analysis of *almost Lyapunov function*. States where $\dot{V} > 0$ are inside Ω and because Ω is "small", the trajectories of solutions have to pass through Ω and the amount V can increase will be compensated by the later decrease. As a result, V is decreasing asymptotically and the system is also shown to be GAS. Compared with the method via finite-step Lyapunov functions, while the idea of "almost Lyapunov" functions is similar in spirit, there is a conceptual difference. The finite-step Lyapunov function approach requires temporal information from the system because the difference between the values of Lyapunov functions over a finite time interval needs to be computed. Thus, the solutions would need to be traced in order to compute the difference. This is a cumbersome and sometimes impossible, in practice, task for a general nonlinear system. By contrast, the "almost Lyapunov" functions approach relies only on the spatial information of the system so that only some bounds on the vector field of the system and the Lyapunov function are needed.

Interestingly enough, all the aforementioned literature only deals with systems without inputs. This is because there are some technical difficulties when generalizing those

approaches to systems with inputs, which will be discussed and handled later in the subsequent sections. In this chapter, we will start with the study of how "almost Lyapunov" function can be used to show stability of an autonomous system, and we will then extend the approaches, via higher order derivatives of Lyapunov functions and "almost Lyapunov" functions, to systems with inputs.

3.1.2 Preliminaries

We first adopt some definition of comparison functions from [19]. A function $\gamma(s) : \mathbb{R}_{\geq 0} \to \mathbb{R}_{\geq 0}$ is said to be positive definite if it is continuous, $\gamma(0) = 0$ and $\gamma(s) > 0$ for all $s > 0$. A function $\gamma(s) : \mathbb{R}_{\geq 0} \to \mathbb{R}_{\geq 0}$ is said to be a class $\mathcal{K}$ function if it is positive definite and strictly increasing. $\gamma(s) : \mathbb{R}_{\geq 0} \to \mathbb{R}_{\geq 0}$ is said to be a class $\mathcal{K}_\infty$ function if $\gamma \in \mathcal{K}$ and $\lim_{s\to\infty} \gamma(s) = \infty$. A function $\beta(s,t) : \mathbb{R}_{\geq 0} \times \mathbb{R}_{\geq 0} \to \mathbb{R}_{\geq 0}$ is said to be a class $\beta \in \mathcal{KL}$ function if for each fixed t, $\beta(\cdot, t) \in \mathcal{K}$ and for each fixed s, $\beta(s, \cdot)$ is decreasing and $\lim_{t\to\infty} \beta(s,t) = 0$.

A function $f : A \to B$ where A, B are two metric spaces is said to be locally Lipschitz if for each compact set $S \subset A$, there exists $L \geq 0$ such that for any $x, y \in S$

$$|f(x) - f(y) \leq L|x - y|.$$

The function is said to be globally Lipschitz if L is independent of the choice of S. Note local Lipschitzness implies continuity and Lipschitzness is a weaker property than differentiability. However, according to Rademacher's theorem, Lipschitzness implies differentiability almost everywhere.

Finally, let $B^n_\gamma(x)$ be the closed ball whose center is at x in $\mathbb{R}^n$ with radius γ. Also define the function $\mathrm{vol}(\cdot)$ to be the standard volume function induced by the Euclidean metric. Recall that a general expression for the volume of a n-dimensional ball of radius γ is:

$$\mathrm{vol}(B^n_\gamma) = \frac{\pi^{\frac{n}{2}}}{\Gamma(\frac{n}{2}+1)}\gamma^n =: \chi(n)\gamma^n, \tag{3.1}$$

where Γ is the standard gamma function [73, Ch. 4.11]. Further notation will be introduced in the context.

Stability definitions We first consider an autonomous system which has no inputs:

$$\dot{x} = f(x), \quad x \in \mathbb{R}^n, \tag{3.2}$$

where $f : \mathbb{R}^n \to \mathbb{R}^n$ is a locally Lipschitz function. The system (3.2) has an equilibrium at origin by assuming $f(0) = 0$. For initial state x_0 at time 0, denote the solution to the differential equation (3.2) at time t by $x(t; x_0)$. When the initial state is clear in the context, it is also abbreviated by $x(t)$. The origin is *globally asymptotically stable* (GAS) for the system[1] if there exists $\beta \in \mathcal{KL}$ such that for any $x_0 \in \mathbb{R}^n, t \geq 0$,

$$|x(t; x_0)| \leq \beta(|x_0|, t). \tag{3.3}$$

GAS can also be shown via a Lyapunov function. Let $V(x) : \mathbb{R}^n \to \mathbb{R}_{\geq 0}$ be a C^1 function. Denote the gradient of V by V_x. It is said to be a Lyapunov function for the system (3.2) if there exists $\alpha_1, \alpha_2 \in \mathcal{K}_\infty$ such that

$$\alpha_1(|x|) \leq V(x) \leq \alpha_2(|x|) \quad \forall x \in \mathbb{R}^n \tag{3.4}$$

and

$$\dot{V}(x) := V_x(x) \cdot f(x) < 0 \quad \forall x \neq 0. \tag{3.5}$$

The system (3.2) is GAS if and only if such a Lyapunov function exists [19, Ch. 4]. A stronger version of Lyapunov function is when V decays at a certain positive rate $a > 0$:

$$\dot{V}(x) < -aV(x) \quad \forall x \neq 0. \tag{3.6}$$

We then consider a time-varying system with inputs

$$\dot{x} = f(t, x, u), \tag{3.7}$$

[1]Since we will always assume the origin to be the only equilibrium of the system, in the later work we will say "the system is GAS" while not explicitly mentioning that the stability is with respect to the origin. This convention also applies to the other stability notations.

where $f : \mathbb{R}_{\geq 0} \times \mathbb{R}^n \times U \to \mathbb{R}^n$ is continuous in t and locally Lipschitz in x and u. $U \subseteq \mathbb{R}^m$ is the input value set and the input function $u(\cdot) \in L^\infty_{\text{loc}}(\mathbb{R}_{\geq 0} \to U) =: \mathcal{M}_U$; that is, $u(\cdot)$ is a locally essentially bounded function. For a specific initial condition x_0 at time t_0 and input u, denote the solution state of (3.7) at time t by $x(t; t_0, x_0, u)$.

The system (3.7) is *globally uniformly asymptotically stable* (GUAS) if there exists $\beta \in \mathcal{KL}$ such that for all $x_0 \in \mathbb{R}, u \in \mathcal{M}_U$ and $t \geq t_0$,

$$|x(t; t_0, x_0, u)| \leq \beta(|x_0|, t - t_0). \tag{3.8}$$

Just like the autonomous case mentioned earlier, GUAS can also be shown via a *time-varying* Lyapunov function. Let $V(t, x) : \mathbb{R} \times \mathbb{R}^n \to \mathbb{R}_{\geq 0}$ be a C^1 function. It is said to be a Lyapunov function for the system (3.7) if there exists $\alpha_1, \alpha_2 \in \mathcal{K}_\infty$ such that

$$\alpha_1(|x|) \leq V(t, x) \leq \alpha_2(|x|) \quad \forall t \in \mathbb{R}, x \in \mathbb{R}^n \tag{3.9}$$

and there exists a positive definite function $\psi(s) : \mathbb{R}_{\geq 0} \to \mathbb{R}_{\geq 0}$ such that

$$\dot{V}(x) := V_t(t, x) + V_x(t, x) \cdot f(t, x, u) \leq \psi(|x|) \quad \forall t \in \mathbb{R}, x \in \mathbb{R}^n, u \in U. \tag{3.10}$$

The system (3.7) is GUAS if and only if such a Lyapunov function exists. Note that the "uniformity" in GUAS is with respect to time. If the system is time-invariant and the input u is fixed, then (3.8), (3.9) and (3.10) reduce to (3.3), (3.4) and (3.5), respectively.

It is also observed by (3.8) that GUAS is a very strong stability property in the sense that the input has no effect on the asymptotic behavior of the solutions; they will converge to the origin anyways. A more practical stability property is *input-to-state stable* (ISS), introduced by Prof. Eduardo Sontag in [74]. A system (3.7) is said to be ISS if there exist $\gamma \in \mathcal{K}_\infty, \beta \in \mathcal{KL}$ such that for all $x_0 \in \mathbb{R}, u \in \mathcal{M}_U$ and $t \geq t_0$,

$$|x(t; t_0, x_0, u)| \leq \beta(|x_0|, t - t_0) + \gamma(\operatorname*{ess\,sup}_{\tau \in [t_0, t]} |u(\tau)|). \tag{3.11}$$

ISS and GUAS are connected via auxiliary system as discussed in the celebrated work

[29]:

Lemma 3.1. *The system* (3.7) *is ISS if and only if its auxiliary system*

$$\dot{x} = f(t, x, \rho(|x|)d) =: f'(t, x, d), \quad |d| \leq 1 \tag{3.12}$$

is GUAS for some $\rho \in \mathcal{K}_\infty$.

From the early discussion, we also conclude that ISS can be shown via a Lyapunov function, which in this case is called an ISS Lyapunov function, such that (3.9) holds and there exists a positive definite function $\psi(s) : \mathbb{R}_{\geq 0} \to \mathbb{R}_{\geq 0}$, $\rho \in \mathcal{K}_\infty$ such that

$$V_t(t, x) + V_x(t, x) \cdot f(t, x, u) \leq \psi(|x|) \quad \forall t \in \mathbb{R}, x \in \mathbb{R}^n, |u| \leq \rho(|x|). \tag{3.13}$$

An extended work on Lemma 3.1 is studied in Chapter 4, where this lemma is also proven to be true in the framework of switched systems.

3.2 Using almost Lyapunov function to show stability of autonomous systems

In this section we discuss how "almost Lyapunov" function techniques can be used to show stability of an autonomous system. There is not much work related to this topic of "almost Lyapunov" functions. We start with giving some results from the work [72],[24] and [27].

3.2.1 Local results

Let the region of interest be of the following form:

$$D := \{x \in \mathbb{R}^n : c_1 \leq V(x) \leq c_2\}, \quad c_2 > c_1 > 0. \tag{3.14}$$

In addition we assume D to be compact.[2] While we only care about stability in D and the property (3.6) does not hold for the entire region of interest D, we set

$$\Omega := \{x \in D : \dot{V}(x) \geq -aV(x)\} \tag{3.15}$$

and when the measure of Ω is "small", we informally say this V is an almost Lyapunov function for the system (3.2) because now

$$\dot{V}(x) < -aV(x) \quad \forall x \in D \backslash \Omega.$$

Note that the solution trajectory passing through Ω does not necessarily imply growth of V; it is only in the subset $\{x \in \Omega : \dot{V}(x) > 0\}$ that growth of V occurs.

Since f is a Lipschitz function and D is compact, we can define the following bounds:

$$\bar{L}_0 := \max_{x \in D} |f(x)|, \tag{3.16}$$

$$\underline{L}_0 := \min_{x \in D} |f(x)|, \tag{3.17}$$

and let L_1 be the Lipschitz constant of f over D:

$$|f(x_1) - f(x_2)| \leq L_1 |x_1 - x_2| \quad \forall x_1, x_2 \in D. \tag{3.18}$$

In addition, since V is assumed to be C^1 and has locally Lipschitz gradient, we also define some bounds on V_x:

$$M_1 := \max_{x \in D} |V_x(x)|, \tag{3.19}$$

and let M_2 be the Lipschitz constant of V_x over D:

$$|V_x(x_1) - V_x(x_2)| \leq M_2 |x_1 - x_2| \quad \forall x_1, x_2 \in D. \tag{3.20}$$

[2]This is true when V is radially unbounded. Otherwise the results of our theorem are still applicable if the initial state of the system is inside a compact connected component of D. In this case we take this compact connected component as the region of interest D.

For $\eta \in [0,1]$, define

$$\Omega_\eta := \{x \in D : \dot{V}(x) \geq -\eta a V(x)\}. \tag{3.21}$$

By this definition, Ω_1 is the same as Ω in (3.15) and $\Omega_{\eta_1} \subseteq \Omega_{\eta_2}$ if $\eta_1 \leq \eta_2$.

We first discuss the case when $c_1 = 0$ in the definition (3.14); that is, D is some sub-level set of V. We can achieve some simple results in this case regarding those bounds from Section 3.1.2:

Lemma 3.2. *For any $x_1, x_2 \in D$,*

$$|V(x_1) - V(x_2)| \leq M_1 |x_1 - x_2|.$$

Proof. If the line segment between x_1, x_2 entirely lies in D, by the mean value theorem there exists x_3 on the segment such that $V(x_2) = V(x_1) + V_x(x_3) \cdot (x_2 - x_1)$. Now by (3.19),

$$|V(x_1) - V(x_2)| = |V_x(x_3) \cdot (x_1 - x_2)| \leq |V_x(x_3)||x_1 - x_2| \leq M_1 |x_1 - x_2|.$$

In the case when the line segment is partially outside of D, let us say that $y_1, y_2 \in \partial D$ are two points on the segment connecting x_1, x_2 such that the line segment between y_1, y_2 is outside D. Since y_1, y_2 are on the boundary of D, the V value must be either c_1 or c_2 at these two points. If $V(y_1) \neq V(y_2)$, say $V(y_1) = c_1$ and $V(y_2) = c_2$, then $V(x) \leq c_1$ or $V(x) \geq c_2$ for all x on the line segment from y_1 to y_2. This cannot happen since V is a continuous function. Therefore $V(y_1) = V(y_2)$. Hence using triangle inequality,

$$\begin{aligned} |V(x_1) - V(x_2)| &= |(V(x_1) - V(y_1)) + (V(y_2) - V(x_2))| \\ &\leq |V(x_1) - V(y_1)| + |V(y_2) - V(x_2)| \\ &\leq M_1 |x_1 - y_1| + M_1 |y_2 - x_2| \\ &\leq M_1 |x_1 - x_2|. \end{aligned}$$

The second to last inequality follows from the fact that the two segments x_1 to y_1 and x_2 to y_2 are contained in D so we can apply our earlier result. The last inequality is simply the fact that the sum of the lengths of the two segments is no greater than the total distance

between x_1 and x_2. In the case when there are multiple segments between x_1 and x_2 that are outside of D, repeating the above analysis on each interval, we still get the same result. $\square$

Lemma 3.3. *For any $x_1, x_2 \in D$,*

$$|\dot{V}(x_1) - \dot{V}(x_2)| \leq \alpha |x_1 - x_2|, \tag{3.22}$$

where $\alpha := M_1 L_1 + M_2 \bar{L}_0$.

Proof. Estimate

$$\begin{aligned}
|\dot{V}(x_1) - \dot{V}(x_2)| &= |V_x(x_1) f(x_1) - V_x(x_2) f(x_2)| \\
&\leq |V_x(x_1)||f(x_1) - f(x_2)| + |f(x_2)||V_x(x_1) - V_x(x_2)| \\
&\leq M_1 |f(x_1) - f(x_2)| + \bar{L}_0 |V_x(x_1) - V_x(x_2)| \\
&\leq M_1 L_1 |x_1 - x_2| + \bar{L}_0 M_2 |x_1 - x_2| \\
&= \alpha |x_1 - x_2|.
\end{aligned}$$

Note that we have used the definitions of M_1 from (3.19) and $\bar{L}_0$ from (3.16) in the second to last inequality and the two Lipschitz constants L_1, M_2 from (3.18),(3.20) in the last inequality.

$\square$

Lemma 3.4. *If $x \in \Omega_\eta$, then $B^n(x, \gamma_\eta V(x)) \subseteq \Omega_1$, where*

$$\gamma_\eta := \frac{(1-\eta)a}{\alpha + a M_1} \tag{3.23}$$

with α defined in Lemma 3.3 and

$$B^n(x, r) := \{y \in D : |x - y| \leq r\}.$$

Proof. Let $x \in \Omega_\eta, y \in D$. By Lemma 3.2, $V(y) \geq V(x) - M_1|x-y|$. Therefore,

$$\begin{aligned}
\dot{V}(y) + aV(y) &\geq \dot{V}(x) - \alpha|x-y| + aV(y) \\
&\geq -\eta a V(x) - \alpha|x-y| + aV(y) \\
&\geq -\eta a V(x) - \alpha|x-y| + aV(x) - aM_1|x-y| \\
&= (1-\eta)aV(x) - (\alpha + aM_1)|x-y|.
\end{aligned}$$

Hence when $|x-y| \leq \gamma_\eta V(x)$, $\dot{V}(y) \geq aV(y)$, implying $y \in \Omega_1$ and the lemma is proven. □

Consider the extreme situation when $\eta = 0$. As discussed earlier, a necessary condition for the system (3.2) to be unstable is $\Omega_0 \neq \emptyset$. Lemma 3.4 suggests that in this case $B^n\left(x, \frac{aV(x)}{\alpha + aM_1}\right) \subseteq \Omega_1$ for any $x \in \Omega_0$. In other words,

Proposition 3.1. *If $B^n\left(x, \frac{aV(x)}{\alpha + aM_1}\right) \not\subseteq \Omega$ for any $x \in \Omega$, then the system (3.2) is asymptotically stable in D.*

Here "asymptotically stable in D" means every solution that starts at $x(0) \in D$ will be bounded in the sub-level set $x \in D : V(x) \leq V(x(0))$ and it will eventually converge to the origin.

Proposition 3.1 is a trivial result since its hypothesis suggests that $\Omega_0 = \emptyset$. We would hope to establish a result that tolerates a larger Ω so that Ω_0 might be non-empty. Following is a such result:

Theorem 3.1. *[72] Let $\rho : (0, +\infty) \to (0, +\infty)$ be the relation such that*

$$\text{vol}(B^n(\cdot, \rho(\epsilon)) = \epsilon,$$

where vol *is the standard volume function. Consider the system (3.2) with a locally Lipschitz right-hand side f, and a function V which is positive definite and $\mathcal{C}^1$ with locally Lipschitz gradient. Let the region D be defined by $D := \{x \in \mathbb{R}^n : V(x) \leq c\}$ for some $c > 0$ and assume that it is compact. Assume that (3.15) holds. Then there exist a constant $\bar{\epsilon} > 0$ and a continuous, strictly increasing function $\bar{R}$ on $[0, \bar{\epsilon}]$ with $\bar{R}(0) = 0$ such that for every*

$\epsilon \in (0, \bar{\epsilon})$, *if* $\mathrm{vol}(\Omega) < \epsilon$, *then for every initial condition* $x_0 \in D$ *with*

$$V(x_0) < c - 2M_1\rho(\epsilon),$$

where M_1 *is defined by* (3.19)*, the corresponding solution* $x(\cdot)$ *of* (3.2) *with* $x(0) = x_0$ *has the following properties:*

1. $V(x(t)) \leq V(x_0) + 2M_1\rho(\epsilon)$ *for all* $t \geq 0$ *(and hence* $x(t) \in D$ *for all* $t \geq 0$*).*
2. $V(x(T)) \leq \bar{R}(\epsilon)$ *for some* $T \geq 0$*.*
3. $V(x(t)) \leq \bar{R}(\epsilon) + 2M_1\rho(\epsilon)$ *for all* $t \geq T$*.*

The result is similar to the next Theorem 3.2 so it will be discussed later. However, compared with Proposition 3.1, Theorem 3.1 is more abstract and the conclusion is weaker than asymptotic stability. However, there is a chance that the almost Lyapunov function assumption is weaker, in the sense that it allows larger Ω. To better understand this theorem, a sketch of the proof is provided here. For any solution $x(\cdot)$ that starts from initial state $x_0 \in D$, the hypothesis of this theorem guarantees that there exists $y_0 \in D\backslash\Omega$ so that $|x_0 - y_0| \leq \rho(\epsilon)$. Consider the other solution $y(\cdot)$ that starts from y_0. The distance between $x(t)$ and $y(t)$ can be evaluated by Grönwall's inequality, and hence $|V(x(t) - V(y(t))|$ can be bounded via Lemma 3.2. On the other hand, from Lemma 3.4 we see that $y(t)$ will stay in $D\backslash\Omega_0$ for some time, hence $V(y(t))$ decreases at first. Thus using triangle inequality we see that $V(x(t))$ has to decrease over a short time when $\rho(\epsilon)$ is small enough. Reset the initial time and repeat this process as the system (3.2) is time-invariant and we will achieve the result. For more details of the proof of Theorem 3.1, please refer to [72]. Note that in the special case when $\dot{V}(x) \leq -aV(x)$ for all $x \in D$ (which implies that ϵ can be any arbitrarily small positive number), Theorem 3.1 reduces to Lyapunov's classical asymptotic stability theorem.

Another observation is that although $V(x(t))$ will eventually be smaller over some positive time span, the function $V(x(t)) - V(x_0)$ is not necessary a decreasing function. Thus there might be a transient overshoot of V initially, which implies that Ω_0 is non-empty.

Nevertheless, we failed to construct a non-trivial example with $\dot{V}(x) > 0$ for some $x \in D$ while maintaining that inequality. This is left as an open question in [72]. An interesting observation is that by perturbing the system dynamics without increasing the Lipschitz constant, which is used in computing $\bar{\epsilon}$, an unstable equilibrium can be constructed away from the origin. There will be a contradiction if Theorem 3.1 is applicable to such a system because a solution starting at that unstable equilibrium will not move, contrary to what is concluded from the theorem that the solution will be attracted to a neighborhood of the origin. Therefore, we may need to impose more structures to the system in order to achieve non-trivial results. One possible way is to assume that f is "non-vanishing":

$$f(x) \neq 0 \quad \forall x \in D, \tag{3.24}$$

which clearly requires that the origin be excluded from D so we must have $c_1 > 0$. Next define

$$b := \max_{x \in D} \dot{V}(x). \tag{3.25}$$

In the non-trivial case when $\Omega_0 \neq 0$, we have $b > 0$. We further require that b is not too large by assuming $b < ac_1$. Following is the main result that we derived in [24]:

Theorem 3.2. *Consider a system (3.2) with a locally Lipschitz right-hand side f, and a function $V : \mathbb{R}^n \to [0, +\infty)$ which is positive definite and C^1 with locally Lipschitz gradient. Let the region D be defined via (3.14) with some c_1, c_2 and assume it is compact. Let $\Omega \subset D$ be a measurable set such that (3.15) holds for some $a > 0$ and let f be non-vanishing in D as defined in (3.24). Assume $b < ac_1$ where b is defined in* (3.25)*. Then there exist constants $\bar{\epsilon} > 0, g > 0, h > 0$ and for any $\epsilon \in [0, \bar{\epsilon})$ such that if $\mathrm{vol}(\Omega^*) \leq \epsilon$ for every connected component Ω^* of Ω , there exists $T_{\max}$ depending on ϵ such that for any initial condition $x_0 \in D$ with $V(x_0) < c_2 - h - g\epsilon$, the solution $x(\cdot)$ of (3.2) has the following properties:*

1. *$V(x(t)) \leq V(x_0) + g\epsilon$ for all $t \geq 0$,*
2. *$V(x(T)) \leq c_1 + h$ for some $T \leq T_{\max}$,*
3. *$V(x(t)) \leq c_1 + h + g\epsilon$ for all $t \geq T$ with the same T above.*

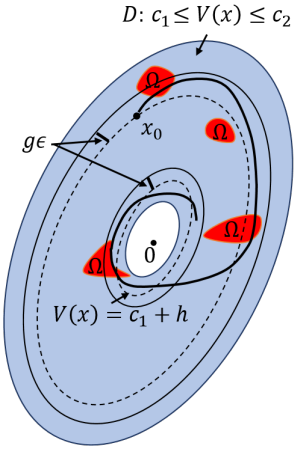

Figure 3.1: Illustration of Theorem 3.2.

Remark 3.1. *The results of Theorem 3.2 are illustrated in Fig. 3.1. The parameter h serves as a "buffer" ensuring that the solution tube is always in D, while $g\epsilon$ is a threshold for possible transient overshoot. They will be defined in* (3.30),(3.31) *respectively and $\bar{\epsilon}$ will be explicitly expressed later in the proof.*

The first statement of Theorem 3.2 says that the solution is always contained in the sub-level set $\{x : V(x) \le V(x_0) + g\epsilon\}$. The second statement says that the solution will eventually converge into the sub-level set of $\{x : V(x) \le c_1 + h\}$. The third statement implies that once the solution arrives at this smaller sub-level set at time T, it will remain inside a slightly inflated one thereafter. Later in the proof of Theorem 3.2 the reader will see that the convergence before time T is in fact exponential, in the form of

$$V(x(t)) \le e^{2\lambda(\epsilon)\frac{g\epsilon}{b}}(V(x_0) + \frac{g}{2}\epsilon)e^{-\lambda(\epsilon)t} + \frac{g}{2}\epsilon,$$

where $\lambda(\epsilon)$ is a positive, continuous and strictly decreasing function on $[0, \bar{\epsilon})$ with $\lambda(0) < a$.

The main idea of the proof is to establish that when the measure of Ω is small enough, there will be too little time for a tube around the solution to stay inside Ω so the growth of V could not be accumulated. The proof contains 4 major steps:

1. The first step is to show that when the time derivative of V is positive, the solution has to be in a connected component Ω^* and a tube around the solution is contained in Ω^*.

2. The second step is to use a non-self-overlapping condition to compute an upper bound on the time that the solution stays in Ω^* based on the volume swept out by the solution tube.

3. The next step is to find a bound on the change of V over the time estimated in the previous step. We will conclude that when the volume of Ω^* is sufficiently small, the change of V will be negative.

4. The last step generalizes previously obtained estimates to the possible scenario of repeated passage of the solution through several, or even infinitely many, connected components of Ω. By connecting segments of the solution, we argue that although there might be temporary overshoots in V, overall the solution will converge to a smaller sub-level set.

Define the normal disk of radius γ centered at x to be

$$N_\gamma(x) = \{y \in B_\gamma^n(x) : (y - x) \cdot f(x) = 0\}, \tag{3.26}$$

which is a ball $B_\gamma^{n-1}(x)$ in the hyperplane

$$\{y \in \mathbb{R}^n : (y - x) \cdot f(x) = 0\}.$$

Define

$$S_{\eta,(s,t)} = \bigcup_{\tau \in (s,t)} N_{\gamma_\eta}(x(\tau)) \tag{3.27}$$

to be the tube of radius γ_η around the solution on the time interval s to t. We will often refer to it as the *solution tube*. We will say the tube is *non-self-overlapping* over time interval (s, t) if

$$N_{\gamma_\eta}(x(\tau_1)) \cap N_{\gamma_\eta}(x(\tau_2)) = \emptyset \quad \forall \tau_1, \tau_2 \in (s, t), \tau_1 \neq \tau_2. \tag{3.28}$$

In a non-self-overlapping tube all the states are swept out only once by such $N_{\gamma_\eta}(x(\tau))$ normal disk at some $\tau \in (s, t)$. There will be more discussion of non-self-overlapping condition later.

Let

$$\mathcal{L}_s^t := \int_s^t |f(x(\tau)|d\tau$$

be the length of the solution trajectory from time s to t. Using bounds (3.16), (3.17) on f, one has

$$\underline{L}_0(t-s) \leq \mathcal{L}_s^t \leq \bar{L}_0(t-s). \tag{3.29}$$

Define

$$g := \frac{b}{\underline{L}_0 \mathrm{vol}(B_{\gamma_\eta}^{n-1})}, \tag{3.30}$$

$$h := M_1 \gamma_\eta. \tag{3.31}$$

Define a shrunk domain

$$D^* := \{x \in \mathbb{R}^n : c_1 + h \leq V(x) \leq c_2 - h\}.$$

For any initial state $x(0) = x_0 \in D$ with $V(x_0) < c_2 - g\epsilon - h$, by the standard theory of ODEs the solution can be continued either indefinitely or to the boundary of D^*. Define

$$T := \inf\{\tau \geq 0 : x(t) \notin D^*\}. \tag{3.32}$$

By this definition, $T = 0$ if $V(x_0) < c_1 + h$. T could also be infinite if the solution stays in D^* forever. Eventually in the proof we will see that T has to be finite and it is impossible for the solution to hit the outer boundary of D^* with $V(x(T)) = c_2 - h$. This T will be the one in the statement of Theorem 3.2 that we are looking for. Define the subset of the time interval when the solution stays in Ω_η as

$$X_\eta = \{\tau \in [0, T) : x(\tau) \in \Omega_\eta\}.$$

While the set X_η might have a complicated structure, the relevant part for us is the interior which must be a union of intervals. The almost Lyapunov function might increase when the solution is considered over such an interval. When the solution is considered over a subset of X_η which has empty interior, the almost Lyapunov function will be decreasing with the

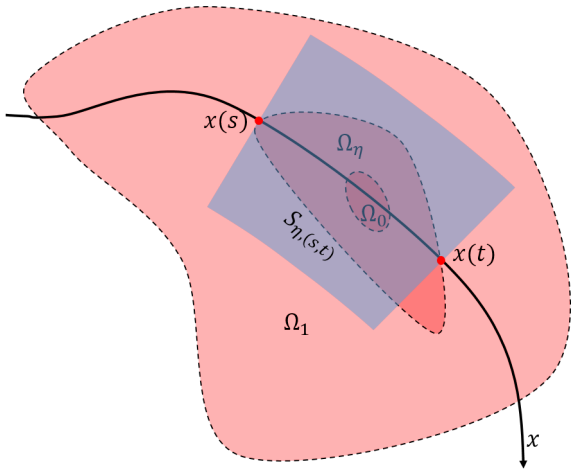

Figure 3.2: A planar example of the solution trajectory passing Ω_η.

rate a. A *maximal interval* contained in X_η is an interval in X_η which cannot be enlarged without leaving X_η. We will also refer to such intervals as *connected components* of X_η.

The sweeping tube $S_{\eta,(s,t)}$ generated over a connected component $(s,t) \subseteq X_\eta$ is illustrated in Fig. 3.2. Intuitively the volume of $S_{\eta,(s,t)}$ is the cross-section area times the trajectory length over (s,t). The next lemma proves this, under the assumption that there is no self-overlapping:

Lemma 3.5. *If the solution is non-self-overlapping over time interval (s,t), then*

$$\mathrm{vol}(S_{\eta,(s,t)}) = \mathrm{vol}(B^{n-1}_{\gamma_\eta})\mathcal{L}^t_s. \tag{3.33}$$

The proof of this lemma is a direct application of results from [73, Chapter 4.10],[75]. The conditions for non-self-overlapping will be discussed later.

Remark 3.2. *The formula in [75] yields a signed volume with multiplicity (which is a result of negative self-overlapping); nevertheless, the non-self-overlapping condition we have ensures that there are no negative or multiple counts of the integrated volume and the result is indeed the absolute volume that we want as a lower bound.*

Note that when $x \in D^*$ and $y \in B^n_{\gamma_\eta}(x)$, we have $|V(y)-V(x)| \le M_1|y-x| \le M_1\gamma_\eta = h$. Thus $c_1 \le V(y) \le c_2$, which implies $y \in D$. This means whenever the solution $x(\tau) \in D^*$

for all $\tau \in (s,t)$, $S_{\eta,(s,t)} \subseteq D$. Combining this result with Lemma 3.4, we have the following corollary:

Corollary 3.1. *$S_{\eta,(s,t)} \subseteq \Omega_1$ for all $(s,t) \subset X_\eta$.*

This can also be viewed in Fig. 3.2 that the sweeping tube is a subset of "bad region" Ω_1. Now if we utilize the fact that $\mathrm{vol}(\Omega_1) \leq \epsilon$ and apply the formula (3.33) here with the assumption that the solution is non-self-overlapping, we have

$$\begin{aligned} \epsilon \geq \mathrm{vol}(\Omega_1) \geq \mathrm{vol}(S_{\eta,(s,t)}) &= \mathrm{vol}(B^{n-1}_{\gamma_\eta})\mathcal{L}^t_s \\ &\geq \mathrm{vol}(B^{n-1}_{\gamma_\eta})\underline{L}_0(t-s) = \frac{b}{g}(t-s). \end{aligned} \tag{3.34}$$

Corollary 3.2. *Let $(s,t) \subset X_\eta$ and assume the solution over this time interval is non-self-overlapping. Then the length of the time interval must satisfy*

$$t - s \leq \frac{g\epsilon}{b}.$$

On non-self-overlapping condition The following proposition gives a geometric criterion of non-self-overlapping.

Proposition 3.2. *Consider a tube of radius ρ_0 around a space curve $\gamma(\tau)$ whose radius of curvature is bounded from below by ρ. If $\rho > \rho_0$ and if the length $\mathcal{L}$ of $\gamma(\tau)$ is bounded:*

$$\mathcal{L} < 2\rho\left(\pi - \sin^{-1}(\frac{\rho_0}{\rho})\right), \tag{3.35}$$

then the tube is non-self-overlapping.

The value on the right-hand side of (3.35) is the curve length of a circular arc with radius of curvature ρ and chord distance of $2\rho_0$ between end points. The proof of this proposition makes use of two classical results of Fenchel's theorem and Schur's comparison theorem (see [76]). Readers are referred to [27] for the proof.

At this point, the solution of our system can be viewed as a space curve $x = \gamma(s)$ in $\mathbb{R}^n$.

Thus we have the curvature

$$k(s) = \frac{[\gamma', \gamma'']}{|\gamma'|^3}(s),$$

where $[*, *]$ is a standard area form. This formula is a simple consequence of the definition of centripetal acceleration $a = v^2 k$. Indeed, $[\gamma', \gamma''] = |\gamma'||\gamma''| \sin\alpha$ where $\sin\alpha$ is the angle between the two vectors γ', γ''. When $[\gamma', \gamma'']$ is divided by $|\gamma'|^3$, we obtain $|\gamma''| \sin\alpha / |\gamma'|^2$, which is the projection of acceleration onto the normal vector to the curve (centripetal acceleration) divided by velocity squared. The second-order derivative in the definition of $\kappa(s)$ involves gradient of $f(x)$, which may not exist if $f(x)$ is only assumed to be Lipschitz. Nevertheless, according to Rademacher's theorem, a Lipschitz vector field is differentiable almost everywhere so curvature exists almost everywhere, which is enough for our subsequent proof as discussed in [76] and the result is similar to the case if the curve is C^2. Hence, applying this bound to our curve $x(s)$ wherever ∇f exists:

$$|k(s)| \leq \frac{|\dot{x}||\ddot{x}|}{|\dot{x}|^3} \leq \frac{|\ddot{x}|}{|\dot{x}|^2} \leq \frac{||\nabla f(x)||\,|\dot{x}|}{|\dot{x}|^2} \leq \frac{||\nabla f(x)||}{|f(x)|} \leq \frac{L_1}{\underline{L}_0}.$$

This implies that $\frac{L_1}{\underline{L}_0}$ is an upper bound of curvature along the solution $x(t)$ almost everywhere. Therefore, since radius of curvature is simply the reciprocal of curvature, Proposition 3.2 implies a sufficient condition for non-self-overlapping solution of our system:

Corollary 3.3. *A tube of radius γ_η around the solution $x(\tau)$ is non-self-overlapping over the interval (s, t) if*

$$\gamma_\eta < \frac{\underline{L}_0}{L_1} \tag{3.36}$$

and

$$\mathcal{L}_s^t < \frac{2\underline{L}_0}{L_1}\left(\pi - \sin^{-1}(\frac{L_1\gamma_\eta}{\underline{L}_0})\right). \tag{3.37}$$

Note that according to (3.23) γ_η is a decreasing function of η and $\gamma_1 = 0$; thus, the inequality (3.36) can always be satisfied by picking η close enough to 1.

Remark 3.3. *Bounded curvature is an important feature for non-vanishing vector fields since bounded curvature prevents the system from some undesired behavior which will not generate new sweeping volume, such as spinning around inside a small region.*

Now we have found a criterion of non-self-overlapping (3.37) in terms of the constraint on the path length, but we need to reformulate this criterion in terms of the measure of the bad set. Suppose that (3.36) holds with the volume bound analog of (3.37)

$$\epsilon < \epsilon_1 := \mathrm{vol}(B^{n-1}_{\gamma_\eta}) \frac{2\underline{L}_0}{L_1} \left(\pi - \sin^{-1}(\frac{L_1 \gamma_\eta}{\underline{L}_0}) \right). \tag{3.38}$$

Then we have the following lemma:

Lemma 3.6. *Assume η satisfies the inequality* (3.36) *and $\epsilon < \epsilon_1$ as defined in* (3.38)*. Then $S_{\eta,(s,t)}$ is non-self-overlapping for any $(s,t) \subseteq X_\eta$.*

Proof. By Corollary 3.1 we have $S_{\eta,(s,t)} \subseteq \Omega_1$ so that $\mathrm{vol}(S_{\eta,(s,t)}) \leq \mathrm{vol}(\Omega_1) \leq \epsilon < \epsilon_1$. Let

$$\tilde{t} := \sup\{\tau \in (s,t] : \text{solution is non-self-overlapping over } [s,\tau)\}.$$

The solution is always non-self-overlapping when τ is sufficiently close to s because of the inequality (3.36), so the above set is non-empty and the supremum exists. Our goal is to show $\tilde{t} = t$. Because (3.37) means any tube generated by any shorter curve will be non-self-overlapping, the solution is non-self-overlapping over $[s,\tau)$ for all $\tau \in (s,\tilde{t})$. Thus by the continuity of $\mathrm{vol}(S_{\eta,(s,\tau)})$ with respect to τ,

$$\begin{aligned}
\mathrm{vol}(B^{n-1}_{\gamma_\eta}) \mathcal{L}_s^{\tilde{t}} &= \lim_{\tau \to \tilde{t}^-} \left(\mathrm{vol}(B^{n-1}_{\gamma_\eta}) \mathcal{L}_s^{\tau} \right) = \lim_{\tau \to \tilde{t}^-} \mathrm{vol}(S_{\eta,(s,\tau)}) \\
&= \mathrm{vol}(S_{\eta,(s,\tilde{t})}) \leq \mathrm{vol}(S_{\eta,(s,t)}) < \epsilon_1 \\
&= \mathrm{vol}(B^{n-1}_{\gamma_\eta}) \frac{2\underline{L}_0}{L_1} \left(\pi - \sin^{-1}(\frac{L_1 \gamma_\eta}{\underline{L}_0}) \right) \\
\Rightarrow \mathcal{L}_{\tilde{s}}^{\tilde{t}} &< \frac{2\underline{L}_0}{L_1} \left(\pi - \sin^{-1}(\frac{L_1 \gamma_\eta}{\underline{L}_0}) \right).
\end{aligned}$$

If $\tilde{t} \neq t$, then since $\mathcal{L}_s^\tau$ is a continuous and strictly increasing function of τ (because of non-vanishing vector field), we can always pick $t^* \in (\tilde{t}, t)$ such that

$$\mathcal{L}_s^{\tilde{t}} < \mathcal{L}_s^{t^*} < \frac{2\underline{L}_0}{L_1} \left(\pi - \sin^{-1}(\frac{L_1 \gamma_\eta}{\underline{L}_0}) \right).$$

Hence by Corollary 3.3 we conclude that the solution is non-self-overlapping up to time t^*, which contradicts maximality of $\tilde{t}$. Thus $\tilde{t} = t$. □

Change of V when passing through Ω_η We now specify the threshold $\bar{\epsilon}$ in the statement of Theorem 3.2

$$\bar{\epsilon} := \min\{\epsilon_1, \epsilon_2\},$$

where ϵ_1 is defined in (3.38) and

$$\epsilon_2 := \mathrm{vol}(B^{n-1}_{\gamma_\eta}) \frac{\underline{L}_0(b + \eta a c_1)^2}{\alpha \bar{L}_0 b}. \tag{3.39}$$

Note that when $\eta < 1$, we have $\gamma_\eta > 0$ and thus both ϵ_1, ϵ_2 are positive, which implies $\bar{\epsilon} > 0$. In addition, when (3.36) is satisfied and $\epsilon < \bar{\epsilon}$, $S_{\eta,(s,t)}$ is non-self-overlapping for any $(s,t) \in X_\eta$ by Lemma 3.6. Hence by Corollary 3.2 we have

$$t - s \le \frac{g\epsilon}{b} < \frac{g\bar{\epsilon}}{b} \le \frac{g\epsilon_2}{b} = \frac{(b + \eta a c_1)^2}{\alpha \bar{L}_0 b}. \tag{3.40}$$

These inequalities in (3.40) are essential and will be repeatedly used in the proofs of subsequent lemmas.

We now show that V will always decrease over any connected component of X_η excluding those containing boundary points $\tau = 0$ and $\tau = T$, if the latter exists. When the solution passes through the connected component containing the initial point $\tau = 0$ or $\tau = T$, then V may actually increase but is bounded by a fixed value. This is summarized in the next lemma:

Lemma 3.7. *Assume $\eta \in (0,1)$ satisfies (3.36) and $\epsilon < \bar{\epsilon}$. For any connected component $(s,t) \subset X_\eta$, define $\Delta V_{(s,t)} := V(x(t)) - V(x(s))$. Then*

1. *If $s = 0$ and $V(x(0)) < c_2 - h - g\epsilon$,*

$$\Delta V_{(s,t)} \le \begin{cases} g\epsilon & \text{if } t = T, \\ \frac{g}{2}\epsilon & \text{if } t \ne T. \end{cases}$$

2. If $s > 0$ and $V(x(s)) < c_2 - h - \frac{g}{2}\epsilon$,

$$\Delta V_{(s,t)} \leq \begin{cases} \frac{g}{2}\epsilon & \text{if } t = T, \\ \phi(t-s) & \text{if } t \neq T, \end{cases}$$

where

$$\phi(\tau) := \begin{cases} \frac{1}{4}\tau^2\alpha\bar{L}_0 - \tau\eta a c_1 & \text{if } \tau\alpha\bar{L}_0 < 2(b+\eta a c_1), \\ b\tau - \frac{(b+\eta a c_1)^2}{\alpha\bar{L}_0} & \text{if } \tau\alpha\bar{L}_0 \geq 2(b+\eta a c_1). \end{cases} \tag{3.41}$$

Remark 3.4. *We observe that when $(t-s)\alpha\bar{L}_0 < 2(b+\eta a c_1)$, b does not appear in the bound for $\Delta V_{(s,t)}$. This corresponds to the case when the bound b is too loose, or the upper bound of $\dot{V}$ is unknown or not pre-determined. We have done studies of such less constrained almost Lyapunov functions previously and an example on which the theorem is applicable is not found yet.*

Proof. The proof consists of four cases:

Case 1: ($s = 0$ and $t = T$).

Note that $\Delta V_{(s,t)} = \int_s^t \dot{V}(x(\tau))d\tau \leq \int_s^t b d\tau = b(t-s) \leq g\epsilon$ for any $(s,t) \subset X_\eta$. The last inequality comes from Corollary 3.2. Thus $g\epsilon$ is an upper bound for $\Delta V_{(s,t)}$ for any connected components (s,t) in X_η, in particular for the special case when both $s = 0$ and $t = T$.

Case 2: ($s = 0$ and $t \neq T$).

In this case t is finite. Since (s,t) is a maximal interval, either $x(t) \in \partial\Omega_\eta$ or $x(t) \in \partial D^*$, the boundary of D^*. If it is the latter, we are only interested in the case when $\Delta V_{(0,t)} > 0$, that is, the case $V(x(t)) = c_2 - h$. Note that in this case $\Delta V_{(0,t)} = V(x(t)) - V(x(0)) > (c_2 - h) - (c_2 - h - g\epsilon) = g\epsilon$. This conflicts with the general upper bound of $g\epsilon$ on $\Delta V_{(s,t)}$ derived in case 1. Thus we must have $x(t) \in \partial\Omega_\eta$ so $\dot{V}(x(t)) = -\eta a V(x(t)) \leq -\eta a c_1$. Next we compute a tighter upper bound on $\Delta V_{(0,t)}$. It follows from (3.22) that for any $t_1, t_2 \in [s,t]$,

$$\begin{aligned} |\dot{V}(x(t_1)) - \dot{V}(x(t_2))| &\leq \alpha|x(t_1) - x(t_2)| \\ &\leq \alpha \int_{t_1}^{t_2} |f(x(\tau))|d\tau \leq \alpha\bar{L}_0|t_1 - t_2|. \end{aligned} \tag{3.42}$$

Thus, $\dot{V}$, when considered as a function of time, is a Lipschitz function with Lipschitz constant $\alpha\bar{L}_0$. We can now estimate $\Delta V_{(0,t)}$ by collecting inequalities:

$$\Delta V_{(0,t)} = \int_0^t \dot{V}(x(\tau))d\tau$$
$$\text{with the bounds } t < \frac{(b+\eta a c_1)^2}{\alpha\bar{L}_0 b}, \dot{V}(x(t)) \leq -\eta a c_1, \dot{V}(x(t_0)) \leq b,$$
$$|\dot{V}(x(t_1)) - \dot{V}(x(t_2))| \leq \alpha\bar{L}_0|t_1 - t_2| \ \forall t_0, t_1, t_2 \in [0,t]. \quad (3.43)$$

The first bound comes from (3.40) and the other bounds have been introduced earlier. We claim that a necessary condition for the inequalities in (3.43) to hold is:

$$\dot{V}(x(\tau)) \leq \min\{b, \alpha\bar{L}_0(t-\tau) - \eta a c_1\},$$

where the first bound b is immediate. The second bound comes from $\dot{V}(x(t)) \leq -\eta a c_1$ and the Lipschitz bound on $\dot{V}$. Hence we conclude that its integration gives an upper bound for $\Delta V_{(0,t)}$:

$$\begin{aligned}\Delta V_{(0,t)} &\leq \int_0^t \min\{b, \alpha\bar{L}_0(t-\tau) - \eta a c_1\}d\tau \\ &= \int_0^t \min\{b, \alpha\bar{L}_0\tau - \eta a c_1\}d\tau.\end{aligned}$$

A change of variable is used for deriving the second line above. Note that the minimum function switches value when $b = \alpha\bar{L}_0\tau - \eta a c_1$, that is, when $\tau = \frac{b+\eta a c_1}{\alpha\bar{L}_0}$. To estimate the integral, consider first the case when $t \geq \frac{b+\eta a c_1}{\alpha\bar{L}_0}$. In this case

$$\begin{aligned}\Delta V_{(0,t)} &\leq \int_0^{\frac{b+\eta a c_1}{\alpha\bar{L}_0}} (\alpha\bar{L}_0\tau - \eta a c_1)d\tau + \int_{\frac{b+\eta a c_1}{\alpha\bar{L}_0}}^t b d\tau \\ &= \frac{1}{2}\alpha\bar{L}_0\left(\frac{b+\eta a c_1}{\alpha\bar{L}_0}\right)^2 - \eta a c_1\frac{b+\eta a c_1}{\alpha\bar{L}_0} + b\left(t - \frac{b+\eta a c_1}{\alpha\bar{L}_0}\right) \\ &= bt + \frac{(b+\eta a c_1)^2 - 2\eta a c_1(b+\eta a c_1) - 2b(b+\eta a c_1)}{2\alpha\bar{L}_0} \\ &= bt - \frac{(b+\eta a c_1)^2}{2\alpha\bar{L}_0} < bt - \frac{bt}{2} \leq \frac{g}{2}\epsilon.\end{aligned}$$

The two inequalities in the last line come from the inequalities in (3.40). Now, if $t < \frac{b+\eta a c_1}{\alpha \bar{L}_0}$, there is no switch and we only need to evaluate one integral:

$$\begin{aligned}\Delta V_{(s,t)} &\leq \int_0^t (\alpha \bar{L}_0 s - \eta a c_1) ds = \frac{1}{2}\alpha \bar{L}_0 t^2 - \eta a c_1 t \\ &= \left(\frac{1}{2}\alpha \bar{L}_0 t - \eta a c_1\right) t < \left(\frac{1}{2}\alpha \bar{L}_0 \left(\frac{b+\eta a c_1}{\alpha \bar{L}_0}\right) - \eta a c_1\right) t \\ &= \frac{1}{2}(b - \eta a c_1) t < \frac{b}{2} t \leq \frac{g}{2}\epsilon.\end{aligned}$$

The last inequality above comes from (3.40). Thus we have shown that $\frac{g}{2}\epsilon$ is an upper bound for $\Delta V_{(s,t)}$ when $s = 0, t \neq T$.

Case 3: $(s \neq 0, t = T)$

We start by considering any connected component (s,t) such that $s \neq 0$. Again because it is maximal, we can only have $x(s) \in \partial\Omega_\eta$. This is because $x(s) \in \partial D^*$ is impossible as otherwise $x(\tau) \notin D^*$ for some $\tau < s$. Thus we should have $\dot{V}(x(s)) = -\eta a V(x(s)) \leq -\eta a c_1$. Similar to (3.43), we obtain a system of inequalities

$$\begin{aligned}\Delta V_{(s,t)} = \int_s^t \dot{V}(x(\tau)) d\tau \\ \text{with bounds } t - s < \frac{(b+\eta a c_1)^2}{\alpha \bar{L}_0 b}, \dot{V}(x(s)) \leq -\eta a c_1, \dot{V}(x(t_0)) \leq b, \\ |\dot{V}(x(t_1)) - \dot{V}(x(t_2))| \leq \alpha \bar{L}_0 |t_1 - t_2| \ \forall t_0, t_1, t_2 \in [s,t], \quad (3.44)\end{aligned}$$

where the first bound again comes from (3.40). The bounds are essentially the same as (3.43) but with the only difference that the boundary condition is $\dot{V}(x(s)) \leq -\eta a c_1$ instead of $\dot{V}(x(t)) \leq -\eta a c_1$. By symmetry considerations (change of variables $\tau' = t + s - \tau$ and then shift the time so $s = 0$), the upper bound will be the same and, thus, we have $\Delta V_{(s,t)} < \frac{g}{2}\epsilon$. This proves the special case when $\tau = T$, if $T < \infty$.

Case 4: $(s \neq 0, t \neq T)$

From the analysis in case 3 we see that $V(x(t)) = V(x(s)) + \Delta V_{(s,t)} < (c_2 - h - \frac{g}{2}\epsilon) + \frac{g}{2}\epsilon = c_2 - h$.

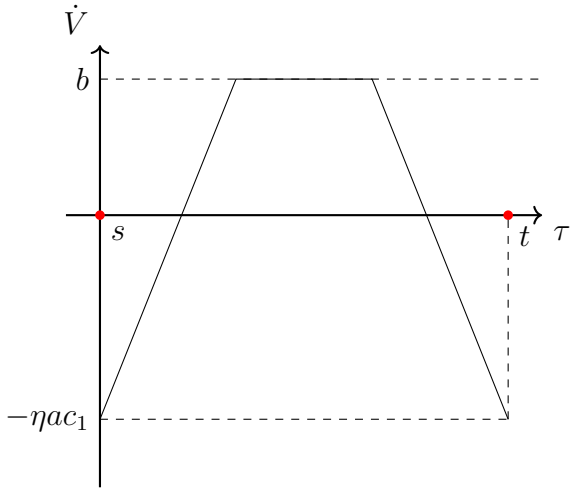

Figure 3.3: Upper bound of $\dot{V}$ vs. τ on the trajectory passing Ω_η.

Hence $x(t) \notin \partial D^*$. So by maximality of (s,t) we must have both $x(s), x(t) \in \partial\Omega_\eta$. Therefore, we have the system of inequalities

$$\begin{aligned}\Delta V_{(s,t)} &= \int_s^t \dot{V}(x(\tau))d\tau \\ &\text{with bounds } (t-s) < \frac{(b+\eta a c_1)^2}{\alpha \bar{L}_0 b}, \dot{V}(x(s)), \dot{V}(x(t)) \leq -\eta a c_1, \\ &\dot{V}(x(\tau)) \leq b, |\dot{V}(x(t_1)) - \dot{V}(x(t_2))| \leq \alpha \bar{L}_0 |t_1 - t_2| \ \forall \tau, t_1, t_2 \in [s,t]. \quad (3.45)\end{aligned}$$

By the same reasoning as that for (3.43), we have the following bound as a necessary condition:

$$\dot{V}(\tau) \leq \min\{b, \alpha \bar{L}_0(\tau - s) - \eta a c_1, \alpha \bar{L}_0(t-\tau) - \eta a c_1\} \quad (3.46)$$

for all $\tau \in [s,t]$. Hence

$$\begin{aligned}\Delta V_{(s,t)} &\leq \int_s^t \min\{b, \alpha \bar{L}_0(\tau - s) - \eta a c_1, \alpha \bar{L}_0(t-\tau) - \eta a c_1\} d\tau \\ &= \int_0^{t-s} \min\{b, \alpha \bar{L}_0 \tau - \eta a c_1, \alpha \bar{L}_0(t - s - \tau) - \eta a c_1\} d\tau.\end{aligned}$$

The upper bound of $\dot{V}$ over $[s,t]$ is plotted in Fig. 3.3, corresponding to the trajectory in Fig. 3.2. If $t - s \leq 2\frac{b+\eta a c_1}{\alpha \bar{L}_0}$, the functions to be minimized in (3.46) have only one switching

point at $\frac{t-s}{2}$, and

$$\begin{aligned}\Delta V_{(s,t)} &\leq \int_0^{\frac{t-s}{2}} (\alpha\bar{L}_0\tau - \eta a c_1)d\tau + \int_{\frac{t-s}{2}}^{t-s} (\alpha\bar{L}_0(t-s-\tau) - \eta a c_1)d\tau \\ &= 2\int_0^{\frac{t-s}{2}} (\alpha\bar{L}_0\tau - \eta a c_1)d\tau = \alpha\bar{L}_0(\frac{t-s}{2})^2 - 2\eta a c_1(\frac{t-s}{2}) \\ &= \frac{1}{4}\alpha\bar{L}_0(t-s)^2 - \eta a c_1(t-s).\end{aligned}$$

If $(t-s) > 2\frac{b+\eta a c_1}{\alpha\bar{L}_0}$, there are two switching points, $\tau = \frac{b+\eta a c_1}{\alpha\bar{L}_0}$ and $\tau = t-s-\frac{b+\eta a c_1}{\alpha\bar{L}_0}$, so we have

$$\begin{aligned}\Delta V_{(s,t)} \leq & \int_0^{\frac{b+\eta a c_1}{\alpha\bar{L}_0}} (\alpha\bar{L}_0\tau - \eta a c_1)d\tau + \int_{\frac{b+\eta a c_1}{\alpha\bar{L}_0}}^{t-s-\frac{b+\eta a c_1}{\alpha\bar{L}_0}} b d\tau \\ & + \int_{t-s-\frac{b+\eta a c_1}{\alpha\bar{L}_0}}^{t-s} (\alpha\bar{L}_0(t-s-\tau) - \eta a c_1)d\tau \\ =& 2\int_0^{\frac{b+\eta a c_1}{\alpha\bar{L}_0}} (\alpha\bar{L}_0\tau - \eta a c_1)d\tau + \int_{\frac{b+\eta a c_1}{\alpha\bar{L}_0}}^{t-s-\frac{b+\eta a c_1}{\alpha\bar{L}_0}} b\, d\tau \\ =& \alpha\bar{L}_0(\frac{b+\eta a c_1}{\alpha\bar{L}_0})^2 - 2\eta a c_1(\frac{b+\eta a c_1}{\alpha\bar{L}_0}) \\ & + b\left((t-s) - 2(\frac{b+\eta a c_1}{\alpha\bar{L}_0})\right) \\ =& b(t-s) - (\frac{b+\eta a c_1}{\alpha\bar{L}_0})^2.\end{aligned}$$

The two bounds are collected to be the ϕ function as stated in the lemma.

□

Now since we have assumed that $b < a c_1$ in the beginning, we can always pick an η sufficiently close to 1 to guarantee that

$$b < \eta a c_1. \tag{3.47}$$

From now on we will assume that η satisfies both (3.36) and (3.47). Note that for the solution outside of Ω_η, the almost Lyapunov function V clearly is decreasing; therefore, Lemma 3.7 also leads us to the following conclusion:

Corollary 3.4. *Consider a solution $x(\tau)$ with $V(x(0)) < c_2 - h - g\epsilon$. Let (s,t) be a maximal connected component of X_η such that $s \neq 0, t \neq T$. Assume also $b < \eta a c_1$ and $\epsilon < \bar{\epsilon}$. Then $\Delta V_{(s,t)} \leq \phi(t-s) < 0$.*

Proof. We prove by induction under an additional assumption that there are finitely many connected components in any bounded subset of X_η. The extension to the general case will be justified at the end of the proof.

Firstly, if $(t-s)\alpha\bar{L}_0 < 2(b+\eta a c_1)$, then (3.47) implies $(t-s)\alpha\bar{L}_0 < 4\eta a c_1$ and hence the first line in (3.41) implies $\phi(t-s) = \frac{1}{4}(t-s)^2\alpha\bar{L}_0 - (t-s)\eta a c_1 < 0$. Otherwise, (3.40) implies $\phi(t-s) = b(t-s) - \frac{(b+\eta a c_1)^2}{\alpha\bar{L}_0} < 0$. Thus we always have $\phi(t-s) < 0$.

Let (s,t) be the first connected component of X_η on the left with $s > 0$. If it is the first connected component on the left (i.e. there is no connected component starting at $\tau = 0$), then $V(x(s)) < V(x(0)) < c_2 - h - g\epsilon$. If there is a connected component starting at $\tau = 0$, say the interval $(0, t_0)$, then still

$$V(x(s)) \leq V(x(0)) + \Delta V_{(0,t_0)} < (c_2 - g\epsilon - h) + \frac{g}{2}\epsilon = c_2 - \frac{g}{2}\epsilon + h.$$

Either way, $V(x(s)) < c_2 - \frac{g}{2}\epsilon + h$. Hence by Lemma 3.7, the base case is true and we have $\Delta V_{(s,t)} \leq \phi(t-s) < 0$. Assume by induction that at some connected component also denoted (s,t) we have $V(x(s)) < c_2 - \frac{g}{2}\epsilon - h$ and $\phi(t-s) < 0$. Then at the next connected component (s^+, t^+) we have

$$\begin{aligned} V(x(s^+)) &= \big(V(x(s^+)) - V(x(t))\big) + \Delta V_{(s,t)} + V(x(s)) \\ &\leq \phi(t-s) + V(x(s)) < c_2 - \frac{g}{2}\epsilon - h \end{aligned}$$

and again by Lemma 3.7 we have $\Delta V_{(s^+,t^+)} \leq \phi(t^+ - s^+) < 0$.

Now, we address the case when X_η is arbitrary, not necessarily consisting of finitely many connected components. Consider any connected component $(s,t) \subset X_\eta$ excluding those which contain boundary points. If the corresponding arc of the solution does not enter Ω_0, then V could only decrease and we declare this component for the purpose of this proof to be outside of X_η. Now consider any connected component of X_η for which the

corresponding solution enters Ω_0. Then, by Lemma 3.4 such a connected component must have a lower bound on its length. Thus, the number of connected components where V might increase has to be finite on a bounded time interval and the above proof by induction applies.

□

Exponential bound when repeatedly passing through Ω_η Corollary 3.4 tells us that the Lyapunov function decreases each time the solution crosses Ω_η. This does not yet guarantee convergence to a smaller set. We now want to find an exponential type bound on V. Define $k(t) : \mathbb{R}_+ \to \mathbb{R}$ by

$$k(t) := \begin{cases} -\frac{1}{t} \ln\left(1 + \frac{1}{c_2}\phi(t)\right) & \text{if } \phi(t) > -c_2, \\ K & \text{if } \phi(t) \leq -c_2, \end{cases}$$

where ϕ is defined in (3.41) and K is a sufficiently large positive constant. Note that $\phi(t)$ is continuous near 0 and $\phi(0) = 0$, so we can define $k(0) = \frac{\eta a c_1}{c_2}$ by extension via L'Hôpital's rule. In addition, define

$$\lambda(\epsilon) := \min_{0 \leq \delta \leq \epsilon} k\left(\frac{g\delta}{b}\right).$$

By this definition, $\lambda(\epsilon)$ is a non-increasing function on $[0, \bar{\epsilon})$. On the one hand, we see from the proof of Corollary 3.4 that $\phi(t) < 0$ for all $t \in (0, \frac{(b+\eta a c_1)^2}{\alpha \bar{L}_0 b})$ and thus we have $k(t) > 0$ for all $t \in [0, \frac{(b+\eta a c_1)^2}{\alpha \bar{L}_0 b})$. In addition, because $\frac{g\bar{\epsilon}}{b} \leq \frac{(b+\eta a c_1)^2}{\alpha \bar{L}_0 b}$ as in (3.40), $\lambda(\epsilon)$ is also positive on $[0, \bar{\epsilon})$. According to Corollary 3.2, $t - s \leq \frac{g\epsilon}{b}$, which implies

$$k(t-s) \geq \min_{0 \leq \delta \leq \epsilon} k\left(\frac{g\delta}{b}\right) = \lambda(\epsilon).$$

Next, we have

$$\begin{aligned} V(x(t)) &= \Delta V_{(s,t)} + V(x(s)) = V(x(s))\left(1 + \frac{\Delta V_{(s,t)}}{V(x(s))}\right) \\ &\leq V(x(s))\left(1 + \frac{\phi(t-s)}{c_2}\right) = V(x(s))e^{-k(t-s)(t-s)} \\ &\leq V(x(s))e^{-\lambda(\epsilon)(t-s)} \end{aligned} \tag{3.48}$$

for any connected component of $(s,t) \subset X_\eta$ that does not contain the end points $\tau = 0$ or $\tau = t_{\max}$. From the second line to the third line the inequality $\Delta V_{(s,t)} \leq \phi(t-s) < 0$ was used. We also have

$$\lambda(\epsilon) \leq \lambda(0) = k(0) = \frac{\eta a c_1}{c_2} < \eta a$$

for all $\epsilon \in [0, \bar{\epsilon})$. Thus, when the solution is inside Ω_η, it has a decay rate slower than when the solution is in $D \backslash \Omega_\eta$, which has decay rate faster than ηa. We can modify $\lambda(\epsilon)$ so that it is a positive, continuous, strictly decreasing function on $[0, \bar{\epsilon})$ with $\lambda(0) < \eta a$ and so the inequality (3.48) still holds.

As a result, for any $s, s' \in (0,T) \backslash \text{int} X_\eta$, we have

$$V(x(s')) \leq V(x(s))e^{-\lambda(\epsilon)(s'-s)}.$$

This exponential decaying bound suggests that T cannot be infinite; otherwise, for $s, s' \in (0,T) \backslash \text{int} X_\eta$ and $s'-s$ large enough, we will have $V(x(s')) < c_1 + h$, implying $x(s') \notin D^*$, and such s' always exists when T is infinite because the possible connected component containing T has maximal length of $\frac{g\epsilon}{b}$.

Take an arbitrary $t \in [0,T]$. Recall that by Lemma 3.7 for any connected components of X_η, even those that contain the end points 0 and t, we still have the bound $\Delta V \leq \frac{g}{2}\epsilon$. Therefore, taking into account boundary components, we have

$$V(x(t)) \leq (V(x(0)) + \frac{g}{2}\epsilon)e^{-\lambda(\epsilon)(s'-s)} + \frac{g}{2}\epsilon \tag{3.49}$$

where $s' = t$ if $t \notin X_\eta$, or s' is the left boundary point of the connected component of X_η

containing t otherwise; $s = 0$ if $s \notin X_\eta$, or s is the right boundary point of the connected component of X_η containing 0 otherwise. From (3.49) we directly see that

$$V(x(t) \leq V(x(0)) + g\epsilon \quad \forall t \in [0, T]. \tag{3.50}$$

The first statement in Theorem 3.2 follows from (3.50) up to time T. In addition, by Corollary 3.2,

$$s \leq \frac{g\epsilon}{b}, \quad t - s' \leq \frac{g\epsilon}{b} \Rightarrow s' - s \geq t - 2\frac{g\epsilon}{b}.$$

Substituting these expressions into (3.49), we have

$$V(x(t)) \leq e^{2\lambda(\epsilon)\frac{g\epsilon}{b}}(V(x(0)) + \frac{g}{2}\epsilon)e^{-\lambda(\epsilon)t} + \frac{g}{2}\epsilon. \tag{3.51}$$

This is also true for $t = T$. By definition of T in (3.32) we see that $x(T) \in \partial D^*$, and because of the exponential bound in (3.51) we must have $V(x(T)) = c_1 + h$. Let $T_{\max}$ solve the equation

$$c_1 + h = e^{2\lambda(\epsilon)\frac{g\epsilon}{b}}(c_2 - h - \frac{g}{2}\epsilon)e^{-\lambda(\epsilon)T_{\max}} + \frac{g}{2}\epsilon.$$

This is the maximum time a solution can remain in D^* and it depends on ϵ alone. As a result, we must have $T \leq T_{\max}$ and the second statement in Theorem 3.2 is proven.

The argument cannot proceed once $V(x(t)) < c_1 + h$ because $B_{\gamma_\eta}(x(t)) \not\subset D$ and the estimation of the sweeping volume, based on the bounds $\underline{L}_0, L_1$ etc. is no longer valid. Nevertheless, once the solution returns to the lower boundary of D^* such that $V(x(t)) = c_1 + h$, it can be again treated as a new solution starting from $x(0) \in D$ with $V(x(0)) < c_2 - h - g\epsilon$, and by the same analysis above we know that it can have an overshoot of $g\epsilon$ at most. This proves the first statement for all $t \geq 0$ and the last statement in Theorem 3.2.

3.2.2 Global results

Our Theorem 3.2 gives a local convergence property. Very often one would like global properties, such as GAS which is introduced ealier in Section 3.1.2. Despite of the characterization via comparison function as in (3.3), a system 3.2 is GAS if it is *globally stable* in the sense

that for any $\varepsilon > 0$, there exists $\delta > 0$ such that if $|x(0)| \leq \delta$, $|x(t)| \leq \varepsilon$ for all $t \geq 0$, and *uniformly attractive* in the sense that for any $\delta > 0, \kappa > 0$, there exists $T = T(\delta, \kappa)$ such that whenever $|x(0)| \leq \kappa$, $|x(t)| \leq \delta$ for all $t \geq T$. We now try to transfer our study to a global result. To do that, instead of a fixed region D defined by two constants c_1, c_2, we let the band-shaped region be defined for any $c > 0$:

$$D(c) := \{x \in \mathbb{R}^n : c \leq V(x) \leq 2c\}. \tag{3.52}$$

Following the definitions of $b, \bar{L}_0, \underline{L}_0, L_1, M_1, M_2$ from (3.25),(3.16),(3.17),(3.18),(3.19),(3.20) over the region $D(c)$, we see that now all of them are functions of c. We present a global uniform asymptotic stability result derived using an almost Lyapunov function:

Theorem 3.3. *Consider a system (3.2) with a globally Lipschitz right-hand side f, and a function $V : \mathbb{R}^n \to [0, +\infty)$ which is positive definite and C^1 with globally Lipschitz gradient. In addition assume $V(x) \geq k_0|x|^2$ for some $k_0 > 0$ and all $x \in \mathbb{R}^n$. For any $c > 0$, let the region $D(c)$ be defined via (3.52) and assume all of them are compact. Let $\Omega \subset \mathbb{R}^n$ be a measurable set such that $\dot{V}(x) < -aV(x)$ for all $x \in \mathbb{R}\backslash\Omega$ with some $a > 0$. Assume $\sup_{c>0} \frac{b(c)}{ac} < 1$ where $b(c)$ is defined via (3.25) over $D(c)$. Let $\underline{L}_0(c)$ be defined via (3.17) over $D(c)$. Then there exist two class $\mathcal{K}_\infty$ functions ρ_1, ρ_2 such that as long as $\text{vol}(\Omega^*(c)) < \min\{\rho_1(\underline{L}_0(c)), \rho_2(c)\}\underline{L}_0$ for all $c > 0$ where $\Omega^*(c)$ is the largest connected component of $\Omega \cap D(c)$, the system (3.2) is GAS.*

Before giving the proof of Theorem 3.3, let us discuss the validity and some variations of the assumptions of this theorem. If we know that the system is globally stable or the working space is some compact set in $\mathbb{R}^n$ instead of $\mathbb{R}^n$ itself, then we can replace global Lipschitzness in f and V_x by local Lipschitzness as it is sufficient for the existence of uniform L_1, M_2 and that is what will be used in the proof. The assumption $V(x) \geq k_0|x|^2$ is quite general since all quadratic Lypunov functions satisfy this assumption. Other assumptions are merely the same as, or general versions of, the assumptions in Theorem 3.2. The non-vanishing assumption is also reflected in the theorem statement that if f vanishes at any state which is different from the origin, $\underline{L}_0(c) = 0$ for some $c > 0$ and this theorem becomes

inconclusive.

Proof. The idea of the proof is to repeatedly apply Theorem 3.2 over the region $D(c)$ for any $c > 0$ and show that $V(x(t))$ is bounded and will decrease by a fixed factor each time.

First of all, globally Lipschitz f and V_x mean there exist $k_1, k_2 > 0$ such that

$$L_1 \le k_1,$$
$$M_2 \le k_2,$$

where L_1, M_2 are the global Lipschitz constants of f, V_x, respectively. In addition, if x^* is the maximizer of $|f(x)|$ in $D(c)$,

$$\bar{L}_0(c) = \max_{x \in D(c)} |f(x)| = |f(x^*)| = |f(x^*) - f(0)| \le L_1 |x^* - 0| \le k_1 |x^*| \le k_1 \sqrt{\frac{V(x^*)}{k_0}} \le k_1 \sqrt{\frac{2c}{k_0}}.$$

By similar argument we also have $M_1 \le k_2 \sqrt{\frac{2c}{k_0}}$. Thus, $\alpha = M_1 L_1 + M_2 \bar{L}_0 \le 2k_1 k_2 \sqrt{\frac{2c}{k_0}}$ and (3.23) in Lemma 3.4 becomes

$$\gamma_\eta = \frac{(1-\eta)ac}{\alpha + \eta a M_1} \ge \frac{(1-\eta)ac}{2k_1 k_2 \sqrt{\frac{2c}{k_0}} + a k_2 \sqrt{\frac{2c}{k_0}}} = \frac{(1-\eta)a\sqrt{k_0}}{\sqrt{2}(2k_1 + a)k_2} c^{\frac{1}{2}} = (1-\eta) K c^{\frac{1}{2}} =: \gamma^*,$$

where $K := \frac{a\sqrt{k_0}}{\sqrt{2}(2k_1 + a)k_2}$ is a constant. For each $c > 0$, pick $\eta(c) \in (\frac{1}{2}, 1)$ such that

$$1 - \eta(c) < \min \left\{ \frac{2k_1 + a}{4a}, \frac{\underline{L}_0(c)}{2k_1 K \sqrt{c}}, 1 - \sup_{c>0} \frac{b(c)}{ac} \right\}, \tag{3.53}$$

This can be done as the right-hand side of (3.53) is always positive. As a result,

$$\gamma^* < \min \left\{ \min \left\{ \frac{2k_1 + a}{4a}, 1 - \sup_{c>0} \frac{b(c)}{ac} \right\} K c^{\frac{1}{2}}, \frac{\underline{L}_0}{2k_1} \right\},$$

which tells us that by a proper choice of $\eta(c)$ satisfying (3.53), γ^* will be the minimum between two class $\mathcal{K}_\infty$ functions of $\underline{L}_0, c$, respectively. Also by definition we know $\gamma^* \le \gamma_\eta$, so the result in Lemma 3.4 holds for γ^* as well. In addition, the second and third elements

in the min function of (3.53) tell us that

$$\gamma^* < \frac{\underline{L}_0}{2k_1} \leq \frac{\underline{L}_0}{2L_1} < \frac{\underline{L}_0}{L_1},$$

$$\eta(c) > \sup_{c>0} \frac{b(c)}{ac} \Rightarrow b(c) < \eta(c)ac.$$

Therefore both (3.36) and (3.47) are satisfied; γ^* is indeed a valid sweeping radius and hence all the subsequent results still follow if we replace every γ_η by γ^*. Now if we let

$$\epsilon < \frac{\underline{L}_0(c)\mathrm{vol}(B^{n-1}_{\gamma^*})}{4b} c =: \epsilon_3, \tag{3.54}$$

the previous definition (3.30) gives us

$$g\epsilon = \frac{b\epsilon}{\underline{L}_0 \mathrm{vol}(B^{n-1}_{\gamma^*})} < \frac{1}{4}c.$$

On the other hand, by substituting the first element of the min function in (3.53), the bound on M_1 and the definition of K into (3.31), we have

$$h = M_1\gamma^* = M_1(1-\eta(c))Kc^{\frac{1}{2}} < k_2\sqrt{\frac{2c}{k_0}}\frac{(2k_1+a)}{4a}\frac{a\sqrt{k_0}}{\sqrt{2}(2k_1+a)k_2}c^{\frac{1}{2}} = \frac{1}{4}c$$

So we have both $g\epsilon, h$ bounded from above by $\frac{1}{4}c$.

Now for any initial state $x(0) \in \mathbb{R}^n$, we let $c = \frac{2}{3}V(x(0))$. Then $x_0 \in D(c)$ and we try to apply Theorem 3.2 on it. Note that $V(x_0) = \frac{3}{2}c < 2c - h - g\epsilon$, thus the initial state satisfies the hypothesis. If the size of ϵ also satisfies the requirement, then we conclude from Theorem 3.2 that $V(x(t)) \leq V(x(0)) + g\epsilon \leq \frac{7}{4}c$, and there is a time T that depends on c, ϵ such that $V(x(t)) \leq c + h < \frac{5}{4}c$ for some $t \leq T$. The global stability part is given by the first conclusion by letting $\delta = \frac{7}{6}\varepsilon$. The second conclusion tells that

$$\frac{V(x(t))}{V(x(0))} < \frac{\frac{5}{4}c}{\frac{3}{2}c} = \frac{5}{6}.$$

Thus over each iteration $|x(t)|$ is decreased by at least a factor of $\frac{5}{6}$, in time at most T. We

then reset time t to be the initial time and can repeat the same argument. Thus while given δ and κ, the total number of iterations is $\lceil \frac{\ln \kappa - \ln \delta}{\ln 6 - \ln 5} \rceil$ for a solution that starts from $\bar{B}^n_\kappa(0)$ and converges to $\bar{B}^n_\delta(0)$. The total time needed is the summation of T's of each iteration and hence only depends on κ, δ.

The only part remaining is to find the bound that ϵ needs to satisfy. Recall from (3.38) and (3.39) that we have

$$\epsilon_1 = \text{vol}(B^{n-1}_{\gamma^*}) \frac{2\underline{L}_0}{L_1} \left(\pi - \sin^{-1}(\frac{L_1 \gamma^*_\eta}{\underline{L}_0}) \right) \geq \text{vol}(B^{n-1}_{\gamma^*}) \underline{L}_0 \frac{2}{k_1} \left(\pi - \sin^{-1}(\frac{1}{2}) \right),$$

$$\epsilon_2 = \text{vol}(B^{n-1}_{\gamma_\eta}) \frac{\underline{L}_0 (b + \eta a c)^2}{\alpha \bar{L}_0 b} \geq \text{vol}(B^{n-1}_{\gamma^*}) \underline{L}_0 \frac{4b\eta ac}{2k_1^2 k_2 \frac{2c}{k_0} b} > \text{vol}(B^{n-1}_{\gamma^*}) \underline{L}_0 \frac{a}{2k_1^2 k_2},$$

where in e_2 the assumption $\eta > \frac{1}{2}$ is used. Meanwhile, from (3.54) we have

$$\epsilon_3 = \frac{\underline{L}_0(c) \text{vol}(B^{n-1}_{\gamma^*})}{4b} c > \text{vol}(B^{n-1}_{\gamma^*}) \underline{L}_0 \frac{1}{4a}.$$

Thus if we define

$$\bar{\epsilon} := \text{vol}(B^{n-1}_{\gamma^*}) \underline{L}_0 \min \left\{ \frac{4\pi}{3k_1}, \frac{a}{2k_1^2 k_2}, \frac{1}{4a} \right\}, \tag{3.55}$$

then $\bar{\epsilon} \leq \min\{\epsilon_1, \epsilon_2, \epsilon_3\}$. Note that the min function in (3.55) is a constant. Recall that γ^* can be chosen to be the minimum between two class $\mathcal{K}_\infty$ functions of $\underline{L}_0, c$, and it implies that $\text{vol}(B^{n-1}_{\gamma^*})$ can also be chosen to be the minimum between two class $\mathcal{K}_\infty$ functions of $\underline{L}_0, c$. Thus we have

$$\bar{\epsilon} = \min\{\rho_1(\underline{L}_0), \rho_2(c)\} \underline{L}_0.$$

This $\bar{\epsilon}$ is a valid upper bound of ϵ in Theorem 3.2. As a result, though the decay rate depends on $\text{vol}(\Omega^*(c))$, as long as $\text{vol}(\Omega^*(c)) < \bar{\epsilon}$ for all $c > 0$ where $\Omega^*(c)$ is the largest connected component of $\Omega \cap D(c)$, the system (3.2) is GAS. $\square$

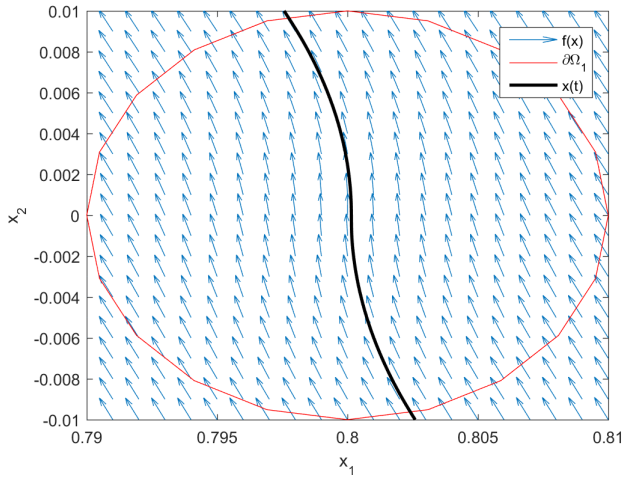

Figure 3.4: Local behavior of the example system.

3.2.3 Example and discussion

Example The system (3.2) is explicitly defined as follows:

$$\begin{pmatrix} \dot{x_1} \\ \dot{x_2} \end{pmatrix} = f(x) = \begin{pmatrix} -\lambda(x) & \mu \\ -\mu & -\lambda(x) \end{pmatrix} \begin{pmatrix} x_1 \\ x_2 \end{pmatrix} \tag{3.56}$$

with

$$\lambda(x) = 1.01 \min \left\{ \frac{|x - x_c|}{\rho}, 1 \right\} - 0.01, \quad x_c = (0.8, 0)^\top, \mu = 2, \rho = 0.01.$$

The relevant part of the phase portrait for the vector field $f(x)$ with a solution $x(t)$ passing through is shown in Fig. 3.4. Note that the spiral-shaped vector field is distorted in the region of $B_\rho(x_c)$. The solution $x(t)$ passing through this region will temporarily move away from the origin when passing through $B_\rho(x_c)$. More explicitly, we consider the function

$$V = |x|^2 = x_1^2 + x_2^2$$

as a candidate Lyapunov function. Then

$$\dot{V}(x) = 2(x_1 \dot{x}_1 + x_2 \dot{x}_2) = -2\lambda(x)(x_1^2 + x_2^2). \tag{3.57}$$

Note that $\lambda(x) = 1$ everywhere except in $B_\rho(x_c)$. Outside this ball $B_\rho(x_c)$ the system is linear and satisfies the decay condition $\dot{V} = -2V$. When $x(t)$ is very close to x_c, $\lambda(x)$ becomes negative and $\dot{V}$ becomes positive. Hence for this system $\Omega_0 \neq \emptyset$ and V is not a Lyapunov function for this system but only an almost Lyapunov function. Nevertheless, we will show by our theorem that convergence to 0 takes place as the effect of Ω is not strong. To do so, choose $d_1 = 0.7, d_2 = 1, c_1 = d_1^2, c_2 = d_2^2$. We find that

$$\begin{aligned}
|f(x)| &= \sqrt{f(x)^\top f(x)} \\
&= \sqrt{\begin{pmatrix} x_1 & x_2 \end{pmatrix} \begin{pmatrix} -\lambda(x) & -\mu \\ \mu & -\lambda \end{pmatrix} \begin{pmatrix} -\lambda(x) & \mu \\ -\mu & -\lambda \end{pmatrix} \begin{pmatrix} x_1 \\ x_2 \end{pmatrix}} \\
&= \sqrt{(\lambda^2(x) + \mu^2)(x_1^2 + x_2^2)} \\
&= |x| \sqrt{(\lambda^2(x) + \mu^2)}.
\end{aligned}$$

Hence on the set $D = \{x : d_1 \leq |x| \leq d_2\}$,

$$\bar{L}_0 = d_2 \times \sqrt{\max \lambda(x)^2 + \mu^2} = \sqrt{5},$$

$$\underline{L}_0 = d_1 \times \sqrt{\min \lambda(x)^2 + \mu^2} = 1.4.$$

The parameter L_1 was computed numerically to be 90.78. Since $V_x(x) = 2(x_1, x_2)$,

$$M_1 = 2d_2 = 2,$$

$$M_2 = 2.$$

In addition, from (3.57) we see that

$$b = -2 \min_{x \in D} \lambda(x) |x|^2.$$

The minimum is achieved at $x = x_c$ and it is computed to be

$$b = 0.0128.$$

Naturally pick $a = 2$ so that $\Omega = B_\rho(x_c)$. Thus,

$$\epsilon = \mathrm{vol}(\Omega) = \pi\rho^2 \approx 3.14 \times 10^{-4}.$$

Also note that this Ω is completely inside D.

Pick $\eta = 0.6$. It can be calculated that

$$\alpha = M_1 L_1 + \bar{L}_0 M_2 \approx 186,$$

$$\gamma_\eta = \frac{(1-\eta)ac_1}{\alpha + \eta a M_1} \approx 0.0021 \leq 0.0154 = \frac{\underline{L}_0}{L_1},$$

so (3.36) is satisfied. In addition,

$$\eta a c_1 = 0.588 > b,$$

so (3.47) is also satisfied. Hence $\eta = 0.6$ is large enough. We can then compute $\bar{\epsilon}$:

$$\begin{aligned}
\epsilon_1 &= 4\gamma_\eta \frac{\underline{L}_0}{L_1}\left(\pi - \sin^{-1}\left(\frac{L_1\gamma_\eta}{\underline{L}_0}\right)\right) \approx 3.86 \times 10^{-4}. \\
\epsilon_2 &= \frac{2\gamma_\eta \underline{L}_0 (b + \eta a c_1)^2}{\alpha \bar{L}_0 b} \approx 3.95 \times 10^{-4}, \\
\Rightarrow \bar{\epsilon} &= \max\{\epsilon_1, \epsilon_2\} = 3.95 \times 10^{-4}
\end{aligned}$$

Indeed we have

$$\epsilon < \bar{\epsilon}.$$

So all the hypotheses in Theorem 3.2 hold. Meanwhile,

$$h = M_1\gamma_\eta \approx 0.0042$$
$$g\epsilon = \frac{b\text{vol}(\Omega_1)}{2\gamma_\eta \underline{L}_0} \approx 6.9 \times 10^{-4} \ll c_2 - c_1.$$

The conclusions in Theorem 3.2 tell us that the system will converge to the set $\{x : V(x) \leq c_1 + h + g\epsilon\} \approx B_{0.7044}(0)$ if it starts at x_0 with $V(x_0) \leq c_2 - h - g\epsilon \approx 0.9951$.

Discussion of the Example Firstly, because our V is chosen to be quadratic and we know from the earlier discussion in Section 3.2.1 that the convergence of V is exponential, we can further conclude that the convergence of the solution to the ball $B_{0.7044}(0)$ is exponentially fast. In addition, since $\dot{V}(x) = -2V(x)$ for all $x \in B_{0.7044}(0) \cup \{x : V(x) > 0.9951\}$, the system is in fact globally exponentially stable.

It is important to note, as discussed earlier, that in this example $\Omega_0 \neq \emptyset$. By continuity of $\dot{V}$ as a function of states, we know that there will be $x' \in \Omega$ such that $V_x(x') \cdot f(x') = \dot{V}(x') = 0$ (which is in fact on $\partial\Omega_0$). If we do not require the vector field to be non-vanishing, then since $V_x(x) = 2x \neq 0$ for all $x \in D$, we either have $f(x') = 0$ or $V_x(x')$ is orthogonal to $f(x')$. In the first case x' is an equilibrium of the system and we will have a solution $x(t) \equiv x'$, which would not converge to a smaller set and hence the conclusion in Theorem 3.2 is no longer true. This indicates that the additional assumption of non-vanishing (which results in the positive bound $\underline{L}_0$) is indeed crucial to establishing the convergence result.

Recall that the significance of Theorem 3.2 and Theorem 3.3 appears when there are multiple "bad regions" with the volume of each of them bounded above. For instance, by modifying the vector field of the above example such that Ω consists of multiple $B_\rho(x_i)$ regions distributed in D with $|x_i| = 0.8$ for all i, Theorem 3.2 and Theorem 3.3 are still applicable and will lead to the same conclusion.

Nevertheless, the obtained $\bar{\epsilon}$ appears to be rather conservative. One can observe in the above example that the radius of the sweeping ball is quite small as $\gamma_\eta \approx \frac{1}{5}\rho$; as a result, $\bar{\epsilon}$ which is proportional to $\text{vol}(B^{n-1}_{\gamma_\eta})$ becomes very small. It is not hard to see from the proofs

of Lemma 3.2, 3.3 and 3.4 that γ_η is a very coarse bound on the radius of the largest ball that is contained in Ω. More careful analysis can be done on tightening γ_η; however, this may require additional information about system dynamics. Our current assumptions on the system, on the other hand, are rather general.

In addition, once η is chosen, a sweeping ball of constant radius is employed for the analysis. We can make γ_η time-varying based on the level set of Ω_η that x is in. Since it is known that the radius of the sweeping ball becomes larger when $\dot{V}$ becomes positive, $\bar{\epsilon}$ will be larger and this modification should yield a better result. However, difficulties arise in converting the bound (3.37) on the length of a particular trajectory to a (3.38)-like bound on the volume of Ω_1.

Lastly, if we compare Theorem 3.2 to Theorem 3.1, we see that asymptotic stability cannot be recovered from Theorem 3.2 even when $\mathrm{vol}(\Omega) = 0$. This is simply because we must have $c_1 > 0$ in this case such that a neighborhood of origin is taken away from D. In addition one may also think that Theorem 3.2 has some drawbacks as it requires more conditions (existence of positive $\underline{L}_0, b$) to hold than Theorem 3.1; meanwhile, the result of Theorem 3.2 seems to be weaker than that of Theorem 3.1 due to the existence of gap h in all three statements, which unlike $g\epsilon$ in Theorem 3.2 or $R(\epsilon)$ in Theorem 3.1 does not vanish as ϵ goes to 0. Nevertheless, we need to point out that the two $\bar{\epsilon}$'s in both theorems are very different; in fact the $\bar{\epsilon}$ in Theorem 3.1 is very conservative compared with that of Theorem 3.2. As already discussed in the Section 3.2.1, we failed to construct a non-trivial example with $\dot{V}(x) > 0$ for some $x \in D$ which satisfies all the assumptions in Theorem 3.1. The previous example in this section will eventually yield $\bar{\epsilon} < \pi\rho^2$, which implies that Theorem 3.1 is inconclusive for this example. Hence we prefer to apply Theorem 3.2 with a modified region D.

3.3 Study of stability of systems with inputs

In this section we will show how non-monotonic Lyapunov functions can be used to show stability of systems with inputs. To be more precise, we will study how "almost" Lyapunov functions or higher order derivatives of Lyapunov functions can be used to verify if a system

with inputs is ISS. As already mentioned in Section 3.1.1, there are some technical problems when generalizing non-monotonic Lyapunov functions to systems with inputs. As we have seen in Section 3.2, the analysis of "almost" Lyapunov function involves some arguments based on the curvature of the solution trajectories. In the presence of inputs, curvature of the solution trajectories is not well defined and hence we cannot follow the same geometric arguments as we did in the autonomous case. On the other hand, higher order derivatives of Lyapunov functions involve differentiating the inputs with respect to time, which is also not well-defined in general. Nevertheless, in this section we will deploy some modifications to the analysis and show how those technical difficulties can be handled and how those non-monotonic Lyapunov techniques can be generalized to systems with inputs when analyzing their stability. The work was published earlier in [25], [26].

3.3.1 Showing ISS via almost Lyapunov functions

For the simplicity of analysis, in this section we restrict ourselves to time-invariant nonlinear systems with inputs

$$\dot{x} = f(x, u). \tag{3.58}$$

Recall that in the case of an autonomous system, the "bad" set Ω is defined to be the set where $\dot{V}$ is not sufficiently negative. In the presence of inputs, $\dot{V}$ depends on input and when the control value set U is unbounded, $\dot{V}$ can also be unbounded. Nevertheless, as we have pointed out in Lemma 3.1, in order to show (3.58) is ISS, it suffices to show that its auxiliary system is GUAS, whose control value set is a unit ball.

Let $V(x) : \mathbb{R}^n \to \mathbb{R}_{\geq 0}$ be a C^1 function satisfying the "sandwich" condition (3.4) for some $\alpha_1, \alpha_2 \in \mathcal{K}_\infty$. To this end, define

$$V'(x) := \sup_{|d|\leq 1} \{V_x(x) \cdot f_\rho(x, d)\} \tag{3.59}$$

for some $\rho \in \mathcal{K}_\infty$ where we recall that the auxiliary vector field f_ρ is given by (3.12). Similar to the autonomous system case, we say V is an "almost Lyapunov" function if there exists

$a > 0$, a subset $\Omega \subset \mathbb{R}^n$ such that

$$V'(x) \leq -aV(x) \quad \forall x \in \mathbb{R}\backslash\Omega. \tag{3.60}$$

Our question again becomes whether we can show (3.58) to be ISS with an "almost Lyapunov" function and sufficiently "small" Ω.

Quantifying the "smallness" of Ω Although the volume of Ω in Euclidean space is used in our previous work for autonomous systems, it appears to be conservative as discussed earlier. The reason is that we have used some geometrical arguments, such as the length or curvature of the solution trajectories for relating the volume of Ω to the time that the solution can stay inside Ω. In the presence of inputs, such geometrical property of solution trajectories may be unavailable. Instead, in [25] we directly impose assumptions on the Ω *dwell time*:

$$T := \sup_{x_0 \in \Omega, \|d\| \leq 1} \inf_{t \geq 0} \{t : x_\rho(t; x_0, d) \notin \Omega\}, \tag{3.61}$$

where $x_\rho(t; x_0, d)$ represents the solution of the auxiliary system

$$\dot{x} = f_\rho(x, d) \tag{3.62}$$

with initial state x_0 at time 0 and input d. Intuitively T is the longest time that the solution can stay inside Ω. We remark here that only an upper bound of T is needed; depending on the size and shape of Ω and the vector field $f(x, u)$, it can be estimated without computing the solutions of the system. Thus while ignoring the shape, volume or other spatial information of Ω, we treat Ω to be "small" if the Ω dwell time is bounded from above by some small number.

As another remark, the assumption on bounded Ω dwell time can be further developed. A simple situation where this property can be shown is when Ω has finite size in some dimension, and the vector field f over the set Ω has a uniform lower bound on the norm of its projection onto this dimension. In this case the vector field is "transversal" to the set Ω and thus the solutions of the system will pass through it. In general, there is no systematic

way to prove bounded Ω dwell time; in other words, to show that Ω is not an invariant set requires not only extra knowledge of the shape and volume of Ω but also knowledge of the vector field f. This can be developed into a separate work and is an interesting future research direction.

Regularity of V' Note that because the set in the supremum function in (3.59) may be unbounded when $x \in \Omega$, $V'(x)$ may not exist. Nevertheless, under the regularity assumptions of the system (3.62) and the function V, the next lemma not only guarantees the existence of $V'(x)$ for all $x \in \mathbb{R}^n$, it also shows that V' is Lipschitz:

Lemma 3.8. *Let $V : \mathbb{R}^n \to \mathbb{R}_{\geq 0}$ be a C_1 positive definite function and assume the system* (3.62) *has an equilibrium at* 0. *Then V' defined via* (3.59) *exists for all $x \in \mathbb{R}^n$ and is Lipschitz when both $f_\rho(x, d), V_x(x)$ are Lipschitz in x.*

Proof. Let L_1, L_2 be the Lipschitz constants of $f_\rho(x, d), V_x(x)$ over compact set $D \times U, D$, respectively with $D := \{|x| \leq r : x \in \mathbb{R}^n\}$ for some $r > 0$. The equilibrium at $x = 0$ and positive definite C^1 function V imply that $f(0, d) = 0$ for all $d \in U$ and $V_x(0) = 0$. Hence for any $x \in D$ and $d \in U$

$$|f_\rho(x, d)| = |f_\rho(x, d) - f_\rho(0, d)| \leq L_1|x|,$$

$$|V_x(x)| = |V_x(x) - V_x(0)| \leq L_2|x|.$$

Thus $V_x(x) \cdot f_\rho(x, d) \leq L_1 L_2 |x|^2$ and $V'(x)$ defined via (3.59) exists. Let $\epsilon > 0$. Pick some $x_1, x_2 \in D$. Equation (3.59) also means there exists $d_1 \in U$ such that $V'(x_1) <$

$V_x(x_1) \cdot f_\rho(x_1, d_1) + \epsilon$. In addition, we have $V'(x_2) \geq V_x(x_2) \cdot f_\rho(x_2, d_1)$. Hence

$$\begin{aligned}
V'(x_1) - V'(x_2) &< V_x(x_1) \cdot f_\rho(x_1, d_1) - V_x(x_2) \cdot f_\rho(x_2, d_1) + \epsilon \\
&= (V_x(x_1) \cdot f_\rho(x_1, d_1) - V_x(x_1) \cdot f_\rho(x_2, d_1)) \\
&\quad + (V_x(x_1) \cdot f_\rho(x_2, d_1) - V_x(x_2) \cdot f_\rho(x_2, d_1)) + \epsilon \\
&\leq |V_x(x_1)||f_\rho(x_1, d_1) - f_\rho(x_2, d_1)| + |V_x(x_1) - V_x(x_2)||f_\rho(x_2, d_1)| + \epsilon \\
&\leq L_2|x_1|L_1|x_1 - x_2| + L_2|x_1 - x_2|L_1|x_2| + \epsilon \\
&= L_1L_2(|x_1| + |x_2|)|x_1 - x_2| + \epsilon.
\end{aligned}$$

Similarly we can swap x_1, x_2 and get the same bound on $V'(x_2) - V'(x_1)$. Now because this is is true for any arbitrary $\epsilon > 0$, we conclude that

$$|V'(x_1) - V'(x_2)| \leq L_1L_2(|x_1| + |x_2|)|x_1 - x_2|. \tag{3.63}$$

Recall $x_1, x_2 \in D$, which implies $|x_1| \leq r, |x_2| \leq r$. Thus $|V'(x_1) - V'(x_2)| \leq 2L_1L_2r|x_1 - x_2|$ and V' is Lipschitz. □

In the case when Ω is bounded, the next lemma guarantees a uniform, finite upper bound on $|V_x'(x) \cdot f_\rho(x, d)|$ for all $d \in U$ and almost all $x \in \Omega$.

Lemma 3.9. *Let $\Omega \subset \mathbb{R}^n$ be a bounded set, and $V : \mathbb{R}^n \to \mathbb{R}_{\geq 0}$ be a C_1 positive definite function satisfying*

$$a_1|x|^2 \leq V(x) \leq a_2|x|^2 \tag{3.64}$$

for some $a_2 \geq a_1 > 0$. Assume the system (3.62) has an equilibrium at 0. Further assume that $f_\rho(x, d), V_x(x)$ are Lipschitz in x. Let V' be defined via (3.59). Then $V_x'(x)$ exists almost everywhere in Ω. In addition, there exists $c > 0$ such that for all $\xi \in \Omega$ where $V_x'(\xi)$ exists and any $d \in U$,

$$|V_x'(\xi) \cdot f_\rho(\xi, d)| \leq cV(\xi). \tag{3.65}$$

Proof. As V' is Lipschitz by Lemma 3.8, Rademacher's theorem directly concludes that V' is differentiable almost everywhere in Ω. Let $d(\cdot) \equiv d$ be a constant input and denote

$x(t) = x(t;\xi,d)$ for abbreviation. We have

$$|V_x'(\xi)\cdot f_\rho(\xi,d)| = \dot{V}'(x(t))\Big|_{t=0^+} = \lim_{t\to 0^+}\frac{|V'(x(t))-V'(\xi)|}{t}.$$

Let $D\supset\Omega$ be a compact set and L_1, L_2 be the Lipschitz constants for f_ρ, V_x as in the proof of Lemma 3.8, and we conclude from (3.63) that $|V'(x(t))-V'(\xi)|\le L_1L_2(|x(t)|+|\xi|)|x(t)-\xi|$. Note that $\lim_{t\to 0^+}|x(t)| = |x(0)| = \xi$; in addition, since

$$|x(t)-\xi| = \left|\int_0^t f_\rho(x(s),d)ds\right| \le \int_0^t |f_\rho(x(s),d)|ds \le \int_0^t L_1|x(s)|ds,$$

$$\lim_{t\to 0^+}\frac{1}{t}|x(t)-\xi| \le \lim_{t\to 0^+}\frac{L_1}{t}\int_0^t |x(s)|ds = L_1|\xi|.$$

Therefore,

$$\begin{aligned}
|V_x'(\xi)\cdot f_\rho(\xi,d)| &\le \lim_{t\to 0^+}\frac{|V'(x(t))-V'(x)|}{t}\\
&\le L_1L_2\lim_{t\to 0^+}\frac{(|x(t)|+|\xi|)|x(t)-\xi|}{t}\\
&\le L_1L_2\left(\lim_{t\to 0^+}|x(t)|+|\xi|\right)\left(\lim_{t\to 0^+}\frac{1}{t}|x(t)-\xi|\right)\\
&\le 2L_1^2L_2|\xi|^2 \le \frac{2L_1^2L_2}{a_1}V(\xi).
\end{aligned}$$

The lemma is proven with $c = \frac{2L_1^2L_2}{a_1}$. □

We are now ready to present the result for this section:

Theorem 3.4. *Consider a control system* (3.62) *with right-hand side* f_ρ *locally Lipschitz in* x *and compact input value set* $U = B_1^m(0)$. *Let* $V:\mathbb{R}^n\to\mathbb{R}_{\ge 0}$ *be a* C_1 *positive definite function satisfying the condition* (3.64) *for some* $a_2\ge a_1>0$ *and assume* V_x *is also locally Lipschitz. Define* $V'(x)$ *via* (3.59) *and for some* $a>0$, *let* $\Omega\subset\mathbb{R}^n$ *be the set such that* (2.53) *holds. If there exists* $c>0$ *such that* (3.65) *holds for all* $x\in\Omega$ *where* V_x' *exists, then there exists an increasing function* $\alpha:[0,1)\to\mathbb{R}_{\ge 0}$ *with* $\alpha(0)=0, \lim_{t\to 1}\alpha(t)=\infty$ *such that as*

long as the Ω *dwell time* T *defined in* (3.61) *satisfies*

$$T < \frac{1}{\sqrt{c}} \min\left\{\frac{\pi}{2}, \alpha\left(\frac{a}{\sqrt{c}}\right)\right\}, \tag{3.66}$$

then the system (3.62) *is GUAS.*

The explicit formula of α is given by

$$\alpha(t) = \ln\left(\frac{1+t}{1-t}\right) + 2\arccos\left((t^2+1)^{-\frac{1}{2}}\right). \tag{3.67}$$

Implied by the connection between GUAS and ISS as stated in Lemma 3.1, we also have the following corollary:

Corollary 3.5. *Consider a control system* (3.58)*. Let* $V : \mathbb{R}^n \to \mathbb{R}_{\geq 0}$ *be a* C_1 *positive definite function satisfying the condition* (3.64) *for some* $a_2 \geq a_1 > 0$*. If its auxiliary system defined by* $f_\rho(x, d) := f(x, \rho(|x|)d)$ *with some* $\rho \in \mathcal{K}_\infty$ *satisfies all the hypotheses in Theorem 3.4, then the system* (3.58) *is ISS.*

Proof. We start by making some direct observations of the hypotheses of Theorem 3.4 here. The definition (3.59) means that at any time t, the time derivative of V along any solution $x(\cdot, x_0, u)$ satisfies:

$$\dot{V}(x(t; x_0, u)) \leq V'(x(t; x_0, u)) \tag{3.68}$$

for all $t \geq 0$. Suppose there exists $t_2 > t_1 \geq 0$ such that the solution trajectory enters Ω at t_1 and leaves at t_2; that is, $x(t; x_0, u) \in \Omega$ for all $t \in (t_1, t_2)$ and $x(t_1, x_0, u), x(t_2, x_0, u) \in \partial\Omega$, the boundary of Ω. By definition (3.61) we have $t_2 - t_1 \leq T$. Thanks to Lemma 1 in [77], the properties that $V'_x(x)$ exists almost everywhere in Ω and (3.65) holds for all $x \in \Omega$ where $V'_x(x)$ exists imply that $V(x(\cdot, x_0, u))$ is absolutely continuous as long as $t \in (t_1, t_2)$ so that $x(t; x_0, u) \in \Omega$. In addition whenever $\dot{V}'(x(t; x_0, u))$ exists,

$$-cV(x(t; x_0, u)) \leq \dot{V}'(x(t; x_0, u)) \leq cV(x(t; x_0, u)). \tag{3.69}$$

Fix $x_0 \in \mathbb{R}^n, u \in \mathcal{M}_U$. Write $V(t), V'(t)$ for abbreviation of $V(x(t; x_0, u))$, $V'(x(t; x_0, u))$. A necessary condition for (3.68), (3.69) to hold is the existence of essentially non-negative

functions $w_1(t), w_2(t), w_3(t)$ defined over (t_1, t_2) such that

$$\dot{V}(t) = V'(t) - w_1(t), \tag{3.70}$$

$$\dot{V}'(t) = cV(t) - w_2(t), \tag{3.71}$$

$$\dot{V}'(t) = -cV(t) + w_3(t). \tag{3.72}$$

Because V, V' are continuous, the above equations can be extended to $[t_1, t_2]$. In addition, because $x(t; x_0, u) \in \partial\Omega$ when $t = t_1$ or t_2, by continuity of V' and the property (2.53), we have

$$V'(t_1) \leq -aV(t_1), \tag{3.73}$$

$$V'(t_2) \leq -aV(t_2). \tag{3.74}$$

Our goal is to show that whenever the solution passes through Ω, $\frac{V(t_2)}{V(t_1)} < 1$. This can be achieved by picking a time $t \in (t_1, t_2)$ and bounding $\frac{V(t)}{V(t_1)}$, $\frac{V(t_2)}{V(t)}$ separately.

We bound $\frac{V(t)}{V(t_1)}$ first. From (3.70),(3.71), we have

$$\begin{pmatrix} \dot{V} \\ \dot{V}' \end{pmatrix} = A_1 \begin{pmatrix} V \\ V' \end{pmatrix} - \begin{pmatrix} w_1 \\ w_2 \end{pmatrix}, \quad A_1 = \begin{pmatrix} 0 & 1 \\ c & 0 \end{pmatrix}.$$

Propagating the solutions from t_1 to t, we have

$$\begin{pmatrix} V(t) \\ V'(t) \end{pmatrix} = e^{A_1(t-t_1)} \begin{pmatrix} V(t_1) \\ V'(t_1) \end{pmatrix} - \int_{t_1}^{t} e^{A_1(t-s)} \begin{pmatrix} w_1(s) \\ w_2(s) \end{pmatrix} ds, \tag{3.75}$$

where

$$e^{A_1 t} = \begin{pmatrix} \cosh\sqrt{c}t & \frac{1}{\sqrt{c}}\sinh\sqrt{c}t \\ \sqrt{c}\sinh\sqrt{c}t & \cosh\sqrt{c}t \end{pmatrix}.$$

Note that for any $s \in [t_1, t]$, the two elements in the first row of $e^{A_1(t-s)}$ are non-negative. In addition, recall that w_1, w_2 are non-negative; thus the integration in (3.75) gives a vector whose first element is always non-negative and because it is subtracted on the right, it implies

that

$$\begin{aligned} V(t) &\leq \cosh\sqrt{c}(t-t_1)V(t_1) + \frac{1}{\sqrt{c}}\sinh\sqrt{c}(t-t_1)V'(t_1) \\ &\leq \left(\cosh\sqrt{c}(t-t_1) - \frac{a}{\sqrt{c}}\sinh\sqrt{c}(t-t_1)\right)V(t_1) \\ &=: R_1(t-t_1)V(t_1), \end{aligned}$$

where (3.73) and the fact that $\sinh\sqrt{c}(t-t_1)$ is non-negative are used for the second inequality. Thus we have $\frac{V(t)}{V(t_1)} \leq R_1(t-t_1)$ for all $t \in [t_1, t_2]$.

Some observations can be made on the function $R_1(t)$. Firstly,

$$\dot{R}_1(t) = \sqrt{c}\sinh\sqrt{c}t - a\cosh\sqrt{c}t = -\frac{1}{2}\left((a-\sqrt{c})e^{\sqrt{c}t} + (a+\sqrt{c})e^{-\sqrt{c}t}\right).$$

The case $c \leq a^2$ is less interesting since then $\dot{R}_1(t) < 0$ for all $t \geq 0$ and $R_1(t)$ is a strictly decreasing function. By picking $t = t_2$ we directly conclude that $\frac{V(t_2)}{V(t_1)} < 1$. In the other case when $c > a^2$,

$$R_1(t) = \frac{1}{2}\left(\left(1 - \frac{a}{\sqrt{c}}\right)e^{\sqrt{c}t} + \left(1 + \frac{a}{\sqrt{c}}\right)e^{-\sqrt{c}t}\right)$$

and we have $R_1(t) > 0$ for all $t \geq 0$, $R_1(0) = 1$, $\dot{R}_1(0) = -a$, $\lim_{t\to\infty} R_1(t) = \infty$ and $\ddot{R}_1(t) = cR_1(t) > 0$. These properties imply that $R(t)$ is convex over $\mathbb{R}_{\geq 0}$, and $R(t) = 1$ has two solutions, one at $t = 0$. Denote the other one t_1^*, $t_1^* > 0$. We also have

$$R_1(t) < 1 \quad \forall t \in (0, t_1^*). \tag{3.76}$$

The graphical illustration of function $R_1(t-t_1)$ with $a = 1, c = 6$ is shown as the blue curve in Fig. 3.5. In fact, t_1^* can be computed analytically:

$$t_1^* = \frac{1}{\sqrt{c}}\ln\frac{\sqrt{c}+a}{\sqrt{c}-a} = \frac{1}{\sqrt{c}}\ln\left(\frac{1+\frac{a}{\sqrt{c}}}{1-\frac{a}{\sqrt{c}}}\right) =: \frac{1}{\sqrt{c}}\alpha_1\left(\frac{a}{\sqrt{c}}\right) \tag{3.77}$$

and it is not hard to check that $\alpha_1(0) = 0, \lim_{t\to 1}\alpha_1(t) = \infty$.

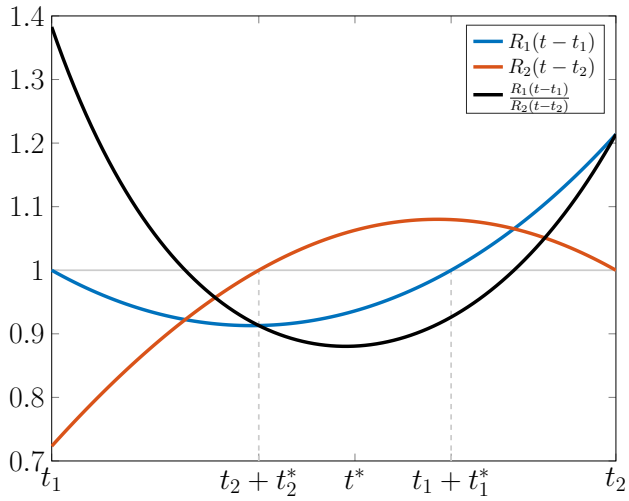

Figure 3.5: Functions R_1, R_2 and R_1/R_2.

Similarly when bounding $\frac{V(t_2)}{V(t)}$, consider the linear system given by (3.70),(3.72):

$$\begin{pmatrix} \dot{V} \\ \dot{V}' \end{pmatrix} = A_2 \begin{pmatrix} V \\ V' \end{pmatrix} + \begin{pmatrix} -w_1 \\ w_3 \end{pmatrix}, \quad A_2 = \begin{pmatrix} 0 & 1 \\ -c & 0 \end{pmatrix}.$$

Propagating the solutions backwards from t_2 to t, we have

$$\begin{pmatrix} V(t) \\ V'(t) \end{pmatrix} = e^{A_2(t-t_2)} \begin{pmatrix} V(t_2) \\ V'(t_2) \end{pmatrix} + \int_{t_2}^{t} e^{A_2(t-s)} \begin{pmatrix} -w_1(s) \\ w_3(s) \end{pmatrix} ds, \tag{3.78}$$

where

$$e^{A_2 t} = \begin{pmatrix} \cos\sqrt{c}t & \frac{1}{\sqrt{c}}\sin\sqrt{c}t \\ -\sqrt{c}\sin\sqrt{c}t & \cos\sqrt{c}t \end{pmatrix}.$$

This case is a bit more complicated compared with the previous case as the elements in $e^{A_2 t}$ are sign indefinite for all $t \leq 0$. Nevertheless, our assumption (3.66) assures that $t_2 - t_1 < \frac{\pi}{2\sqrt{c}}$. As a result, for all $s \in [t, t_2]$, $\sqrt{c}(s - t_2) \in (-\frac{\pi}{2}, 0]$ and thus $\cos(\sqrt{c}(s-t_2)) > 0$, $\sin(\sqrt{c}(s-t_2)) \leq 0$. In addition, note that the integration in (3.78) is backwards and recall that w_1, w_3 are non-negative; hence, the first element of the vector obtained after integration is always non-negative. Because it is added on the right-hand side in (3.78), we

have

$$\begin{aligned} V(t) &\geq \cos\sqrt{c}(t-t_2)V(t_2) + \frac{1}{\sqrt{c}}\sin\sqrt{c}(t-t_2)V'(t_2) \\ &\geq \left(\cos\sqrt{c}(t-t_2) - \frac{a}{\sqrt{c}}\sin\sqrt{c}(t-t_2)\right)V(t_2) \\ &:= R_2(t-t_2)V(t_2), \end{aligned}$$

where (3.74) and the fact $\sin\sqrt{c}(t-t_2)$ is non-positive are used for the second inequality. Thus we have $\frac{V(t)}{V(t_2)} \geq R_2(t-t_2)$ for all $t \in [t_1, t_2]$.

Recall that we are only interested in the non-trivial case when $c > a^2$ (otherwise we already have $\frac{V(t_2)}{V(t_1)} < 1$ as in the discussion for R_1). Some observations can be made on $R_2(t)$: $R_2(0) = 1$, $\dot{R}_2(0) = -a$, $R_2(-\frac{\pi}{2\sqrt{c}}) = \frac{a}{\sqrt{c}} < 1$. In addition, for all $t \in [-\frac{\pi}{2\sqrt{c}}, 0]$, $R_2(t) > 0$ and $\ddot{R}_2(t) = -cR_2(t) < 0$. Hence $R_2(t)$ is concave over $[-\frac{\pi}{2\sqrt{c}}, 0]$, and $R_2(t) = 1$ have two solutions, one at $t = 0$. Denote the other by t_2^*, $t_2^* < 0$. We also have that

$$R_2(t) > 1 \quad \forall t \in (t_2^*, 0). \tag{3.79}$$

The function $R_2(t-t_2)$ with $a = 1, c = 6$ is plotted as the red curve in Fig. 3.5. Similarly to t_1^*, t_2^* can also be computed analytically:

$$t_2^* = -\frac{2}{\sqrt{c}}\arccos\sqrt{\frac{c}{a^2+c}} = -\frac{2}{\sqrt{c}}\arccos\left(\left(\frac{a}{\sqrt{c}}\right)^2 + 1\right)^{-\frac{1}{2}} =: -\frac{1}{\sqrt{c}}\alpha_2\left(\frac{a}{\sqrt{c}}\right). \tag{3.80}$$

We find that α_2 is an increasing function such that $\alpha_2(0) = 0, \alpha_2(1) = \frac{\pi}{2}$.

Define $\alpha := \alpha_1 + \alpha_2$. By this construction α satisfies the hypothesis in Theorem 3.4. The assumption (3.66) also implies that

$$t_2 - t_1 \leq T < \frac{1}{\sqrt{c}}\alpha\left(\frac{a}{\sqrt{c}}\right) = \left(\frac{1}{\sqrt{c}}\alpha_1\left(\frac{a}{\sqrt{c}}\right)\right) - \left(-\frac{1}{\sqrt{c}}\alpha_2\left(\frac{a}{\sqrt{c}}\right)\right) = t_1^* - t_2^*. \tag{3.81}$$

Thus $t_1 + t_1^* > t_2 + t_2^*$ and the interval $(\max\{t_1, t_2 + t_2^*\}, \min\{t_2, t_1 + t_1^*\}) = (t_1, t_1 + t_1^*) \cap$

$(t_2 + t_2^*, t_2)$ is non-empty. Pick some point t^* in that interval by defining

$$t^* := (1-\zeta)\max\{t_1, t_2 + t_2^*\} + \zeta \min\{t_2, t_1 + t_1^*\} \tag{3.82}$$

for some $\zeta \in (0,1)$. Now write $s = t_2 - t_1$, then (3.82) becomes $t^* = t_1 + (1-\zeta)\max\{0, s + t_2^*\} + \zeta \min\{s, t_1^*\}$. When $s \leq \min\{-t_2^*, t_1^*\}$, this reduces to $t^* = t_1 + \zeta s$. Define

$$h(s) := \frac{R_1(t^* - t_1)}{R_2(t^* - t_1 - s)}.$$

Since R_1, R_2 are smooth and positive, so is $h(s)$ over the domain $[0,T]$. We also have $h(0) = \frac{R_1(0)}{R_2(0)} = 1$. Recall that $t^* = t_1 + \zeta s$ when s is small, so

$$h'(0) = \frac{d}{ds}\left(\frac{R_1(\zeta s)}{R_2((\zeta-1)s)}\right)\bigg|_{s=0} = \frac{\zeta \dot{R}_1(0) R_2(0) - (\zeta-1) R_1(0) \dot{R}_2(0)}{(R_2(0))^2} = -a.$$

In addition, $t^* \in (t_1, t_1 + t_1^*) \cap (t_2 + t_2^*, t_2)$ by its definition (3.82), so (3.76) and (3.79) imply $R_1(t^* - t_1) < 1, R_2(t^* - t_1 - s) > 1$; hence $h(s) < 1$ for all $s \in (0,T]$. It can also be seen from the black curve in Fig. 3.5 that $\frac{R(t^* - t_1)}{R_2(t^* - t_2)} < 1$. The next lemma claims that $h(s)$ is in fact bounded from above by some exponentially decaying function:

Lemma 3.10. *Let $h : [0,T] \to \mathbb{R}$ be a continuous function such that $h(0) = 1$ and $h(s) \in (0,1)$ for all $s \in (0,T]$. Suppose $h(s)$ is differentiable at 0 and $h'(0) = -a$. Then there exists $\eta \in (0,1]$ such that for all $s \in [0,T]$, $h(s) \leq e^{-\eta a s}$.*

Proof. Define $\phi : (0,T] \to \mathbb{R}$ by $\phi(s) := -\frac{\ln(h(s))}{as}$. It is continuous since $h(s)$ is continuous over $(0,T]$. As $h(s) \in (0,1)$ for all $s \in (0,T]$, $\ln(h(s)) < 0$ and so $\phi(s) > 0$ for all $s \in (0,T]$. Extend $\phi(s)$ continuously to $s = 0$ and by L'Hospital's rule we have

$$\phi(0) = \lim_{s \to 0^+} -\frac{\ln(h(s))}{at} = \lim_{s \to 0^+} -\frac{h'(s)}{a h(s)} = 1.$$

Let $\eta := \min_{s \in [0,T]} \phi(s)$, existence guaranteed by Weierstrass extreme value theorem, and $\eta > 0$ since $\phi(s) > 0$ for all $s \in [0,T]$. In addition, $\eta \leq \phi(0) = 1$. By construction, $\eta \leq -\frac{\ln(h(s))}{at}$ and thus $h(s) \leq e^{-\eta a s}$ for all $s \in [0,T]$. □

As a result, as long as $t_2 - t_1 \leq T$,

$$\frac{V(t_2)}{V(t_1)} \leq \left(\frac{V(t^*)}{V(t_1)}\right)\left(\frac{V(t_2)}{V(t^*)}\right) \leq \frac{R_1(t^* - t_1)}{R_2(t^* - t_2)} = h(t_2 - t_1) \leq e^{-\eta a(t_2 - t_1)}. \tag{3.83}$$

Finally consider the solution $x(\cdot, x_0, u)$ of the system (3.62) from time 0 to t. At each time it either stays in $\mathbb{R}^n \backslash \Omega$ and according to (2.53) that $V(x(\cdot, x_0, u))$ decreases at exponential rate $-a$, or it will pass through Ω over some time interval (t_1, t_2), where $V(x(\cdot, x_0, u))$ is decreased by the ratio $e^{-\eta a(t_2 - t_1)}$ from (3.83). Cascading them together we see that $V(x(\cdot, x_0, u))$ decreases at exponential rate bounded from above by $-\eta a$. There may be overshoots in V, due to the possibilities that $x_0 \in \Omega$ or $x(t; x_0, u) \in \Omega$. Compared with the exponential decaying rate $-\eta a$, the overshoot in the first possibility is bounded by $(\min_{t\in[-T,0]} R_2(t))^{-1} e^{\eta a T}$ and the overshoot in the second possibility is bounded by $\max_{t\in[0,T]} R_1(t) e^{\eta a T}$. As a result, we will have

$$V(x(t, x_0)) \leq C e^{-\eta a t} V(x_0)$$

for any $x_0 \in \mathbb{R}^n$ and $u \in \mathcal{M}_U$, where $C = \frac{\max_{t\in[0,T]} R_1(t)}{\min_{t\in[-T,0]} R_2(t)} e^{2\eta a T}$. Therefore the system (3.62) is GUAS. □

Example Consider the two-dimensional system with inputs $u \in \mathbb{R}^2$:

$$\dot{x} = \begin{pmatrix} -\lambda(x) & -\mu \\ \mu & -\lambda(x) \end{pmatrix} x + u =: A(x)x + u \tag{3.84}$$

where

$$\lambda(x) = \left(\frac{a+b}{2}\right) \min\left\{\frac{|x - x_c|}{r}, 1\right\} - \frac{b}{2} + k \tag{3.85}$$

for some $a, b, k, r > 0, x_c \in \mathbb{R}^2$. This is modified from the autonomous system example in Section 3.2.3 by adding inputs.

If λ is a constant and when $u = 0$, it is easy to see by changing into polar coordinates that the solution of the system (3.84) is converging to the origin along a spiral trajectory. Moreover, the tangential velocity is μ counter-clockwise and the radial velocity is $\lambda|x|$ towards

the origin. The dependence of λ on x as described in the definition (3.85) perturbs the spiral vector field in the region

$$\Omega = \{x \in \mathbb{R}^2 : |x - x_c| < r\}.$$

Pick the standard $V = \frac{1}{2}|x|^2$ and define $\rho \in \mathcal{K}_\infty$ by $\rho(s) = ks$. The auxiliary system thus is

$$\dot{x} = A(x)x + k|x|d, \quad |d| \leq 1.$$

In this case,

$$\begin{aligned}\dot{V}(x) = x \cdot (A(x)x + k|x|u) &= -\lambda(x)|x|^2 + k|x|x \cdot u \\ &\leq (-\lambda(x) + k)|x|^2 = 2(-\lambda(x) + k)V(x) =: V'(x).\end{aligned}$$

In addition, since $\lambda(x) = \frac{a}{2} + k$ for all $x \in \mathbb{R}^2 \backslash \Omega$, we have

$$V'(x) \leq -aV(x) \quad \forall x \in \mathbb{R}^2 \backslash \Omega,$$

exactly the same as the required assumption (2.53). Note that when $x \in \Omega$, $V'(x) > -aV(x)$ and in particular when $x = x_c$, $V'(x) = bV(x) > 0$ so the classical Lyapunov theorem is not applicable here. In order to apply our Theorem 3.4, we need to compute the upper bound on $|V'_x \cdot (A(x)x + u)|$. We differentiate $\lambda(x)$ for $x \in \Omega$ first. Note that in this case (3.85) implies $\lambda(x) = \frac{(a+b)|x-x_c|}{2r} - \frac{b}{2} + k \leq \frac{a}{2} + k$ and

$$\nabla\lambda(x) = \frac{(a+b)(x - x_c)}{2r|x - x_c|},$$

which exists everywhere in Ω except for $x = x_c$. Hence

$$\begin{aligned}
|\nabla V' \cdot (A(x)x + k|x|d)| &= 2|(-\nabla\lambda(x)V(x) \\
&\quad + (-\lambda(x) + k)V_x(x)) \cdot (A(x)x + k|x|d)| \\
&= 2\left|\left((-\frac{(a+b)(x-x_c)}{2r|x-x_c|}V(x) + (-\lambda(x)+k)x\right)(A(x)x + k|x|d)\right| \\
&\leq \left|\frac{(a+b)(x-x_c)}{r|x-x_c|} \cdot (A(x)x + k|x|d)\right| V(x) + 2|(-\lambda(x)+k)x \cdot (A(x)x + k|x|d)| \\
&\leq \frac{(a+b)}{r}(\|A(x)\| + k)|x|V(x) + 2| - \lambda(x) + k||x \cdot (A(x)x + k|x|d)| \\
&\leq \frac{(a+b)}{r}(k + \sqrt{\lambda(x)^2 + \mu^2})(|x_c| + r)V(x) + 4| - \lambda(x) + k|^2 V(x) \\
&\leq \left(\frac{(a+b)}{r}\left(k + \sqrt{\left(\frac{a}{2} + k\right)^2 + \mu^2}\right)(|x_c| + r) + a^2\right)V(x).
\end{aligned}$$

We take $c = \frac{(a+b)}{r}\left(k + \sqrt{\left(\frac{a}{2} + k\right)^2 + \mu^2}\right)(|x_c| + r) + a^2$ so that (3.65) holds for all $x \in \Omega\backslash\{x_c\}$. Automatically we have $c > a^2$. For the Ω dwell time, recall the solution of the system (3.84) is rotating at constant tangential velocity μ. Also Ω is bounded in a sector with center angle $2\arcsin\frac{r}{|x_c|}$ so $T \leq \frac{2}{\mu}\arcsin\frac{r}{|x_c|}$.

Take numerical values $a = 1, b = 0.5, k = 0.1, r = 0.1, \mu = 2$ and $x_c = \begin{pmatrix} 0.8 \\ 0 \end{pmatrix}$. It is then computed $c \approx 30.54$ and $T < 0.125$. In addition, $\frac{\pi}{2\sqrt{c}} \approx 0.284$ and eventually by (3.81) and the formulas (3.67), we find

$$\frac{1}{\sqrt{c}}\alpha\left(\frac{a}{\sqrt{c}}\right) \approx 0.131.$$

Thus $T < \frac{1}{\sqrt{c}}\min\left\{\frac{\pi}{2}, \alpha\left(\frac{a}{\sqrt{c}}\right)\right\}$ and the system (3.84) is exp-ISS with linear ISS gain $\rho^{-1} = \frac{1}{k} = 10$. The vector field $A(x)x$ is shown in Fig. 3.6 by the blue arrows. Ω is the red shaded region. A solution generated with constant input $u = \begin{pmatrix} 0.01 \\ 0 \end{pmatrix}$ and initial state $x_0 = \begin{pmatrix} 0.9 \\ -0.4 \end{pmatrix}$ is drawn by the black curve in the figure. Although it is temporarily affected by the distorted vector field in Ω, the solution passes through Ω and eventually converges to the ball $|x| \leq 10|u| = 0.1$, determined by the ISS gain and shown as the green circle in

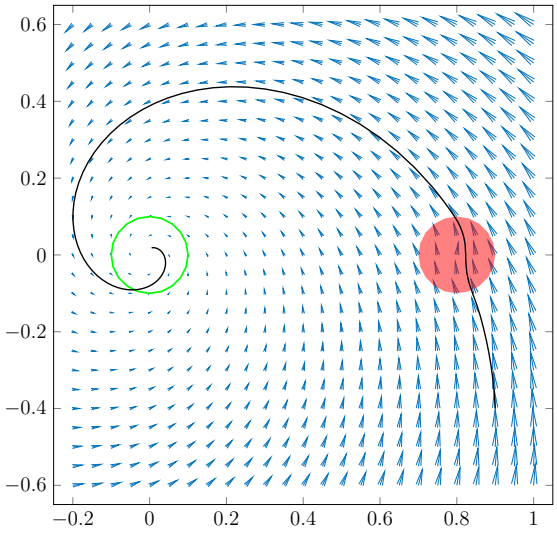

Figure 3.6: An illustration of the system (3.84) solution.

Fig. 3.6. Compared with the analysis in Section 3.2.3, we observe that while all the other parameters are kept the same, the radius of Ω, $r = 0.1$ is much larger than the old one (which was 0.01) and the maximum increasing rate of V, $b = 0.5$ is also much larger than the old one (which was 0.01). Hence not only is the proposed Theorem 3.4 capable of dealing with the stability of systems with inputs, it is less conservative and able to address "worse behavior" systems.

3.3.2 Showing ISS via higher order derivatives of Lyapunov functions

In this subsection we will switch gears and use higher order derivatives of Lyapunov functions to analyze the stability of a time-varying system with inputs (3.7).

Sign definite functions For convenience we adopt some definitions of sign definite functions for a function $P(x) : \mathbb{R}^n \to \mathbb{R}$. We say P is *positive definite* ($P \succ 0$) if $P(0) = 0$ and $P(x) > 0$ when $x \neq 0$. We say P is *positive semi-definite* ($P \succeq 0$) if $P(0) = 0$ and $P(x) \geq 0$ when $x \neq 0$. P is said to be *negative definite* ($P \prec 0$) or *negative semi-definite* ($P \preceq 0$), if $-P$ is positive definite or positive semi-definite, respectively. We say P is *sign indefinite* if P is neither positive semi-definite nor negative semi-definite. In addition for a

function $V(t,x):\mathbb{R}\times\mathbb{R}^n\to\mathbb{R}$, we abuse the same terminology and say $V(t,x)\succ 0$ positive definite if there exists a positive definite function $P(x):\mathbb{R}^n\to\mathbb{R}$ and $V(t,x)\geq P(x)$ for all $t\in\mathbb{R}, x\in\mathbb{R}^n$. This convention for $V(t,x)$ is generalized to negative definite, semi-definite or sign indefinite functions. We also write $P\succ Q$ if $P-Q\succ 0$ and similar notations for the other sign definite relations.

Construction of higher order derivatives of V We start with a quick review of how higher order derivatives of Lyapunov functions can be used to show stability of an autonomous system (3.2).

Theorem 3.5. *Let $V(x):\mathbb{R}^n\to\mathbb{R}_{\geq 0}$ be a function satisfying the condition* (3.4) *for some $\alpha_1,\alpha_2\in\mathcal{K}_\infty$. If there exists $m\in\mathbb{N}_{\geq 2}$ and $a_1,\cdots a_{m-1}\geq 0$ such that V is $m-1$ times differentiable and f is $m-2$ times differentiable and*

$$V^{(m)}+a_{m-1}V^{(m-1)}+\cdots+a_1\dot{V}\prec 0, \tag{3.86}$$

then (3.2) *is GAS.*

The theorem is taken from [71] and the readers can find the proof in that paper. Nevertheless, as an intuitive interpretation of the theorem, (3.86) implies that at least one of the higher order derivatives of V has to be negative definite, say $V^{(i)}$. This means $V^{(i-1)}$ is decreasing when evaluated along a solution and it has to be eventually negative as well. Recursively V itself is asymptotically decreasing and hence the origin is asymptotically stable.

When extending this idea to systems with inputs (3.7) and higher order derivatives of V in [26], there are two technical issues that need to be resolved. First, if we use the same definition in (3.10) for "$\dot{V}$", it will become input dependent and hence undesired for our study because our GUAS property is uniform with respect to input. A good way to get rid of the dependence on u is to take the supremum of those "$\dot{V}$" with respect to u:

$$V_1(t,x):=\frac{\partial V(t,x)}{\partial t}+\sup_{u\in U}\left(\frac{\partial V(t,x)}{\partial x}f(t,x,u)\right).$$

This V_1 seems to be a good candidate for our first-order derivative of V for the system (3.7).

The second technical issue is that we cannot directly differentiate V twice along a solution in order to get an expression for the second-order derivative because it involves the derivative of u with respect to t, which may not even exist as u is not assumed to be differentiable. On the other hand, we cannot differentiate V_1 to get the second-order derivative either because differentiability of V_1 is unclear due the sup function used in its definition. Note that we only need upper bounds for the derivatives; they do not need to be tight and thus a solution to this technical issue is by finding a smooth upper bound $v_1 \succeq V_1$. This v_1 will be the actual first-order derivative of V used for our analysis. An advantage of using smooth functions is that they can be used to generate the subsequent higher order derivatives. In other words, we define $v_0(t,x) := V(t,x)$, and for all $i = 1, 2, \cdots$, iteratively define and construct

$$\begin{aligned} &V_i(t,x) := \frac{\partial v_{i-1}(t,x)}{\partial t} + \sup_{u\in U}\left(\frac{\partial v_{i-1}(t,x)}{\partial x} f(t,x,u)\right), \\ &v_i(t,x) \in C^1(\mathbb{R}_{\geq 0}\times\mathbb{R}^n) \text{ s.t. } v_i \succeq V_i. \end{aligned} \tag{3.87}$$

We call those v_i functions the higher order derivatives of V if they exist. We say the higher order derivatives of V up to order m are *globally decrescent* if there exists $\phi' \in \mathcal{K}_\infty$ such that

$$v_i(t,x) \leq \phi'(|x|) \quad \forall t \geq t_0, x \in \mathbb{R}^n, i = 0, \cdots m.$$

Because of the assumption (3.9) on V, it is equivalent to write the above requirements in a compact form:

$$v_i \preceq \phi(V) \quad \forall i = 0, \cdots m \tag{3.88}$$

for some $\phi \in \mathcal{K}_\infty$. Now suppose for some $m \in \mathbb{N}$, there exist

$$a_0 > 0,\ a_i \geq 0 \quad \forall i = 1, \cdots, m \tag{3.89}$$

such that

$$\sum_{i=0}^{m} a_i v_i \preceq 0, \tag{3.90}$$

and we want to conclude stability properties for the system. They are summarized as our

main theorem in this subsection:

Theorem 3.6. *Given a system* (3.7) *and a positive definite function* $V(t,x)$ *satisfying* (3.9)*, generate the higher order derivatives* v_i *via* (3.87) *by* f *and* V*. If the global decrescent condition* (3.88) *is satisfied and* (3.90) *holds for some* $m \in \mathbb{N}$ *with* a_i*'s satisfying* (3.89)*, then the system* (3.7) *is GUAS.*

Inspired by Lemma 3.1, we also conclude a result on showing ISS of the system (3.7) via higher order derivatives of V:

Corollary 3.6. *Given a system* (3.7) *and a positive definite function* $V(t,x)$ *satisfying* (3.9)*, generate the higher order derivatives* v_i *via* (3.87) *by* f' *and* V *where* f' *is defined in* (3.12) *with some* $\rho \in \mathcal{K}_\infty$*. If all the hypotheses in Theorem 3.6 are satisfied, then the system* (3.7) *is ISS.*

In the case when both V and f are smooth enough and there are no inputs, v_i's reduce to the usual higher order derivatives of V. When the equality in (3.90) is achieved everywhere, it becomes a linear differential equation

$$a_m v^{(m)} + \cdots + a_1 \dot{v} + a_0 = 0, \tag{3.91}$$

which is associated with a characteristic polynomial

$$a_m s^m + \cdots + a_1 s + a_0 = 0. \tag{3.92}$$

Recall that (3.89) is only a necessary condition for the above polynomial to be Hurwitz. This means that it is possible that there exist some a_i's satisfying (3.89) but a solution $v(t)$ of (3.91) diverges as t increases. Since $v(t)$ also satisfies the differential relation (3.90), at a first glance it contradicts the result in Theorem 3.6 that the system is GUAS. However, we argue that this v cannot be a positive definite Lyapunov function and hence Theorem 3.6 is not conflicted. Note that (3.92) has no non-negative real roots when the coefficients satisfy (3.89). It then must have positive complex roots if the solution of (3.91) diverges. Hence

$v(t)$ will oscillate stronger and stronger in order to diverge, so $v(t)$ will become negative for some t large enough. In other words:

Corollary 3.7. *If the characteristic polynomial* (3.92) *of the linear differential equation* (3.91) *is not Hurwitz but the coefficients a_i's satisfy the condition* (3.89)*, then the solution of* (3.91) *with any initial condition $v(0) > 0$ has to be negative for some $t > 0$.*

Without loss of generality we can always assume v_m is the highest order term in (3.90) with non-zero coefficient a_m. By scaling we can also assume that $a_m = 1$. Consider a solution $x(t; x_0, u)$ with arbitrary initial condition $x_0 \in \mathbb{R}^n$ and $u \in M_U$. Simplify the notation with $x(t) = x(t; x_0, u)$, representing the state of the system at time t. By the construction (3.87) we see that for all $t \geq t_0, i \in \mathbb{N}$,

$$\dot{v}_{i-1}(t, x(t)) = \frac{\partial v_{i-1}(t, x(t))}{\partial t} + \frac{\partial v_{i-1}(t, x(t))}{\partial x} \cdot f(t, x(t), u(t)) \leq v_i(t, x(t)), \tag{3.93}$$

which can be written as $\dot{v}_{i-1} \preceq v_i$ in short. Interesting results can be developed based on this sequence of first-order differential relations.

Lemma 3.11. *Let $x(t)$ be an arbitrary solution of system* (3.7) *with $t_0 = 0$. Under assumptions* (3.89) *and* (3.90)*, for any $b > 0$ if $v_0(t, x(t)) \geq b$ for all $t \in [0, T]$ for some $T \geq 0$, then*

$$v_0(t, x(t)) \leq -b \sum_{j=1}^{m} a_{m-j} \frac{t^j}{j!} + \sum_{j=0}^{m-1} \sum_{i=0}^{j} \frac{t^j}{j!} a_{m+i-j} v_i(0, x_0) \tag{3.94}$$

for all $t \in [0, T]$.

Proof. This proof is inspired by the work in [71]. We claim that for any $k = 0, 1, \cdots m-1$,

$$\sum_{i=1}^{m-k} a_{i+k} v_{i-1}(t, x(t)) \leq -b \sum_{j=1}^{k+1} a_{k+1-j} \frac{t^j}{j!} + \sum_{j=0}^{k} \sum_{i=0}^{m-k-1+j} \frac{t^j}{j!} a_{i+k-j+1} v_i(0, x_0). \tag{3.95}$$

Recall we have safely assumed $a_m = 1$ so (3.94) is simply the incidence when $k = m - 1$. We use mathematical induction to prove the claim (3.95). First, for $k = 0$, we need to show that

$$\sum_{i=1}^{m} a_i v_{i-1}(t, x(t)) \leq -b a_0 t + \sum_{i=0}^{m-1} a_{i+1} v_i(0, x_0). \tag{3.96}$$

To show that, we plug (3.93) into (3.90):

$$a_0 v_0(t, x(t)) + \sum_{i=1}^{m} a_i \dot{v}_{i-1}(t, x(t)) \leq \sum_{i=0}^{m} a_i v_i(t, x(t)) \leq 0.$$

Shift the v_0 term to the right, integrate both sides from 0 to t and recall that $a_0 > 0, v_0(\tau, x(\tau)) \geq b$,

$$\sum_{i=1}^{m} a_i \Big(v_{i-1}(t, x(t)) - v_{i-1}(0, x_0) \Big) \leq -a_0 \int_0^t v_0(\tau, x(\tau)) d\tau \leq -b a_0 t.$$

Shift the initial terms $v_{i-1}(0, x_0)$ to the right and increase their indices by 1 and we have proven (3.96).

Second, suppose (3.95) holds for some $k = 0, 1, \ldots, m-2$. We show that (3.95) also holds for the incidence $k+1$. To do that, we plug (3.93) into (3.95):

$$\begin{aligned} a_{1+k} v_0(t, x(t)) + \sum_{i=2}^{m-k} a_{i+k} \dot{v}_{i-2}(t, x(t)) &\leq \sum_{i=1}^{m-k} a_{i+k} v_{i-1}(t, x(t)) \\ &\leq -b \sum_{j=1}^{k+1} a_{k+1-j} \frac{t^j}{j!} + \sum_{j=0}^{k} \sum_{i=0}^{m-k-1+j} \frac{t^j}{j!} a_{i+k-j+1} v_i(0, x_0). \end{aligned}$$

Shift the v_0 term to the right, integrate both sides from 0 to t and recall that $a_{1+k} \geq 0, v_0(\tau, x(\tau)) \geq b$,

$$\begin{aligned} &\sum_{i=2}^{m-k} a_{i+k} \Big(v_{i-2}(t, x(t)) - v_{i-2}(0, x_0) \Big) \\ &\leq -a_{1+k} \int_0^t v_0(\tau, x(\tau)) d\tau - b \sum_{j=1}^{k+1} a_{k+1-j} \int_0^t \frac{\tau^j}{j!} d\tau + \sum_{j=0}^{k} \sum_{i=0}^{m-k-1+j} \int_0^t \frac{\tau^j}{j!} d\tau a_{i+k-j+1} v_i(0, x_0) \\ &\leq -a_{1+k} b t - b \sum_{j=1}^{k+1} a_{k+1-j} \frac{t^{j+1}}{(j+1)!} + \sum_{j=0}^{k} \sum_{i=0}^{m-k-1+j} \frac{t^{j+1}}{(j+1)!} a_{i+k-j+1} v_i(0, x_0). \end{aligned}$$

Note that the first term $-a_{1+k} b t$ can be combined into the first summation with an index

$j = 0$. In addition, shift the initial terms $v_{i-2}(0, x_0)$ to the right and we have

$$\sum_{i=2}^{m-k} a_{i+k} v_{i-2}(t, x(t)) \leq -b \sum_{j=0}^{k+1} a_{k+1-j} \frac{t^{j+1}}{(j+1)!} + \sum_{j=0}^{k} \sum_{i=0}^{m-k-1+j} \frac{t^{j+1}}{(j+1)!} a_{i+k-j+1} v_i(0, x_0) + \sum_{i=2}^{m-k} a_{i+k} v_{i-2}(0, x_0).$$

Rearrange the summation indices; namely, let the summation on the left side start with $i = 1$, the first summation on the right start with $j = 1$, the outer summation of the second term start with $j = 1$ and the last summation start with $i = 0$. Then we have

$$\sum_{i=1}^{m-k-1} a_{i+k+1} v_{i-1}(t, x(t)) \leq -b \sum_{j=1}^{k+2} a_{k-j+2} \frac{t^j}{j!} + \sum_{j=1}^{k+1} \sum_{i=0}^{m-k+j-2} \frac{t^j}{j!} a_{i+k-j+2} v_i(0, x_0) + \sum_{i=0}^{m-k-2} a_{i+k+2} v_i(0, x_0).$$

Note that the last term can be combined into the nested summations with an index $j = 0$. As a result, we have

$$\sum_{i=1}^{m-(k+1)} a_{i+(k+1)} v_{i-1}(t, x(t)) \leq -b \sum_{j=1}^{(k+1)+1} a_{(k+1)-j+1} \frac{t^j}{j!} + \sum_{j=0}^{k+1} \sum_{i=0}^{m-(k+1)-1+j} \frac{t^j}{j!} a_{i+(k+1)-j+1} v_i(0, x_0).$$

Compared with (3.95), the above inequality is exactly the incidence of $k + 1$ and hence we have proven the lemma. □

Lemma 3.12. *Suppose all the hypotheses in Lemma 3.11 hold. For any $\delta > 0, \epsilon > 0$, there exist a function $\bar{v}(\delta) \in \mathcal{K}_\infty$, a set $D = \{(\delta, \epsilon) \in \mathbb{R}^2 : \delta > 0, 0 < \epsilon \leq \bar{v}(\delta)\}$ and a function $\bar{T}(\delta, \epsilon) : D \to \mathbb{R}_{\geq 0}$ with the following properties:*

1. *$\bar{T}(\delta, \epsilon)$ is increasing in δ when ϵ is fixed, and decreasing in ϵ when δ is fixed.*

2. *$\bar{T}(\delta, \bar{v}(\delta)) = 0$ and $\lim_{\epsilon \to 0^+} \bar{T}(\delta, \epsilon) = \infty$ for all $\delta > 0$.*

Then if $v_0(0, x_0) = \delta$, we have the following conclusions:

a. $v_0(t, x(t)) \le \bar{v}(\delta)$ *for all* $t \ge 0$*;*

b. $v_0(t, x(t)) \le \epsilon$ *for all* $t \ge \bar{T}(\delta, \epsilon)$*.*

Proof. We pick $b \in (0, \delta]$ and let $t \ge 0$ be the maximal time such that $v_0(t, x(t)) \ge \delta$ for all $t \in [0, T]$. Then by Lemma 3.11 we have (3.94) for all $t \in [0, T]$. Split the second summation term in (3.94) into two parts so that one of them involves v_0 terms only:

$$v_0(t, x(t)) \le -b \sum_{j=1}^{m} a_{m-j} \frac{t^j}{j!} + \sum_{j=0}^{m-1} a_{m-j} \frac{t^j}{j!} v_0(0, x_0) + \sum_{j=1}^{m-1} \sum_{i=1}^{j} \frac{t^j}{j!} a_{m+i-j} v_i(0, x_0). \tag{3.97}$$

By global decrescent condition (3.88) we have $\phi \in \mathcal{K}_\infty$ such that for all $i = 1, \cdots m-1$,

$$v_i(0, x_0) \le \phi(V(0, x_0)) = \phi(v_0(0, x_0)) = \phi(\delta).$$

Substitute the above uniform bounds on v_i's into (3.97),

$$v_0(t, x(t)) \le -b \sum_{j=1}^{m} a_{m-j} \frac{t^j}{j!} + \delta \sum_{j=0}^{m-1} a_{m-j} \frac{t^j}{j!} + \phi(\delta) \sum_{j=1}^{m-1} \sum_{i=1}^{j} \frac{t^j}{j!} a_{m+i-j}. \tag{3.98}$$

To find the $\bar{v}$ function, we consider the case $b = \delta$. Thus we have

$$v_0(t, x(t)) \le -\delta a_0 \frac{t^m}{m!} + \delta + \phi(\delta) \sum_{j=1}^{m-1} \sum_{i=1}^{j} \frac{t^j}{j!} a_{m+i-j} =: p_\delta(t). \tag{3.99}$$

Note that $p_\delta(t)$ is an m-th degree polynomial in t, whose coefficients depend on δ. In addition, the coefficient of the highest degree term is negative so $p_\delta(t)$ is bounded from above for all $t \ge t_0$. By simple computation, $p_\delta(0) = \delta$, $\frac{d}{dt} p_\delta(0) = \phi(\delta) > 0$ so it can be concluded that the maximum value of $p_\delta(t)$ is achieved somewhere at $t^* > 0$ and $p_\delta(t^*) > \delta$; in addition since $p_0(t) \equiv 0$ the maximum value of $p_\delta(t)$ approaches 0 as δ decreases to 0. Consequently it can be concluded that there exists $\bar{v} \in \mathcal{K}_\infty$ so that $p_\delta(t) \le \bar{v}(\delta)$ for all $t \ge t_0$. We claim this $\bar{v}$ is the desired upper bound for $v_0(t, x(t))$. Indeed if this is not true, then it means there exists $s^* > 0$ such that $v_0(s^*, x(s^*)) > \bar{v}(\delta)$. As $v_0(t_0, x_0) = \delta$, there exists $s_0 \in [0, s^*)$ such that

$v_0(s_0, x(s_0)) = \delta$ and $v_0(t, x(t)) \geq \delta$ for all $t \in [s_0, s^*]$. We shift s_0 to be the initial time 0 and the assumptions in Lemma 3.11 are satisfied with $T = s^*$. Note that semi-definite relation (3.90) and the global decrescent condition (3.88) still hold for all $t \geq s_0$ so by same analysis we will still have the inequality (3.99). Hence we must have $v_0(s^*, x(s^*)) \leq p_\delta(s^* - s_0) \leq \bar{v}(\delta)$, which is a contradiction.

To find the $\bar{T}$ function, we let $b = \bar{v}^{-1}(\epsilon)$. In this way because $\epsilon \leq \bar{v}(\delta)$, indeed we have $b \leq \delta$, which does not conflict with our previous choice of $b \in (0, \delta]$. Thus (3.98) becomes:

$$\begin{aligned}
v_0(t, x(t)) &\leq -\bar{v}^{-1}(\epsilon) \sum_{j=1}^{m} a_{m-j} \frac{t^j}{j!} + \delta \sum_{j=0}^{m-1} a_{m-j} \frac{t^j}{j!} + \phi(\delta) \sum_{j=1}^{m-1 \sum_{i=1}^{j}} \frac{t^j}{j!} a_{m+i-j} \\
&= -\bar{v}^{-1}(\epsilon) a_0 \frac{t^m}{m!} + (\delta - \bar{v}^{-1}(\epsilon)) \sum_{j=1}^{m-1} a_{m-j} \frac{t^j}{j!} + \delta + \phi(\delta) \sum_{j=1}^{m-1} \sum_{i=1}^{j} a_{m+i-j} \frac{t^j}{j!} \\
&= -\bar{v}^{-1}(\epsilon) a_0 \frac{t^m}{m!} + \delta + \sum_{j=1}^{m-1} \frac{t^j}{j!} \left(\phi(\delta) \sum_{i=1}^{j} a_{m+i-j} + (\delta - \bar{v}^{-1}(\epsilon)) a_{m-j} \right) \\
&=: p_{\delta,\epsilon}(t).
\end{aligned}$$

Again $p_{\delta,\epsilon}(t)$ is an m-th degree polynomial in t. Define $\bar{T}(\delta, \epsilon) := \arg\min_{t \geq t_0} \{p_{\delta,\epsilon}(t) \leq \bar{v}^{-1}(\epsilon)\}$, which is finite since the highest degree term in the polynomial $p_{\delta,\epsilon}(t)$ has negative coefficient and thus decreases to $-\infty$ when t increases, and is positive when $p_{\delta,\epsilon}(0) = \delta > \bar{v}^{-1}(\epsilon)$. We claim this is the $\bar{T}$ function that we are looking for.

To show the first property of $\bar{T}(\delta, \epsilon)$ in Lemma 3.12, we see that when ϵ is fixed, $\delta_1 > \delta_2$ implies $p_{\delta_1,\epsilon}(t) - \bar{v}^{-1}(\epsilon) > p_{\delta_2,\epsilon}(t) - \bar{v}^{-1}(\epsilon)$ for all $t \geq t_0$ and hence $\bar{T}(\delta_1, \epsilon) > \bar{T}(\delta_2, \epsilon)$; when δ is fixed, $\epsilon_1 > \epsilon_2$ implies $p_{\delta,\epsilon_1}(t) - \bar{v}^{-1}(\epsilon_1) < p_{\delta,\epsilon_2}(t) - \bar{v}^{-1}(\epsilon_2)$ for all $t > 0$ and hence $\bar{T}(\delta, \epsilon_1) < \bar{T}(\delta, \epsilon_2)$. To show the second property, we see that $p_{\delta,\bar{v}(\delta)}(0) = \delta = \bar{v}^{-1}(\bar{v}(\delta))$ so $\bar{T}(\delta, \bar{v}(\delta)) = 0$. In addition, $p_{\delta,0}(t) = \delta > 0$ for all $t \geq t_0$ and because $p_{\delta,\epsilon}(t)$ is continuous in ϵ, we must have $\lim_{\epsilon \to 0^+} \bar{T}(\delta, \epsilon) = \infty$.

Eventually, to show $v_0(t, x(t)) \leq \epsilon$ for all $t \geq \bar{T}(\delta, \epsilon)$, recall $v_0(t, x(t)) \geq b = \bar{v}^{-1}(\epsilon)$ and it is bounded from above by $p_{\delta,\epsilon}(t)$ for $t \in [0, T]$. By the definition of $\bar{T}$ we must have $T \leq \bar{T}$. In other words there exists $\bar{t} \leq \bar{T}$ such that $v(\bar{t}, x(\bar{t})) = \bar{v}^{-1}(\epsilon)$. Hence by the first conclusion on $\bar{v}$ we have $v_0(t, x(t)) \leq \epsilon$ for all $t \geq \bar{T}(\delta, \epsilon) \geq \bar{t}$. □

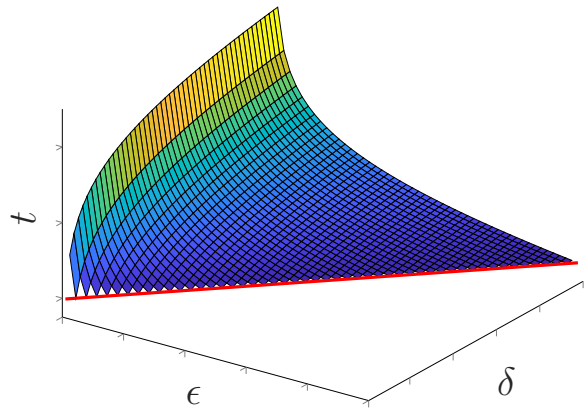

Figure 3.7: A graphical view of $\bar{T}$ function.

Proof of Theorem 3.6: Briefly speaking, the first property in Lemma 3.12 implies global stability and the second property implies uniform attractivity and hence the system is GUAS. We present an alternative proof here via the construction of a class $\mathcal{KL}$ function as required by (3.8).

Without loss of generality and by majorization, we can always assume $\bar{T}$ from Lemma 3.12 is a continuous function over D while preserving its properties. A graphical view of the $\bar{T}$ function is given in Fig. 3.7. For each $\delta > 0$, define $W_\delta(\epsilon) = \bar{T}(\delta, \epsilon)$. By the properties of $\bar{T}$ in Lemma 3.12, we see that its inverse function $W_\delta^{-1} : \mathbb{R}_{\geq 0} \to (0, \bar{v}(\delta)]$ exists and is a decreasing function such that $W_\delta^{-1}(0) = \bar{v}(\delta)$, $\lim_{t\to\infty} W_\delta^{-1}(t) = 0$. In addition, from the second conclusion on $v_0(t, x(t))$ after $\bar{T}$ we see that when $v_0(t_0, x_0) = \delta$, $v_0(t, x(t)) \leq W_\delta^{-1}(t - t_0)$.

Define

$$\bar{\beta}(\delta, t) := \begin{cases} W_\delta^{-1}(t) & \delta > 0, \\ 0 & \delta = 0. \end{cases}$$

We claim that $\bar{\beta} \in \mathcal{KL}$. We are left to show that $\bar{\beta}(\delta, t)$ is increasing in δ and it is continuous at $\delta = 0$. Let $\delta_1 > \delta_2 > 0$ and $t \geq t_0$. Since t is in the range of the function $\bar{T}(\delta, \epsilon)$ for any $\delta > 0$, $t = \bar{T}(\delta_1, \epsilon_1) = \bar{T}(\delta_2, \epsilon_2)$ for some ϵ_1, ϵ_2. Then we must have $\epsilon_1 > \epsilon_2$ because $\bar{T}(\delta, \epsilon)$ is increasing in δ and decreasing in ϵ. In other words,

$$\bar{\beta}(\delta_1, t) = W_{\delta_1}^{-1}(t) = \epsilon_1 > \epsilon_2 = W_{\delta_2}^{-1}(t) = \bar{\beta}(\delta_2, t).$$

So $\bar{\beta}(\delta, t)$ is increasing in δ. In addition, we have $\bar{\beta}(\delta, t) \leq \bar{\beta}(\delta, 0) = \bar{v}(\delta) \to 0$ as $\delta \to 0$ so $\lim_{\delta \to 0} \bar{\beta}(\delta, t) = 0 = \bar{\beta}(0, t)$ and the function is continuous at $\delta = 0$.

Last, from the earlier analysis we have $v_0(t, x(t)) \leq \bar{\beta}(v_0(t_0, x_0), t - t_0)$ for any $x_0 \in \mathbb{R}^n, u \in \mathcal{M}_U, t \geq t_0$. As $v_0 = V$ by definition, combine this result with (3.9) and we have

$$\begin{aligned} |x(t)| \leq \alpha_1^{-1}(V(t, x(t))) &\leq \alpha_1^{-1} \circ \bar{\beta}(V(t_0, x_0), t - t_0) \\ &\leq \alpha_1^{-1} \circ \bar{\beta}(\alpha_2(|x_0|), t - t_0) =: \beta(|x(0)|, t - t_0). \end{aligned}$$

By construction $\beta \in \mathcal{KL}$ and hence the system (3.7) is GUAS.

□

Examples

Linear system with unaligned V

Consider a 2-dimensional linear system given by

$$\dot{x} = f(x, u) = Ax + u, \tag{3.100}$$

where $A = \begin{pmatrix} -0.1 & -1 \\ 2 & -0.1 \end{pmatrix}$. It is not hard to check that A is Hurwitz so the system (3.100) is ISS. This can be verified by picking a proper quadratic Lyapunov function $V := x^\top P x$ where P satisfies the Lyapunov equation:

$$AP + PA^\top = -Q \tag{3.101}$$

for some positive definite Q. Consider the canonical Lyapunov function $V = |x|^2$ so that P is the identity matrix. By (3.101) we find $Q = \begin{pmatrix} 0.2 & -1 \\ -1 & 0.2 \end{pmatrix}$, which is not positive definite. Hence such V is not a Lyapunov function for system (3.100); in other words, even in the

case when $u = 0$, we have

$$\dot{V} = -0.2x_1^2 + 2x_1x_2 - 0.2x_2^2 = -0.2(x_1 - 5x_2)^2 + 4.8x_2^2,$$

which may be positive when $x_1 = 5x_2 \neq 0$. Nevertheless, in spite of the sign indefiniteness of $\dot{V}$, we look at its higher order derivatives and we still want to show that (3.100) is ISS. Pick $\rho(s) = \dfrac{s}{20}$ and consider the auxiliary system

$$\dot{x} = f'(x, u) = Ax + \rho(|x|)u$$

with $|u| \leq 1$. As usual $v_0 = V$ and note that

$$\frac{\partial v_i}{\partial x} f'(x, u) = (V_i)_x \left(Ax + \frac{|x|}{20} u \right) \leq (V_i)_x Ax + \frac{|(V_i)_x||x|}{20}.$$

When v_i is quadratic in x, $|(V_i)_x| \leq R_i|x|$ for some $R_i \geq 0$ and hence according to (3.87) we can recursively define

$$v_{i+1} := (V_i)_x Ax + \frac{R_i}{20}|x|^2,$$

which is also quadratic in x. According to this rule the first few v_i's can be generated:

$$\begin{aligned} v_1 &= -0.1x_1^2 + 2x_1x_2 - 0.1x_2^2, \\ v_2 &= 4.13x_1^2 - 0.6x_1x_2 - 1.87x_2^2, \\ v_3 &= -1.5907x_1^2 - 15.62x_1x_2 + 1.4093x_2^2. \end{aligned}$$

It is observed that (3.88) is satisfied since all v_i's are quadratic. Letting $a_0 = 0.1, a_1 = 8, a_2 = 0.5, a_3 = 1$, we have

$$\sum_{i=0}^{3} a_i v_i = -0.2257x_1^2 + 0.08x_1x_2 - 0.2257x_2^2 = -x^\top \begin{pmatrix} 0.2257 & -0.04 \\ -0.04 & 0.2257 \end{pmatrix} x \prec 0,$$

hence according to our Corollary 3.6 the system (3.100) is ISS.

Slowly varying between two stable modes

Consider the following 2-dimensional, time-varying system:

$$\dot{x} = f(t, x, u) = \sin^2(kt)A_1 x + \cos^2(kt)A_2 x + u =: A(k, t)x + u, \tag{3.102}$$

where

$$A_1 = \begin{pmatrix} -0.1 & -1 \\ 2 & -0.1 \end{pmatrix}, \quad A_2 = \begin{pmatrix} -0.1 & -2 \\ 1 & -0.1 \end{pmatrix}$$

and k is a sufficiently small positive number, representing a slow enough variation of the system (3.102) between the two linear sub-systems $\dot{x} = A_1 x + u$ and $\dot{x} = A_2 x + u$. The two sub-systems are taken from Chapter 2.1 of [28]. Both sub-systems are stable when there are no inputs; however, as discussed in the cited book, the trajectory of a switched system may diverge for some particular sequence of switches between the two sub-systems. Hence the switched system is not stable under arbitrary switches; there is no common Lyapunov function between the two sub-systems so there exist no time-independent Lyapunov functions for (3.102). Nevertheless we want to show that the canonical positive definite function $V(x) = |x|^2$ when applied on (3.102) satisfies (3.90) and hence proves ISS of the system when k is sufficiently small. Again pick $\rho(s) = \frac{s}{20}$ and the auxiliary system is $\dot{x} = f'(t, x, d) = A(k, t)x + \frac{|x|}{20}d$. It can be inductively shown that the higher order derivatives of v_i are of quadratic form $v_i(t, x) = x^\top M_i(k, t)x$ because

$$\begin{aligned}
&\frac{\partial v_i}{\partial t} + \frac{\partial v_i}{\partial x} \cdot f'(t, x, d) \\
&\quad = x^\top \frac{dM_i}{dt} x + x^\top \left(M_i + M_i^\top\right) \left(Ax + \frac{|x|}{20}d\right) \\
&\quad \leq x^\top \frac{dM_i}{dt} x + x^\top \left(M_i + M_i^\top\right) Ax + \frac{1}{20}\|M_i + M_i^\top\||x|^2 \\
&\quad = x^\top \left(\frac{dM_i}{dt} + \left(M_i + M_i^\top\right) A + \frac{1}{20}\|M_i + M_i^\top\| I_{2\times 2}\right) x \\
&\quad =: v_{i+1}.
\end{aligned}$$

Hence we also have the recursive relations

$$M_{i+1} = \frac{dM_i}{dt} + \left(M_i + M_i^\top\right) A + \frac{1}{20}\|M_i + M_i^\top\| I_{2\times 2}.$$

In addition, if $M_i(k,t) = P_i(k,t) + o(k)Q_i(k,t)$ such that $o(k)$ converges to 0 as k converges to 0 and $\|Q_i(k,t)\|$ is bounded uniformly with respect to all $k \in \mathbb{R}, t \geq t_0$, then the sign definiteness of $\sum_{i=0}^m a_i M_i$ is the same as $\sum_{i=0}^m a_i P_i$ when k is sufficiently small. Hence we only need to compute those P_i's. Because we use $V(x) = |x|^2$, $P_0 = M_0 = I_{2\times 2}$ as a start. The other matrices can be generated accordingly:

$$
\begin{aligned}
P_1 &= \begin{pmatrix} -0.1 & -C \\ -C & -0.1 \end{pmatrix}, \\
P_2 &= \begin{pmatrix} C^2 - 3C + 0.13 & 0.3C \\ 0.3C & C^2 + 3C + 0.13 \end{pmatrix}, \\
P_3 &= \begin{pmatrix} -0.5C^2 + 1.5C + 0.224 & -C^3 + 8.81C \\ -C^3 + 8.81C & -0.5C^2 - 1.5C + 0.224 \end{pmatrix},
\end{aligned}
$$

where $C = \cos(2kt)$. Use the same coefficients as in the previous example; that is, $a_0 = 0.1, a_1 = 8, a_2 = 0.5, a_3 = 1$ and we have

$$
\sum_{i=0}^{3} a_i P_i = \begin{pmatrix} -0.411 & -C^3 + 0.96C \\ -C^3 + 0.96C & -0.411 \end{pmatrix}.
$$

Note that $\max_t |\cos^3 2kt - 0.96 \cos 2kt| = 0.256\sqrt{2} < 0.411$ so the above matrix is negative definite. Thus when k is sufficiently small,

$$
\sum_{i=0}^{3} a_i v_i \approx \sum_{i=0}^{3} a_i x^\top P_i x \prec 0
$$

and the system (3.102) is ISS by Corollary 3.6.

3.4 Discussion and future work

It is appreciated that the stability of nonlinear systems can be shown either by finding standard Lyapunov functions, or via the analysis via some non-monotonic Lyapunov functions; each approach has its own pros and cons. Because of the negative definite requirement on

the time derivative of the standard Lyapunov function, Lyapunov's direct method is not trivial in general; in addition, we point out that for a time-varying system, such a standard Lyapunov function may also need to be time-varying and hence difficult to find. As shown in our second example, no standard time-independent Lyapunov function exists for this time varying system (3.102); on the contrary, starting from a simple $V(x) = |x|^2$ and using our techniques via non-monotonic Lyapunov functions, we are able to show ISS.

In terms of almost Lyapunov function techniques, we have seen that provided that the "bad set" where V does not decrease along the solutions is "small" enough, the system is guaranteed to be GUAS if it is autonomous, or ISS if it has inputs, as discussed in Section 3.2.2 and Section 3.3.1, respectively. Depending on how we quantify the size of the "bad set", we may have different results. We also see that the more we know about the system structure, the less conservative the bound on the size of the "bad set" we can derive. While using the upper bound of Ω dwell time gives us less conservative results for ISS, for practical purposes, we would like to avoid computing solutions of the systems and thus this temporal information of the system is very often intangible. We point out here that converting spatial bounds on Ω to temporal bounds on Ω is possible; nevertheless the connection between the two is highly non-trivial; this problem has its own interest and can be further developed.

On the other hand, while our method for checking stability of the systems via higher order derivatives as studied in Section 3.3.2 gives freedom in the choice of the candidate positive definite function V, as a trade-off the negative semi-definite linear combination condition is analytically difficult to check. Nevertheless, very often when all the higher order derivatives are polynomials, our negative semi-definite linear combination condition is related to the sum-of-squares (SOS) techniques in semi-definite programming (SDP) (i.e., [78]). It is worth devoting more effort to the study of numerical SOS SDP implementation, and there is a good chance that such problems can be solved efficiently.

The connection between higher order derivatives and the standard Lyapunov function is observed in the work [79]. For an asymptotically stable system with no inputs, if there exists a function $V \in C^\infty(\mathbb{R}^n \to \mathbb{R})$ with $V(0) = 0$ and some coefficients $a_0, a_1, \cdots, a_m$ such that the negative definite linear combination condition $\sum_{i=1}^m a_i V^{(i)} \prec 0$ holds where $V^{(i)}$ is

the i-th time derivative of V, then

$$W(x) := \sum_{i=1}^{m} a_i V^{(i-1)}(x) \tag{3.103}$$

is a standard positive definite Lyapunov function with negative definite time derivative. Note that there is no assumption of positive definiteness on V, nor any sign requirements like (3.89) on the coefficients a_i. Compared with our theorem, the result in [79] seems to be much less conservative. However, we point out that because of the presence of inputs in the system, W constructed via a formula similar to (3.103) may not be a standard Lyapunov function in our case. To be more precise, because of the inputs, we only have inequality in the relations (3.93) between higher order derivatives, rather than equality as we have for the case when there are no inputs. Thus as long as there are some negative a_i's, we will not be able to compare $\dot{W}$ with $\sum_{i=1}^{m} a_i V^{(i)}$ and hence the negative definite time derivative of W cannot be concluded.

As a comparison to the classical Lyapunov function theorem, another interesting question to study is whether there also exists a converse theorem with respect to the higher order derivatives. That is, given a positive definite V and a stable system, whether there always exist some non-negative coefficients such that the negative semi-definite linear combination condition of the higher order derivatives of V with these coefficients is satisfied. If starting with any arbitrary V seems too optimistic, we then can consider those "almost" Lyapunov functions whose time derivative is negative everywhere except at small regions in the state space, as studied in our earlier work [24]. It is very likely that such V can be adjusted to be negative definite by adding some higher order derivatives to it. This remains as an interesting future research direction.

CHAPTER 4

STABILITY ANALYSIS FOR STATE-DEPENDENT SWITCHED SYSTEMS

4.1 Stability and state-dependent switched systems

In this chapter we study several stability properties for state-dependent switched systems. We examine the gap between global asymptotic stability and uniform global asymptotic stability, and illustrate it with an example. Several regularity assumptions are proposed in order to obtain the equivalence between these two stability properties. Based on this equivalence, we are able to show that global stability and asymptotic gain imply input-to-state stability for state-dependent switched systems, which is the main result of this chapter. The proof consists of a bypass via an auxiliary system which takes in a bounded disturbance, and showing that this system is uniformly globally asymptotically stable.

4.1.1 GS + AG vs. ISS

In Chapter 2, we have already seen how ISS can be used to describe the stability of a dynamical system. Defined by (3.11), ISS is normally defined in terms of the sum of an initial-state-dependent, time-decaying estimate and an input-dependent estimate. On the other hand, it also has many other characterizations, each with its own advantages. For example, ISS is equivalent to the validity of a dissipation inequality for an appropriately defined energy storage function; ISS is also equivalent to the uniform asymptotic gain (UAG) property (see, e.g., [80]). Here we are interested in the close relation of ISS with the global stability (GS) property and the asymptotic gain (AG) property; these two properties combined were shown to be equivalent to ISS for single-mode, Lipschitz systems in [29].

In our prior work, we have designed state feedback controllers with quantized state

measurements, via zoom-in/out techniques, for achieving disturbance attenuation. This controller design can be applied to single-mode linear systems with inputs [81], or to switched linear systems with inputs [82]. The closed-loop system was proven to be GS and AG with respect to the external disturbance, yet this does not immediately result in ISS as the closed-loop system is a switched system and so the theorem from [29] is not directly applicable. A strictly weaker version of ISS with parametrization was shown in [83], with significant extra effort.

Motivated by the above reasons, we want to study ISS for switched systems, in particular the implication from GS plus AG to ISS. It is observed that in quantized controller design, the zoom events and transitions of control law typically occur when the error exceeds certain bounds; in other words, the switch is triggered when the system state reaches certain regions in the state space. Accordingly, we choose to focus on state-dependent switched systems; see, e.g., [28]. (We note that event-triggered control systems [84] can also be captured in a similar modeling framework.) As a popular type of hybrid system, state-dependent switched systems have attracted a lot of research recently (see, e.g., [85], [86] among many other works). Our main task here is to formulate assumptions under which the implication from GS plus AG to ISS holds for state-dependent switched systems.

It is identified in [30] that the major gap between GS plus AG and ISS is the uniformity of convergence time. Briefly speaking, the lack of uniformity lies in the nature of state-dependent switched systems, namely, in the fact that solutions evolving from adjacent initial states may behave very differently because they are in different modes. As a result, while AG guarantees that all solutions will converge to the equilibrium, the time to converge to a small set is no longer continuous with respect to the initial states and hence a uniform upper bound on the convergence time may not exist; consequently the system may not be ISS. This gap can be filled by imposing suitable regularity conditions; for example, in the hybrid system framework of [87], the system solution space is closed, and it is concluded that global pre-asymptotic stability is equivalent to uniform global pre-asymptotic stability. It is also noted that GS plus AG is related to the nonuniform ISS defined in [88], which is shown to imply ISS if this nonuniform ISS still holds when either the dynamics of the system or switch guards/rules are perturbed.

Motivated by [89], we would like to impose transversality of solutions with respect to switch guards in our model. The idea of transversal solutions can be traced back to [90] in the 1980s. In [91] the transversality condition is also shown to be essential for trajectory sensitivity analysis. With this assumption of transversality, we can eventually draw the equivalence between GS plus AG and ISS.

4.1.2 Preliminaries

Basic definitions and notations Our state-dependent switched system deploys a model from [89], which has a similar setup as the state-dependent switched system model in [28] and the references therein. Let $I = \{1, 2, \cdots, l\}$ be the set of modes of the system and for each $i \in I$, define functions

$$f_i(x, u) : \mathbb{R}^n \times \mathcal{U} \to \mathbb{R}^n.$$

These are the dynamics for each mode and we require $f_i(x, u)$ to be locally Lipschitz in both x and u for all $i \in I$. Here $\mathcal{U} \subseteq \mathbb{R}^m$ is the input value set. We then define $\mathcal{M}_{\mathcal{U}}$ as the set of all locally essentially bounded functions from $\mathbb{R}_{\geq 0}$ to $\mathcal{U}$. Let $S_i \subseteq \mathbb{R}^n$ be the admissible regions of the state x in mode i. S_i's are not necessarily disjoint, meaning the system can have the same state while in different modes. Define the total admissible hybrid state space to be $\mathcal{S} = \cup_{i \in I}(S_i, \{i\})$. Define the switch guards $E_{i,j} \subset \mathbb{R}^n$ so that a switch from mode i to j occurs when $x \in E_{i,j}$ and $\sigma = i$. By convention $E_{i,i} = \emptyset$ and $E_{i,j}$ can be empty for lots of other indices j, meaning that the switch from mode i to j will never happen. Following are some regularity assumptions on the switch guards:

Assumption 4.1.

$$E_{i,j} \subseteq intS_j \quad \forall i, j \in I, \qquad and \tag{4.1}$$

$$\cup_{j \in I} E_{i,j} = \partial S_i \quad \forall i \in I. \tag{4.2}$$

Assumption 4.2. *Each $E_{i,j}$ is closed and*

$$E_{i,j} \cap E_{i,k} = \emptyset \quad \forall j \neq k,\ i, j, k \in I. \tag{4.3}$$

Here (4.1) ensures that the solution is still in the admissible hybrid state space after each switch. Equation (4.2) ensures the occurrence of a switch when the state is at the boundary of an admissible region, and (4.3) guarantees that when a switch is about to occur, the mode-to-be is unique.

The dynamics of a forward complete, state-dependent switched system (Σ) is defined as follows:

$$\begin{cases} \dot{x} = f_\sigma(x,u) & \text{if } x \in \text{int}S_\sigma \\ x^+ = x & \text{if } x \in \partial S_\sigma \end{cases} \tag{4.4}$$

$$\begin{cases} \sigma^+ = \sigma & \text{if } x \in \text{int}S_\sigma \\ \sigma^+ = j & \text{if } x \in E_{\sigma,j} \end{cases} \tag{4.5}$$

with initial condition $(x_0, \sigma_0) \in \mathcal{S}$. We denote the state and mode of the solution at time t as $x(t, x_0, \sigma_0, u), \sigma(t, x_0, \sigma_0, u)$ respectively. When $(x_0, \sigma_0) \in \mathcal{S}$ is given and $u \in \mathcal{M}_\mathcal{U}$ is fixed, we can simplify the two notations to be $x(t), \sigma(t)$, respectively. Sometimes we will simply call $x(t, x_0, \sigma_0, u)$ the solution of system (Σ) while ignoring the current modes the system is in. Because of Assumption 4.1, we see that $(x(t), \sigma(t)) \in \mathcal{S}$ for all $t \geq 0, u \in \mathcal{M}_\mathcal{U}$. In addition, (4.5) is well defined when $x \in \partial S_\sigma$ because (4.3) in Assumption 4.2 tells us that the mode-to-be is unique.

For any $r > 0$ and set Ω, define ball

$$B_r(\Omega) := \{x : |x - y| < r \text{ for some } y \in \Omega\}.$$

Let $\bar{B}_r(\Omega)$ be the closure of $B_r(\Omega)$. In case $\Omega = \{0\}$, we simplify the notations to be $B_r, \bar{B}_r$, respectively. The ambient space where Ω is in will be made clear in the context.

For two sets $A, B \subset \mathbb{R}^n$ define the metric

$$d(A, B) := \inf_{x \in A, y \in B} |x - y|.$$

It naturally reduces to the case when one of them is only a single point $x \in \mathbb{R}^n$ and we abuse the same notation

$$d(A, x) := \inf_{y \in A} |x - y|.$$

Finally, we say a function $\rho(t) : [0,\infty) \to [0,\infty)$ is a class $\mathcal{K}_\infty$ function if it is strictly increasing with $\rho(0) = 0$ and $\lim_{t\to\infty} \rho(t) = \infty$. We say a function $\beta(\xi, t) : [0,\infty) \times [0,\infty) \to [0,\infty)$ is a class $\mathcal{KL}$ function if it is strictly increasing in ξ, decreasing in t, $\beta(0,t) = 0$ for all $t \geq 0$ and $\lim_{t\to\infty} \beta(\xi, t) = 0$ for all $\xi \geq 0$.

Auxiliary system As in Chapter 3, we rely on the relation between the system (Σ) and its auxiliary system when studying its stability properties. The auxiliary system is defined similarly.

Let $r > 0$ and let ρ be a class $\mathcal{K}_\infty$ function. Define

$$f_i^\rho(x,d) := f_i(x, \rho(|x|)d), \quad i \in I. \tag{4.6}$$

Define the auxiliary system (Σ^ρ) for (Σ) as follows:

$$\begin{cases} x = f_\sigma^\rho(x,d) & \text{if } x \in \text{int}S_\sigma \\ x^+ = x & \text{if } x \in \partial S_\sigma \end{cases} \tag{4.7}$$

$$\begin{cases} \sigma^+ = \sigma & \text{if } x \in \text{int}S_\sigma \\ \sigma^+ = j & \text{if } x \in E_{\sigma,j} \end{cases} \tag{4.8}$$

with initial condition $(x_0, \sigma_0) \in \mathcal{S}$ and disturbance $d \in \mathcal{M}_\mathcal{D}$, $\mathcal{D} = \bar{B}_1$. Similarly we denote the state and mode of this auxiliary system (Σ^ρ) by $x^\rho(t, x_0, \sigma_0, d), \sigma^\rho(t, x_0, \sigma_0, d)$ respectively. Note that by this definition, $x^\rho(t, x_0, \sigma_0, d) = x(t, x_0, \sigma_0, \rho(|x|)d)$, $\sigma^\rho(t, x_0, \sigma_0, d) = \sigma(t, x_0, \sigma_0, \rho(|x|)d)$ for all $t \geq 0, (x_0, \sigma_0) \in \mathcal{S}, d \in \mathcal{M}_\mathcal{D}$. The construction of an auxiliary system is a common technique practiced in the literature (see, e.g., [29],[92]) and we also would like to mimic those techniques here. The relation between (Σ) and (Σ^ρ) will be discussed in Section 4.3.

Stability definitions First of all, $f_i(0,0) = 0$ for all $i \in I$ such that $0 \in S_i$ imply $x(t, 0, \sigma_0, 0) \equiv 0 \quad \forall t \geq 0, (0, \sigma_0) \in \mathcal{S}$. In this case we say 0 is an equilibrium to the system (Σ).

Consider the case when $\mathcal{U} = \mathbb{R}^m$; that is, when the control is unconstrained. ISS is

defined similarly to that in Chapter 3, and we say the system (Σ) is ISS if

$$\exists \beta \in \mathcal{KL}, \gamma \in \mathcal{K}_\infty \text{ s.t. } \forall (x_0, \sigma_0) \in \mathcal{S}, \forall u \in \mathcal{M}_\mathcal{U},$$
$$|x(t, x_0, \sigma_0, u)| \leq \beta(|x_0|, t) + \gamma(\|u\|_{[0,t]}).$$

We say the system (Σ) has global stability (GS) property if bounded initial states and controls produce uniformly bounded trajectories and, in addition, small initial states and controls produce uniformly small trajectories:

$$\exists \sigma, \gamma \in \mathcal{K}_\infty \text{ s.t. } \forall (x_0, \sigma_0) \in \mathcal{S}, \forall u \in \mathcal{M}_\mathcal{U},$$
$$\sup_{t \geq 0} |x(t, x_0, \sigma_0, u)| \leq \max\{\sigma(|x_0|), \gamma(\|u\|_\infty)\}.$$

The system (Σ) has asymptotic gain (AG) property if every trajectory must ultimately stay not far from the origin, depending on the magnitude of the input:

$$\exists \gamma \in \mathcal{K}_\infty \text{ s.t. } \forall (x_0, \sigma_0) \in \mathcal{S}, \forall u \in \mathcal{M}_\mathcal{U},$$
$$\limsup_{t \to \infty} |x(t, x_0, \sigma_0, u)| \leq \gamma(\|u\|_\infty).$$

The next few stability definitions will only be used on the auxiliary system (Σ^ρ) whose input value set $\mathcal{D}$ is the unit ball. Nevertheless, we state the definitions for the general state-dependent switched systems (Σ) when $\mathcal{U}$ is bounded. We say a system (Σ) is globally asymptotically stable (GAS) if the system is *stable* in the sense that

$$\forall \epsilon > 0, \exists \delta > 0 \text{ s.t. } \forall (x_0, \sigma_0) \in \mathcal{S} \text{ with } |x_0| \leq \delta,$$
$$\sup_{t \geq 0, u \in \mathcal{M}_\mathcal{U}} |x(t, x_0, \sigma_0, u)| \leq \epsilon$$

and is *attractive* in the sense that

$$\forall (x_0, \sigma_0) \in \mathcal{S}, u \in \mathcal{M}_\mathcal{U}, \quad \lim_{t \to 0} x(t, x_0, \sigma_0, u) = 0.$$

It is worth pointing out that GAS is strictly weaker than global uniform asymptotic stability

(GUAS) in the sense that attractivity is not uniform with respect to time. In addition to the GUAS definition via comparison functions as we did in Chapter 3, The system (Σ) is GUAS if the system is stable and is *uniformly attractive* in the sense that

$$\forall \epsilon > 0, \kappa > 0, \exists T \geq 0 \text{ s.t. } \forall (x_0, \sigma_0) \in \mathcal{S} \text{ with } |x_0| \leq \kappa,$$
$$\sup_{t \geq T, u \in \mathcal{M}_{\mathcal{U}}} |x(t, x_0, \sigma_0, u)| \leq \epsilon.$$

4.2 Main results

Before studying the state-dependent switched system, we would like to review some ideas behind the elegant proof in [29] of the equivalence between GS plus AG and ISS for single-mode Lipschitz systems. Fig. 4.1 shows a proof flow of the main result in that paper:

$$\begin{array}{lccccccc} \Sigma\text{:} & \text{GS} & + & \text{AG} & & \xleftarrow{\text{(f)}} & & \text{ISS} \\ & \downarrow\text{(a)} & & \downarrow\text{(b)} & & & & \uparrow\text{(c)} \\ \Sigma^{\rho}\text{:} & \text{stability} & + & \text{attractivity} & \xrightarrow{\text{(d)}} & \text{GAS} & \xrightarrow{\text{(e)}} & \text{GUAS} \end{array}$$

Figure 4.1: Proof flow of AG+GS=ISS.

In their proof, while the implication (f) in Fig. 4.1 is trivial, the proof of the other direction is done by a detour via arguments on the auxiliary system (Σ^{ρ}). Firstly (a) and (b) are proven by straightforward comparison function manipulation; (c) can be either concluded directly by invoking the converse Lyapunov theorem from [92], or again proven via comparison functions. In addition, (d) is the definition of GAS. The essential step is (e), which heavily depends on the property of continuous dependence of solutions on initial conditions induced by a Lipschitz vector field and an approximation of the limit of a sequence of infinite time horizon solutions with arbitrarily small error. Thanks to this key result of (e), there is no necessity to mention uniform convergence time for systems with Lipschitz vector fields whenever we are dealing with stability of systems and convergence of solutions. For example, ISS (with uniform convergence time implicitly embedded in the class $\mathcal{KL}$ function β) applied to an autonomous system yields the so-called 0-GAS property, which in fact should be more

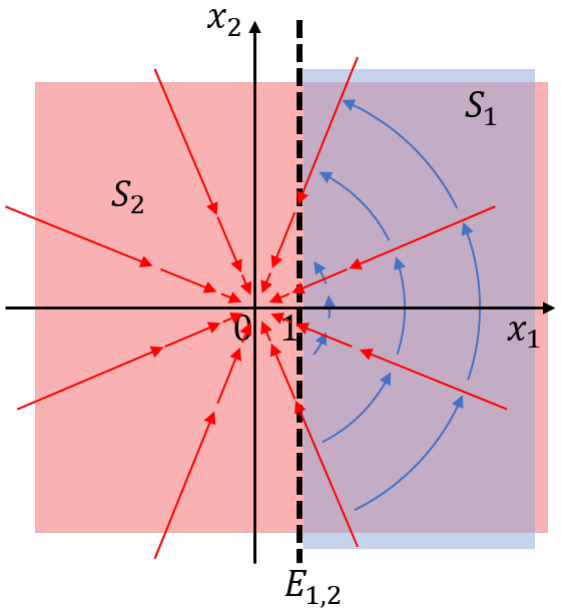

Figure 4.2: A 2-dimensional example which is GAS but not GUAS.

precisely referred to as 0-GUAS. However, this equivalence between GAS and GUAS cannot be simply transferred to state-dependent switched systems, as illustrated by the following counterexample taken from [30]:

Counterexample Consider a 2-dimensional, 2-mode system with

$$S_1 = \{(x_1, x_2) \in \mathbb{R}^2 : x_1 \geq 1\},\ S_2 = \mathbb{R}^2,$$
$$E_{1,2} = \partial S_1 = \{(1, x_2) : x_2 \in \mathbb{R}\}.$$

The subsystem dynamics of each mode is given by:

$$f_1(x) = (\sqrt{x_1^2 + x_2^2} - 1)\begin{pmatrix} -x_2 \\ x_1 \end{pmatrix},\ f_2(x) = -\begin{pmatrix} x_1 \\ x_2 \end{pmatrix}.$$

The mode regions and corresponding vector fields are shown in Fig 4.2. It is not hard to see that in Mode 1, the system solution is rotating counter-clockwise around the origin with angular velocity $|x| - 1$. Since S_1 is only the right half-plane with respect to the line $x_1 = 1$, the rotation velocity is always positive in $\text{int}S_1$ and the solution will eventually hit the boundary and switch to Mode 2. In Mode 2, the solution converges to the origin

exponentially fast. Therefore, this system is stable and attractive, so it is GAS. Nevertheless, consider a solution with initial condition $x_0 = (r, 0), \sigma_0 = 1$ where $r > 1$ but very close to 1. It needs to rotate an angle of $\arccos(\frac{1}{r})$ before it hits $E_{1,2}$; hence, it has to stay in mode 1 for a time $\frac{\arccos(\frac{1}{r})}{r-1}$, which tends to infinity when $r \to 1^+$. Thus the convergence time is not uniformly bounded; the system is not uniformly attractive. Therefore, this system is not GUAS.

Additional assumptions For simplicity, the assumptions in this subsection are expressed in terms of f_i^ρ, which can be translated to assumptions in terms of f_i via (4.6). It is observed that in the previous example, the ill behavior of solutions arises in the neighborhood of state $(1, 0)$ in S_1, on which $f_1(x)$ becomes parallel to the boundary $x_1 = 1$ and hence the time needed for a switch to occur approaches infinity. Therefore, we need a suitable transversality assumption imposed on the system:

Assumption 4.3. *There exist functions $g_i \in C^1(\mathbb{R}^n)$ such that each admissible region S_i can be defined by g_i:*

$$S_i = \{x \in \mathbb{R}^n : g_i(x) \geq 0\}, \quad i \in I.$$

In addition,

$$f_i^\rho(x, d) \cdot \nabla g_i(x) < 0 \quad \forall d \in \mathcal{D}, x \in \partial S_i, i \in I. \tag{4.9}$$

By this assumption, the boundaries of regions of system modes are $\partial S_i = \{x \in S_i : g_i(x) = 0\}$. For any $K \subset \mathcal{S}$ (in most cases the mode element in K is a singleton), the reachable set of the solutions of (Σ^ρ) over the time interval $[0, T]$ starting from K is denoted to be $\mathcal{R}^T(K)$. In other words,

$$\mathcal{R}^T(K) := \{x^\rho(t, x_0, \sigma_0, d) : t \in [0, T], (x_0, \sigma_0) \in K, d \in \mathcal{M}_\mathcal{D}\}.$$

To make the analysis easier, we also impose the two following assumptions here:

Assumption 4.4. *For any $T \geq 0$ and compact set $K \subset \mathcal{S}$, there exists $c > 0$ such that $\mathcal{R}^T(K) \subseteq B_c$.*

Assumption 4.5. *The sets $F_i(x) := \{f_i^\rho(x, d) : d \in \mathcal{D}\}$ are convex for all $x \in \mathbb{R}^n, i \in I$.*

Assumption 4.4 means the reachable space over a compact set of initial conditions and finite time horizon is bounded. While this assumption is always true for single-mode Lipschitz systems (see [92]), it is not clear for state-dependent switched systems. Nevertheless, if we are working on a compact state space, or $|f_i|$ are globally bounded, or some more knowledge of the system directly tells that every solution is bounded, then Assumption 4.4 would be true. We postpone the discussion of Assumption 4.5 to Lemma 4.7 where it is used.

With the assumptions proposed in the previous section, we can prove the following theorem regarding GAS and GUAS here:

Theorem 4.1. *Let a state-dependent switched system* (Σ^ρ) *be defined via* (4.7), (4.8). *When Assumption 4.1 to Assumption 4.5 hold,* (Σ^ρ) *is GAS if and only if it is GUAS.*

Theorem 4.1 also leads to the main result of our work:

Theorem 4.2. *Let a state-dependent switched system* (Σ) *be defined via* (4.4), (4.5) *and assume it is GS and AG. There exists* $\rho \in \mathcal{K}_\infty$ *such that if Assumption 4.1 to Assumption 4.5 hold with* f_i^ρ *defined via* (4.6), *then* (Σ) *is ISS.*

Referring to Fig. 4.1 and following the same proof flow, we will first prove some simple arrows in the figure, that is, (a) by Lemma 4.1, (b) by Lemma 4.2, and (c) by Lemma 4.4, respectively. We will then prove Theorem 4.1, which also leads to the arrow (e) in the figure. As that proof is the most critical component of the flow, it will be contributed by the entire Section 4.3.2, consisting of several lemmas. Now note that the arrow (d) is simply the definition of GAS and (f) is still trivial in this case; subsequently we can conclude Theorem 4.2.

4.3 Connection between (Σ) and (Σ^ρ)

Without loss of generality we can assume the two γ functions in the definition of GS and AG are identical and smooth. Define

$$\rho(s) := \gamma^{-1}(\frac{s}{2}). \tag{4.10}$$

Since $\gamma \in \mathcal{K}_\infty$, $\rho(s)$ is also a class $\mathcal{K}_\infty$ function and $\gamma \circ \rho(s) = \frac{s}{2}$. Using this ρ and defining the corresponding auxiliary system, we can prove several relations between (Σ) and (Σ^ρ) in the following subsections.

4.3.1 Easier implications

GS to stability

Lemma 4.1. *If (Σ) is GS, then its auxiliary system (Σ^ρ) is stable, where ρ is defined via (4.10).*

Proof. Let $\epsilon > 0$. Pick $\delta = \sigma^{-1}(\epsilon)$. GS implies

$$\begin{aligned}
\sup_{t\geq 0} |x^\rho(t, x_0, \sigma_0, d)| &= \sup_{t\geq 0} |x(t, x_0, \sigma_0, \rho(|x^\rho(t)|)d)| \\
&\leq \max\{\sigma(|x_0|), \gamma(\|\rho(|x^\rho(t)|)d(t)\|_\infty)\} \\
&\leq \max\{\sigma(|x_0|), \gamma(\|\rho(|x^\rho(t)|)\|_\infty)\} \\
&\leq \max\{\sigma(|x_0|), \|\gamma(\rho(|x^\rho(t)|))\|_\infty\} \\
&= \max\{\sigma(|x_0|), \frac{1}{2}\|x^\rho(t)\|_\infty\}.
\end{aligned}$$

Since $\|x^\rho(t)\|_\infty$ is nothing but a different notation of $\sup_{t\geq 0} |x^\rho(t, x_0, \sigma_0, u)|$, the bound $\frac{1}{2}\|x^\rho(t)\|_\infty$ is redundant. Hence when $|x_0| \leq \delta$, $\sup_{t\geq 0} |x^\rho(t, x_0, \sigma_0, u)| \leq \sigma(|x_0|) \leq \sigma(\delta) = \epsilon$ and the auxiliary system (Σ^ρ) is stable. □

AG to attractivity

Lemma 4.2. *If (Σ) is AG, then its auxiliary system (Σ^ρ) is attractive, where ρ is defined via (4.10).*

Proof. By lemma II.1 in [29], AG is equivalent to the property

$$\limsup_{t\to\infty} |x(t, x_0, \sigma_0, u)| \leq \gamma\left(\limsup_{t\to\infty} |u(t)|\right)$$

for all $(x_0, \sigma_0) \in \mathcal{S}, u \in \mathcal{M}_{\mathcal{U}}$ where γ is the same as the one in the definition of AG. Fixing $(x_0, \sigma_0) \in \mathcal{S}$ and $d \in \mathcal{M}_{\mathcal{D}}$ and denoting $x^\rho(t) := x^\rho(t, x_0, \sigma_0, d)$, we have

$$\begin{aligned}
\limsup_{t\to\infty} |x^\rho(t)| &= \limsup_{t\to\infty} |x^\rho(t, x_0, \sigma_0, d)| \\
&= \limsup_{t\to\infty} |x(t, x_0, \sigma_0, \rho(|x^\rho(t)|)d(t))| \\
&\leq \gamma\left(\limsup_{t\to\infty} \rho(|x^\rho(t)|)|d(t)|\right) \\
&\leq \limsup_{t\to\infty} \gamma(\rho(|x^\rho(t)|)) \\
&\leq \frac{1}{2} \limsup_{t\to\infty} |x^\rho(t)|,
\end{aligned}$$

which implies $\limsup_{t\to\infty} x^\rho(t) = 0$. Thus the system (Σ^ρ) is attractive. □

GUAS and ISS Recall that in Chapter 3, GUAS can also be defined via a class $\mathcal{KL}$ function:

Lemma 4.3. *A system (Σ^ρ) is GUAS if and only if there is a class $\mathcal{KL}$ function β such that*

$$|x^\rho(t, x_0, \sigma_0, d)| \leq \beta(|x_0|, t) \tag{4.11}$$

for all $(x_0, \sigma_0) \in \mathcal{S}, d \in \mathcal{M}_{\mathcal{D}}$.

The proof is similar to that for the autonomous version of Lemma 4.5 in [19], which can be found in its appendix and hence omitted here. It is noted that since converse Lyapunov theorem may not hold for state-dependent switched systems, the existence of a Lyapunov function V cannot be assumed when showing GUAS implies ISS; nevertheless, by using the alternative definition of GUAS in Lemma 4.11 and assuming that (Σ) is GS, we can still derive this implication via comparison functions:

Lemma 4.4. *Assume that the system (Σ) is GS. Then it is also ISS if and only if its auxiliary system (Σ^ρ) is GUAS where ρ is defined via* (4.10).

Proof. When (Σ) is ISS, by definition there exists $\beta \in \mathcal{KL}, \gamma \in \mathcal{K}_\infty$ such that for all $(x_0, \sigma_0) \in$

$\mathcal{S}, u \in \mathcal{M}_{\mathcal{U}}$,

$$|x(t, x_0, \sigma_0, u)| \leq \beta(|x_0|, t) + \gamma(\|u\|_{[0,t]}).$$

For any $d \in \mathcal{M}_{\mathcal{D}}$,

$$\begin{aligned}
|x^\rho(t, x_0, \sigma_0, d)| &= |x(t, x_0, \sigma_0, \rho(|x^\rho(t)|)d)| \\
&\leq \beta(|x_0|, t) + \gamma\left(\rho(|x^\rho(t)|)\|d\|_{[0,t]}\right) \\
&\leq \beta(|x_0|, t) + \gamma \circ \rho(|x^\rho(t)|) \\
&= \beta(|x_0|, t) + \frac{|x^\rho(t)|}{2}.
\end{aligned}$$

Hence $|x^\rho(t, x_0, \sigma_0, d)| \leq 2\beta(|x_0|, t)$. Because 2β is also a class $\mathcal{KL}$ function, by Lemma 4.3 (Σ^ρ) is GUAS.

To show that GUAS (Σ^ρ) implies ISS (Σ), consider a solution of (Σ). For any initial state $(x_0, \sigma_0) \in \mathcal{S}$, any control $u \in \mathcal{M}_{\mathcal{U}}$, define $t_0 := \inf\{t \geq 0 : \|u\|_{[t,\infty)} \geq \rho(|x(t)|)\}$ ($t_0 = \infty$ when the set is empty). Let

$$d(t) := \begin{cases} \frac{u(t)}{\rho(|x(t)|)} & t < t_0, \\ 0 & t \geq t_0. \end{cases}$$

By definition of t_0, $|u(t)| \leq \rho(|x(t)|)$ for all $t \in [0, t_0)$ hence $d(t) \in \mathcal{M}_{\mathcal{D}}$. Thus for $t \in [0, t_0)$

$$x(t, x_0, \sigma_0, u) = x(t, x_0, \sigma_0, \rho(|x|)d) = x^\rho(t, x_0, \sigma_0, d).$$

Then by Lemma 4.3, we have $|x(t, x_0, \sigma_0, u)| \leq \beta(|x_0|, t)$. Note that this β is independent of t_0. ISS is shown when $t_0 = \infty$. Otherwise, note that $\|u\|_{[t,\infty)}$ is a non-increasing function of t and $\rho(|x(t)|)$ is continuous with respect to t, so from the definition of t_0 we must have $\|u\|_{[t_0,\infty)} \geq \rho(|x(t_0)|)$. Because the system (Σ) is assumed to be GS and time-invariant, take t_0 as the initial time and we have that for all $t \geq t_0$,

$$\begin{aligned}
|x(t)| &\leq \max\{\sigma(|x(t_0)|), \gamma(\|u\|_{[t_0,\infty)})\} \\
&\leq \max\{\sigma \circ \rho^{-1}(\|u\|_{[t_0,\infty)}), \gamma(\|u\|_{[t_0,\infty)})\} \\
&\leq \gamma'(\|u\|_{[t_0,\infty)}) \leq \gamma'(\|u\|_\infty),
\end{aligned}$$

where $\gamma'(s) = \max\{\sigma \circ \rho^{-1}(s), \gamma(s)\}$. Combining the two parts we have $|x(t)| \leq \beta(|x_0|, t) + \gamma'(\|u\|_\infty)$ for all $t \geq 0$. Observe that t_0 does not appear in the above bound so it is true for all x_0, σ_0, u. Appealing to causality we can replace $\|u\|_\infty$ by $\|u\|_{[0,t]}$ and hence we have shown ISS. □

4.3.2 Key implication: GAS to GUAS

The special properties of state-dependent switched systems are not required for the proofs for the lemmas in Section 4.3; they will only appear when we show the implication from GAS to GUAS. For convenience we will omit the superscripts of ρ on f_i^ρ and x^ρ only in this section as everything will be discussed on the auxiliary system.

Transversality We first conclude an important result from the transversality Assumption 4.3. The following lemma suggests that whenever a solution is very close to the switching guards, it is guaranteed to hit the switching guards within a time that is proportional to the distance from the current state to the guards.

Lemma 4.5. *When Assumption 4.3 is true, for any $T > 0$ and any compact set $K \subseteq \mathcal{S}$, there exists $r_1 > 0, \mu > 0$ such that if $|x(s, x_0, \sigma_0, d) - y| \leq r_1$ for some $s \leq T, (x_0, \sigma_0) \in K, d \in \mathcal{M}_\mathcal{D}$ and $y \in \partial S_{\sigma(s)}$, then $x(s + \Delta, x_0, \sigma_0, d) \in \partial S_{\sigma(s)}$ for some $\Delta \leq \mu |x(s, x_0, \sigma_0, d) - y|$.*

Proof. By Assumption 4.4 there exists $c' > 0$ such that $\mathcal{R}^T(K) \subseteq B_{c'}$. Letting $h > 0$ and $c = c' + h$, then B_c contains the dilated reachable set $B_h(\mathcal{R}^T(K))$. Define

$$M := \sup_{x \in \bar{B}_c, d \in \mathcal{D}, i \in I} |f_i(x, d)|. \tag{4.12}$$

Since $g_i \in C^1$, let L_2 be the common Lipschitz constant on all g_i's over $\bar{B}_c$ (recall g_i's define the guards for switch). For any $\gamma > 0$, define sets

$$N_i(\gamma) := \{x \in \bar{B}_c : d(x, \partial S_i) \leq \gamma\}, \quad i \in I.$$

Note that by this definition, $N_i(\gamma)$ is compact. Thus by Assumption 4.3 and continuity of

the function $f_i(x,d)\cdot\nabla g_i(x)$ with respect to x and d, we know that there exists $a>0, r_1>0$ such that $f_i(x,d)\cdot\nabla g_i(x)\le -a$ for all $i\in I, u\in\mathcal{D}, x\in N_i(r_1)$. We pick r_1 sufficiently small so that $r_1\le \min\{h, \frac{ah}{ML_2}\}$. When $y\in\partial S_{\sigma(s)}$, $g_{\sigma(s)}(y)=0$ by definition of ∂S_i. If $|x(s)-y|\le r_1$, we have $d(x(s),\partial S_i)\le r_1$; in addition, $x(s)\in B_{c'}\subset \bar{B}_c$ so $x(s)\in N_i(r_1)$. Evaluating $g_{\sigma(s)}(x(t))$ as a function of time along the solution starting at time s,

$$\frac{d}{dt}g_{\sigma(s)}(x(t))|_{t=s}=\nabla g_{\sigma(s)}(x)\cdot f_{\sigma(s)}(x,u)|_{t=s}\le -a,$$

$$g_{\sigma(s)}(x(s))=g_{\sigma(s)}(x(s))-g_{\sigma(s)}(y)\le L_2|x(s)-y|.$$

It means that $g(x(t,\xi,u))$ is decreasing at rate $-a$ at least, starting from a value no larger than $L_2|x(s)-y|$. By taking r_1 sufficiently small, $x(t)$ will stay in $N_{\sigma(s)}(r_1)$ while decreasing $g(x(t))$ and hence the value has to drop to 0, that is, $x(t)$ will hit $\partial S_{\sigma(s)}$ after time $\Delta\le \mu|x(s)-y|$ where $\mu:=\frac{L_2}{a}$. In addition for any $\tau\in[s,s+\mu r_1]$,

$$|x(\tau)|\le |x(s)|+M\mu r_1\le c'+\frac{ML_2}{a}r_1\le c'+h=c,$$

which implies $x(\tau)\in B_c$ so L_2, M are indeed valid along the solution over time $[s,s+\Delta]\subseteq[s,s+\mu r_1]$. □

Now with the help of the other assumptions, we can show there are more advantageous properties of this type of state-dependent switched system.

Convergent switching time With the help of Lemma 4.5 and the other assumptions in the theorem statement, we can now show that adjacent solutions of the state-dependent switched system switch at similar times. To be more precise, let $K\subseteq\mathcal{S}$ be a compact set and pick a convergent sequence of initial conditions $(x_0^k,\sigma_0)\in K$. Denote $x^k(t):=x^\rho(t,x_0^k,\sigma_0,d^k)$, $\sigma^k(t):=\sigma^\rho(t,x_0^k,\sigma_0,d^k)$ where $d^k\in\mathcal{M}_\mathcal{D}$. Suppose that $x^k(t)\to\theta(t)\in\mathbb{R}^n$ for all $t\ge 0$ point-wise. Clearly we should have $\theta(0)=\lim_{t\to\infty}x_0^k$. It is not hard to see that $x^k(t)$ are locally equicontinuous so the limit $\theta(t)$ is continuous. Keep in mind that θ may

not be a solution so "switches" on θ are not defined. Alternatively, we can recursively define

$$t_0 = 0,\ t_j = \min\{t \geq t_{j-1} : \theta(t) \in \partial S_{\sigma_{j-1}}\}, \tag{4.13}$$

with σ_j defined such that $\theta(t_j) \in E_{\sigma_{j-1},\sigma_j}$ for $j \geq 1$. Similar switching time means:

Lemma 4.6. *For any $T > 0$, there exists a $\bar{k}$ such that for each $j \geq 1$ and $t_j < T$ as defined via (4.13), there will be a sequence of time t_j^k when all the solutions $x^k(t)$ with $k \geq \bar{k}$ will switch, in the sense that $\sigma^k(t_j^k) = \sigma_{j-1}$, $x^k(t_j^k) \in E_{\sigma_{j-1},\sigma_j}$. In addition, $\lim_{k\to\infty} t_j^k = t_j$ and $\lim_{k\to\infty} x^k(t_j^k) = \theta(t_j)$.*

Proof. We start from $j = 1$. From the given T and K we can derive r_1, μ according to Lemma 4.5. Because $x^k \to \theta$ uniformly over time $[0, t_1]$, there exists k_1 such that $\|x^k - x^{k'}\|_{[0,t_1]} \leq r_1$ for all $k, k' \geq k_1$; in particular, we conclude $|x^k(t_1) - \theta(t_1)| \leq r_1$. If there is no switch on $x^k(t)$ over time $[0, t_1]$, the solution is still in mode σ_0 at t_1. Because $\theta(t_1) \in \partial S_{\sigma_0}$, by Lemma 4.5, there will be a switch at $t_1^k = t_1 + \Delta$ with $\Delta \leq \mu|x^k(t_1) - \theta(t_1)|$. In addition, $x^k(t_1) \to \theta(t_1)$ as $k \to \infty$ implies $t_1^k \to t_1$. The lemma is almost proven if there are only finitely many solution switches at t_1^k with $t_1^k \leq t_1$. Otherwise, consider the subsequence of such "early switched" solutions and still call them x^k, from which we compare two solutions with index k, k'. Without loss of generality we assume $t_1^k \leq t_1^{k'}$. Because $|x^{k'}(t_1^k) - x^k(t_1^k)| \leq r_1$ and $x^k(t_1^k) \in \partial S_{\sigma_0}$, again by Lemma 4.5 we conclude that $|t_1^k - t_1^{k'}| \leq \mu|x^k(t_1^k) - x^{k'}(t_1^k)| \leq \mu\|x^k - x^{k'}\|_{[0,t_1]}$. The right-most term can be made arbitrarily small by taking k, k' large enough, which means t_1^k is convergent by the Cauchy convergence theorem. Denote $\lim_{k\to\infty} t_1^k =: \tilde{t}_1^k$. Equicontinuity of x^k implies the sequence of states $x^k(t_1^k)$ converges as well and $\lim_{k\to\infty} x^k(t_1^k) = \lim_{k\to\infty} x^k(\tilde{t}_1) = \theta(\tilde{t}_1)$. Now let $\partial S_i^* := \partial S_i^* \cap \bar{B}_c, \partial E_{i,j}^* := E_{i,j} \cap \bar{B}_c$ where c is the radius of ball $B_c \supseteq \mathcal{R}^{T+\mu r_1}(K)$ from Assumption 4.4. By definition all of $\partial S_i^*, E_{i,j}^*$ are compact and thus from Assumption 4.1 and Assumption 4.2 we know that there exists $r_2, r_3 > 0$ such that for all $i, j, k \in I, i \neq j$,

$$r_2 \leq d(E_{k,i}^*, E_{k,j}^*), \tag{4.14}$$

$$r_3 \leq d(E_{i,j}^*, \partial S_j^*). \tag{4.15}$$

Convergence of $x^k(t_1^k)$ suggests that there exists k_2 such that $|x^k(t_1^k) - x^{k'}(t_1^{k'})| < r_2$ for all $k, k' \geq k_2$. Hence they should be hitting the same switch guard, say $x^k(t_1^k) \in E_{\sigma_0,i}$. This means $\sigma^k(t_1^k) = i$ for all $k \geq \max\{k_1, k_2\}$. In addition because switch guards are closed, as the limit of $x^k(t_1^k)$, $\theta(\tilde{t}_1) \in E_{\sigma_0,i}$ as well. Now because the definition of t_j in (4.13) suggests that it is the first time θ hits any switch guards, we must have $\tilde{t}_1 = t_1$ and $i = \sigma_1$. The lemma is proven for the case $j = 1$.

For $j > 1$, convergence of t^k means $|t_1^k - t_1^{k'}| < \frac{r_3}{M}$ for all $k, k' \geq k_3$ where M is defined via (4.12) over $\bar{B}_c$. Denote $\bar{t}_1 := \sup\{t_1^k\} = \max\{t_1^k, t_1\}$. Then we see $|x^k(t_1^k) - x^k(\bar{t}_1)| \leq M|t_1^k - \bar{t}| < r_3$, meaning there is no second switch on any solution x^k before time $\bar{t}_1$. In other words, $\sigma^k(\bar{t}_1^+) = \sigma_1$ for all $k \geq \bar{k} := \max\{k_1, k_2, k_3\}$. Reset $\bar{t}_1^+$ to be the initial time and we can inductively prove the rest cases. □

Compact infinite time horizon solution space The next lemma is similar to Lemma III.2 in [29]. It is noted that their lemma only guarantees the existence of an approximated solution, which is based on construction of reverse time solution. However, in the case of state-dependent switched system with overlapped admissible regions S_i, the reverse time solution is actually not well defined so we cannot use that approach. Instead, we try to directly prove that there exists a limit curve and it is an infinite horizon solution, with the convexity Assumption 4.5. First, for any set $\Omega \subseteq \mathbb{R}^n$, define function $\tau_\Omega : C^0(\mathbb{R}^n_{\geq 0} \to \mathbb{R}^n) \to \mathbb{R}^n_{\geq 0}$:

$$\tau_\Omega(x) := \inf_{t \geq 0}\{t : x(t) \in \Omega\}.$$

This is the hitting time of a solution to the set Ω. To be complete, we say $\tau_\Omega(x) = \infty$ if $x(t) \notin \Omega$ for all $t \geq 0$.

Lemma 4.7. *Let $K \subseteq \mathcal{S}$ be a compact subset and $\Omega \subseteq \mathbb{R}^n$ be an open subset. If*

$$\sup_{(x_0,\sigma_0)\in K, d\in\mathcal{M}_\mathcal{D}} \tau_\Omega(x(t, x_0, \sigma_0, d)) = \infty,$$

then there exists $(x^*, \sigma^*) \in K, v \in \mathcal{M}_\mathcal{D}$ such that

$$\tau_\Omega(x(t, x^*, \sigma^*, v)) = \infty.$$

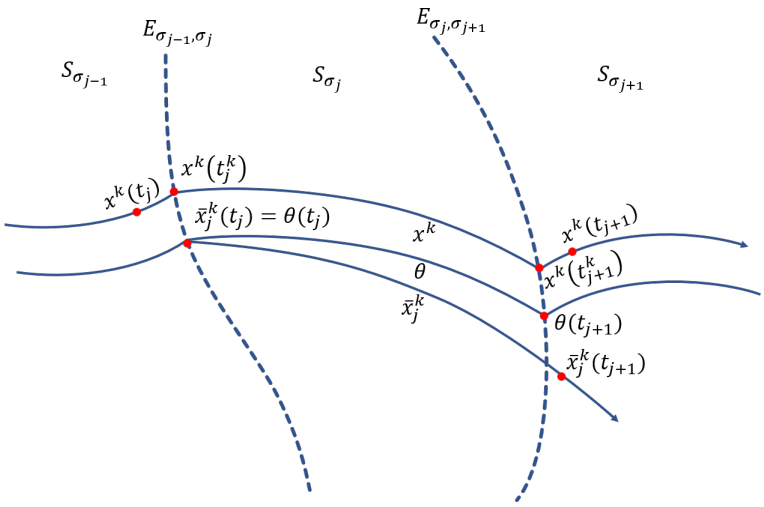

Figure 4.3: An illustration of x^k, θ and $\bar{x}_j^k$.

Proof. The proof consists of two parts. The first part is to show that under the hypothesis, there exists a curve that never intersects Ω. To do this, observe that the hypothesis in this lemma means there exists a sequence of solutions $x^k(t)$ such that $\tau_\Omega(x^k) > k$ for all $k \in \mathbb{N}$. Because all $x^k(t)$ are uniformly bounded and equicontinuous over time $[0, 1]$, by the Azela-Ascoli theorem there exists a convergent subsequence $x^{g_1(k)}$ from x^k that converges uniformly over the time interval $[0, 1]$. Note that the same argument can be applied inductively on any time interval $[0, i], i \in \mathbb{N}$ and there will exist a subsequence $x^{g_i(k)}$ from $x^{g_{i-1}(k)}$ with $g_0(k) = k$ that converges uniformly over $[0, i]$. In addition, we see that their limits are partially identical: $\lim_{k\to\infty} x^{g_i(k)}(t) = \lim_{k\to\infty} x^{g_j(k)}(t)$ for all $t \in [0, \min\{i, j\}]$. Thus we have constructed a continuous curve $\theta(t)$ such that for any $T > 0$, the sequence $x^{g_{\lceil T\rceil}(k)}(t)$ converges to $\theta(t)$ uniformly for $t \in [0, T]$. Recall that by definition the solution $x^{g_{\lceil T\rceil}(k)}$ has a hitting time larger than $g_{\lceil T\rceil}(k)$ and in addition since it is a subsequence of x^k, $\tau_\Omega(x^{g_{\lceil T\rceil}(k)}) > g_{\lceil T\rceil}(k) \geq k$ so $x^{g_{\lceil T\rceil}(k)}(t) \in \mathbb{R}^n\backslash\Omega$ for all $t \in [0, k]$. Because Ω is open, $\mathbb{R}^n\backslash\Omega$ is closed so $\theta(t) = \lim_{k\to\infty} x^{g_{\lceil T\rceil}(k)}(t) \in \mathbb{R}^n\backslash\Omega$ for all $t \in [0, T]$. Lastly, because this T is arbitrary, $\theta(t) \notin \Omega$ for all $t \geq 0$. This completes the first part of the proof.

The second part is to show that θ indeed is a solution to the system (Σ^ρ). Without loss of generality assume the second element in K is a singleton; hence we must have $\sigma^* = \sigma_0$. Define the sequence of t_j on $\theta(t)$ as in (4.13). By Assumption 4.1 we know that in fact $t_j < t_{j+1}$ for all j. From now on we relabel the convergent subsequence $x^{g_{\lceil T\rceil}(k)}$ as x^k for

convenience. We define a solution $\bar{x}_j^k(t)$ over the time interval $[t_j, t_{j+1}]$ by the dynamics

$$\dot{\bar{x}}_j^k(t) = f_{\sigma_j}(\bar{x}_j^k, d^k)$$

with initial condition $\bar{x}_j^k(t_j) = \theta(t_j)$. Fig. 4.3 is an illustration of the relation between x^k, θ and $\bar{x}_j^k$. In order to prove that θ is a solution, we first show that $\bar{x}_j^k \to \theta$ uniformly over $[t_j, t_{j+1}]$ for all $j \geq 0$ and $t_{j+1} \leq T$. Pick any arbitrary $\delta_1, \delta_2 > 0$. By Lemma 4.6, there exists $k_1 \in \mathbb{N}$ such that as long as $k \geq k_1$, $|t_j^k - t_j| \leq \delta_1$, $\quad |t_{j+1}^k - t_{j+1}| \leq \delta_1$ and $x^k(t_j^k) \in E_{\sigma_{j-1},\sigma_j}, x^k(t_{j+1}^k) \in E_{\sigma_j,\sigma_{j+1}}$. In addition because $x^k(t)$ converges to $\theta(t)$ uniformly over $[t_j, t_{j+1}] \subseteq [0, T]$, we should have $k_2 \in \mathbb{N}$ such that for all $k \geq k_2$, $|x^k(t) - \theta(t)| \leq \delta_2$ for all $t \in [t_j, t_{j+1}]$. Now if $t_j^k \leq t_j$, $|x^k(t_j) - \bar{x}_j^k(t_j)| = |x_k(t_j) - \theta(t_j)| \leq \delta_2$. Otherwise, $\sigma^k(t) = \sigma_{j-1}$ for all $t \in [t_j, t_j^k]$, meaning there is no switch on the solution x^k over this time interval so $|x^k(t) - x^k(t_j)| \leq M|t - t_j|$. Thus we have

$$\begin{aligned}|x^k(t) - \bar{x}_j^k(t)| \leq & |x^k(t) - x^k(t_j)| + |x^k(t_j) - \bar{x}_j^k(t_j)| + |\bar{x}_j^k(t_j) - \bar{x}_j^k(t)| \\ \leq & 2M(t_j^k - t_j) + \delta_2 \leq 2M\delta_1 + \delta_2.\end{aligned}$$

So we have $|x^k(t) - \bar{x}_j^k(t)| \leq 2M\delta_1 + \delta_2$ for all $t \in [t_j, \max\{t_j, t_j^k\}]$.

Now for $t \in [\max\{t_j, t_j^k\}, \min\{t_{j+1}, t_{j+1}^k\}]$, we see that $\sigma^k(t) = \sigma_j$, that is, x^k follows dynamics $\dot{x}^k = f_{\sigma_j}^{\rho}(x^k, u^k)$, the same as $\bar{x}_j^k$. Hence we can apply Grönwall's lemma, $|x^k(t) - \bar{x}_j^k(t)| \leq |x^k(t_j^k) - \bar{x}_j^k(t_j^k)|e^{L_1(t-t_j^k)} \leq (2M\delta_1 + \delta_2)e^{L_1(t_{j+1}-t_j)}$. In the case $t_{j+1}^k \geq t_{j+1}$, that is exactly the upper bound for the separation over the whole time interval $[t_j, t_{j+1}]$. Otherwise, for $t \in [t_{j+1}^k, t_{j+1}]$,

$$\begin{aligned}|x^k(t) - \bar{x}_j^k(t)| \leq & |x^k(t) - x^k(t_j)| + |x^k(t_{j+1}) - \bar{x}_j^k(t_{j+1})| + |\bar{x}_j^k(t_{j+1}) - \bar{x}_j^k(t)| \\ \leq & 2M(t_j^k - t_j) + (2M\delta_1 + \delta_2)e^{L_1(t_{j+1}-t_j)} \\ \leq & 2M\delta_1 + (2M\delta_1 + \delta_2)e^{L_1(t_{j+1}-t_j)}.\end{aligned}$$

Comparing it with the earlier bounds, we see that the inequality above is in fact true for all

$t \in [t_j, t_{j+1}]$. Using triangle inequality again, we have

$$\begin{aligned}|\bar{x}_j^k(t) - \theta(t)| &\leq |\bar{x}_j^k(t) - x^k(t)| + |x^k(t) - \theta(t)| \\ &\leq 2M\delta_1 + (2M\delta_1 + \delta_2)e^{L_1(t_{j+1}-t_j)} + \delta_2 \\ &= (2M\delta_1 + \delta_2)\left(1 + e^{L_1(t_{j+1}-t_j)}\right).\end{aligned}$$

For all $k \geq \max\{k_1, k_2\}, t \in [t_j, t_{j+1}]$. As δ_1, δ_2 are taken arbitrarily so the separation can be made arbitrarily small, we conclude that $\bar{x}_j^k(t)$ converges to $\theta(t)$ uniformly over $[t_j, t_{j+1}]$. Thus by Filippov's theorem [93] and using the Assumption 4.5 that f_i are convex, there exists a control $v_j \in \mathcal{M}_{\mathcal{D}}$ that $\dot{\theta} = f_{\sigma_j}(\theta, v_j)$ over $[t_j, t_{j+1}]$. By defining $x^* = \theta(0)$ and $v \in \mathcal{M}_{\mathcal{D}}$ by $v(t) := v_j(t) \quad \forall t \in [t_j, t_{j+1})$, we finally have $x(t, x^*, \sigma_0, v) = \theta(t)$ and hence $\tau(x^*, \sigma_0, \Omega, v) = \infty$. □

Proof of Theorem 4.1. Let $\kappa, \epsilon > 0$ be arbitrary. The system (Σ) being GAS means it is stable and attractive. Let $\delta > 0$ be given by stability so that $(\xi, i) \in \mathcal{S}$ with $|\xi| \leq \delta$ implies $|x(t, \xi, i, d)| \leq \epsilon$ for all $t \geq 0, d \in \mathcal{M}_{\mathcal{D}}$. Let $\Omega = \{x \in \mathbb{R}^n : |x| < \delta\}$ and $K = \{(\xi, i) \in \mathcal{S} : |\xi| \leq \kappa\}$. On the other hand, attractivity implies that $\tau(\xi, i, \Omega, d) < \infty$ for all $(\xi, i) \in \mathcal{S}, d \in \mathcal{M}_{\mathcal{D}}$. Hence by the contrapositive argument of Lemma 4.7 we conclude that $\sup_{(\xi,i)\in K, d\in\mathcal{M}_{\mathcal{D}}} \tau(\xi, i, \Omega, u) < \infty$. In other words, there exists $T := T(\kappa, \delta)$ such that $x(\tau, \xi, i, u) \in \bar{\Omega}$ for some $\tau \leq T$ and all $(\xi, i) \in K, d \in \mathcal{M}_{\mathcal{D}}$. Because the system is time-invariant, with the aforementioned stability we conclude that $\limsup_{t\geq T, u\in\mathcal{M}_{\mathcal{U}}} |x(t, \xi, i, d)| \leq \epsilon$ for all $(\xi, i) \in \mathcal{S}$ with $|\xi| \leq \kappa$. Because T only depends on κ and δ, which further depends on ϵ, the system (Σ) is uniformly attractive in addition to being stable, and hence GUAS. □

4.4 Continuous dependence on initial conditions

A byproduct of the hypothesis in Theorem 4.1 also gives us a conclusion on continuous dependence of initial conditions for solutions of state-dependent switched systems. A similar result supporting that the transversality condition leads to continuous dependence on initial conditions can be found in [89], with a slightly different problem formulation.

Lemma 4.8. *For any $T > 0$, $\sigma_0 \in I$ and compact set $K \subseteq S_{\sigma_0}$, there exists $C \geq 1, \bar{L} > 0, \eta > 0$ so that*

$$|x(t, x_0, \sigma_0, u) - x(t, x_0', \sigma_0, u)| \leq |x_0 - x_0'| C e^{\bar{L}t}$$

for any $x_0, x_0' \in K$ with $|x_0 - x_0'| \leq \eta$ and all $u \in \mathcal{M}_{\mathcal{U}}, t \in [0, T]$.

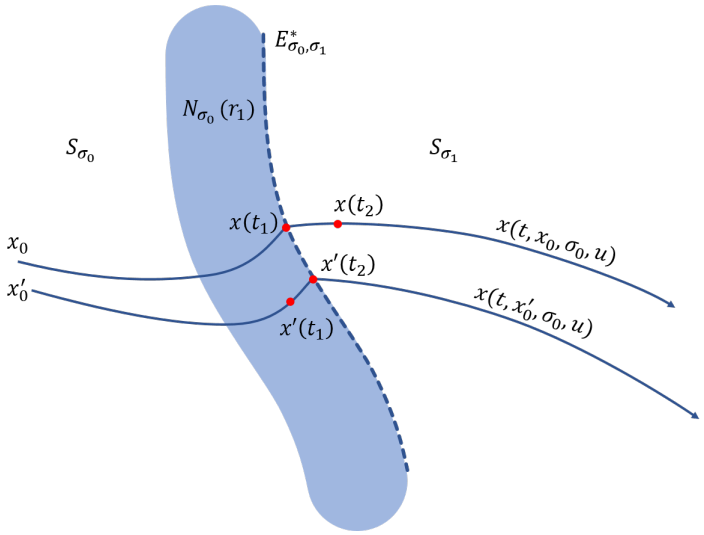

Figure 4.4: A sketch of two adjacent solutions generated by same control but different initial conditions.

Proof. We start by considering two adjacent solutions as shown in Fig. 4.4. We again make some abbreviations such that $x(t) := x(t, x_0, \sigma_0, u), x'(t) = x(t, x_0', \sigma_0, u)$. By Assumption 4.4, there exists $c > 0$ such that $\mathcal{R}^T(K) \subseteq B_c$. Thus we can also derive M as in (4.12). In addition we have r_1, k from Lemma 4.5 and we also define the minimal separations r_2, r_3 as in (4.14),(4.15) here. We then define

$$C := 1 + 2Mk,$$

$$\bar{L} = \frac{M}{r_2} \ln C + L_1.$$

If neither of the two solutions switches, then it reduces to a Lipschitz system dynamics and by Grönwall lemma we conclude

$$|x(t) - x'(t)| \leq |x_0 - x_0'| e^{L_1 t} \leq |x_0 - x_0'| C e^{\bar{L}t}.$$

Otherwise, without loss of generality we assume that the first switch occurs from mode σ_0 to σ_1 on the solution $x(t)$ at time $t_1 \leq T$. Let

$$\eta = \min\{r_1, r_2, r_3\} C^{-1} e^{-\bar{L}T}.$$

Then when $|x_0 - x_0'| \leq \eta$, using the Grönwall inequality we have

$$|x(t_1) - x'(t_1)| \leq \eta e^{L_1 t_1} \leq r_1 C^{-1} e^{-\bar{L}T} e^{L_1 t_1} \leq r_1.$$

Note that $x(t_1) \in E^*_{\sigma_0,\sigma_1} \subseteq \partial S^*_{\sigma_0}$, so we have $x'(t_1) \in N^*_{\sigma_0}(r_1)$; hence by Lemma 4.5, $x'(t_2) \in \partial S^*_{\sigma_0}$ for some $t_2 \geq t_1$ such that $t_2 - t_1 \leq k|x(t_1), x'(t_1)|$. Note that for $t \in (t_1, t_2]$, $\sigma(t), \sigma^\rho(t)$ are different so we cannot use the Grönwall inequality again for comparing the two solutions. However, we can still compute their difference from another perspective. First we see that when $t \in (t_1, t_2]$,

$$\begin{aligned} |x(t) - x(t_1)| &\leq M(t - t_1) \leq M(t_2 - t_1) \leq Mk|x(t_1), x'(t_1)| \\ &\leq Mk|x_0 - x_0'|e^{L_1 t_1} \leq Mk\eta e^{L_1 t_1} \leq Mkr_2 C^{-1} e^{-\bar{L}T} e^{L_1 t_1} < r_2. \end{aligned}$$

This suggests that there is no more switch occurring on the solution $x(t)$ and $\sigma(t) = \sigma_1$ for $t \in (t_1, t_2]$. We can do a similar computation on the solution $x'(t)$ and use triangular

inequality to compute $|x(t_1) - x'(t)|$. This time we use r_3 in the expression for η:

$$\begin{aligned}
|x(t_1) - x'(t)| =& |x(t_1) - x'(t_1) + x'(t_1) - x'(t)| \\
\leq& |x(t_1) - x'(t_1)| + |x'(t_1) - x'(t)| \\
\leq& |x(t_1) - x'(t_1)| + M(t - t_1) \\
\leq& |x(t_1) - x'(t_1)| + Mk|x(t_1) - x'(t_1)| \\
\leq& (1 + Mk)\, |x_0 - x_0'| e^{L_1 t_1} \\
\leq& (1 + Mk)\, \eta e^{L_1 t_1} \\
\leq& (1 + Mk)\, r_3 C^{-1} e^{-\bar{L}T} e^{L_1 t_1} \\
<& r_3.
\end{aligned}$$

In particular, we have $|x(t_1) - x'(t_2)| < r_3$, meaning we must have $x'(t_2) \in E^*_{\sigma_0,\sigma_1}$ as well. Hence $\sigma^\rho(t_2^+) = \sigma_2 = \sigma(t_2)$. Now use triangle inequality again,

$$\begin{aligned}
|x(t) - x'(t)| =& |x(t) - x(t_1) + x(t_1) - x'(t)| \\
\leq& |x(t) - x(t_1)| + |x(t_1) - x'(t)| \\
\leq& (1 + 2Mk)\, |x(t_1) - x'(t_1)| \\
\leq& (1 + 2Mk)\, |x_0 - x_0'| e^{L_1 t_1} \\
\leq& (1 + 2Mk)\, |x_0 - x_0'| e^{L_1 t}
\end{aligned}$$

For all $t_1 \leq t \leq \min\{t_2, T\}$. Trivially this upper bound is true for $t \leq t_1$ so the lemma is proven if $t_2 \geq T$. Now suppose that $t_2 < T$ and the next switch occurs at some $t_3 > t_2$. Since $\sigma(t_2^+) = \sigma^\rho(t_2^+) = \sigma_1$, we can again use the Grönwall inequality to compute $|x(t) - x'(t)|$ for $t \in (t_2, \min\{t_3, T\}]$:

$$|x(t) - x'(t)| \leq |x(t_2) - x'(t_2)| e^{L_1(t - t_2)} = C|x_0 - x_0'| e^{L_1 t}.$$

Thus this upper bound is in fact true for all $t \leq t_3$. The lemma will also be proven if $t_3 \geq T$. In case $t_3 < T$, note that there is a positive dwell time (see, e.g. [28]) in our

system; namely, in order for a second switch to occur, it needs to spend at least time of $\frac{r_2}{M}$ for the system solution to reach the next switching event. In other words, we have $t_3 \geq \min\{t_1 + \frac{r_2}{M}, t_2 + \frac{r_2}{M}\} = t_1 + \frac{r_2}{M} \geq \frac{r_2}{M}$. Now, because we still have $\sigma(t_3) = \sigma_1 = \sigma^\rho(t_3)$, we reset time t_3 to be the initial time and note that we have $x(t, x(t_3), \sigma_1, u(t + t_3)) = x(t + t_3), x(t, x'(t_3), \sigma_1, u(t + t3)) = x'(t + t_3)$. In addition, the time horizon is shortened to be $T - t_3$, hence the new bound η' on initial continuous states separation is also changed to be

$$\eta' = \min\{r_1, r_2, r_3\}C^{-1}e^{-\bar{L}(T-t_3)} = e^{\bar{L}t_3}\eta = C^{\frac{M}{r_2}t_3}e^{L_1 t_3}\eta$$

Note that $|x(t_3) - x'(t_3)| \leq \eta'$ is automatically satisfied because $t_3 \geq \frac{r_2}{M}$ and

$$|x(t_0') - x'(t_0')| \leq C|x_0 - x_0'|e^{L_1 t_3} \leq C^{\frac{M}{r_2}t_3}e^{L_1 t_3}\eta$$

Thus the earlier analysis will still hold for the solution after t_3, up to the 3rd switch, and so on. Note that over time t, there are at most $\lceil \frac{Mt}{r_2} \rceil \leq \frac{Mt}{r_2} + 1$ switches in total. Hence cascading solutions between switches together,

$$\begin{aligned} |x(t) - x'(t)| &\leq |x_0 - x_0'|C^{\frac{Mt}{r_2}+1}e^{L_1 t} \\ &= |x_0 - x_0'|Ce^{\left(\frac{M}{r_2}\ln C + L_1\right)t} \\ &= |x_0 - x_0'|Ce^{\bar{L}t} \end{aligned}$$

for all $t \in [0, T]$. □

4.5 Discussion and future work

We would like to discuss another possible approach to showing the equivalence between GAS and GUAS via some results given in [87]. For a hybrid system $\mathcal{H}$ defined via

$$\begin{cases} \dot{x} \in F(x) & \text{if } x \in C \\ x^+ \in G(x) & \text{if } x \in D \end{cases},$$

Theorem 7.12 in [87] says that as long as C, D are closed, G, F are outer semicontinuous, locally bounded and $F(x)$ is convex for all $x \in C$, then GAS is equivalent to GUAS. In order to deploy this theorem, we need to combine state x and mode σ as the hybrid state as well as define $C := \cap_{i\in I}(\bar{S}_i, \{i\}), D := \cap_{i\in I}(\partial S_i, \{i\})$. Note that by this transformation, although C and D are both closed, there are possible overlaps between them. As a result, when a solution reaches ∂S_i, $\mathcal{H}$ either allows the solution to keep flowing continuously inside ∂S_i without switch, or a switch occurs and the mode jumps. In other words, $\mathcal{H}$ is different from (Σ^ρ) as it allows non-unique solutions. Nevertheless, under the transversality assumption, the first situation cannot happen; thus indeed the system $\mathcal{H}$ has the same solutions as (Σ^ρ). Additionally, using this approach we see that Lipschitzness on f_i's can be replaced by outer semicontinuity and Assumption 4.4 becomes redundant. Nevertheless, it is worth pointing out that our approach is from scratch and does not require the framework of hybrid systems from [87], the transformation of models from state-dependent switched system to hybrid system is not apparent, and analysis in hybrid time domain requires some extra work. Besides, Lemma 4.5, Lemma 4.6 and their proofs also reveal some robustness related properties on the state-dependent switched system with the presence of transversality.

In addition, we have required in Assumption 4.5 that the vector fields f_i's be convex. As discussed earlier, this assumption is needed to show that the limit of sequence of solutions is also a solution. In fact, we can relax this; as long as we can approximate the limit of a sequence of solutions by a solution on the infinite time horizon within an arbitrary uniform ε-tube, we can still show the existence of a uniform convergence time. This is closely related to the Filippov-Wazewski relaxation theorem, and [94] gives an infinite time horizon version. This relaxation in the context of state-dependent switched systems will be another possible research direction.

CHAPTER 5

CONCLUSION

Both synthesis of control strategy for motion planning and analysis of stability of nonlinear and switched systems have been researched in this work.

In terms of control strategy, we proposed a novel approach to the long-standing problem of motion planning for non-holonomic systems. An arbitrary curve of states between initial state and goal state is first sketched and then deformed into a curve via solving a set of PDEs. Along with the deformation, the value of an energy functional evaluated on the curve is minimized. Controls are subsequently extracted from that energy minimizing curve and they generate an admissible path for the non-holonomic system. It has been theoretically proven that under some mild assumptions on the system, the non-holonomic system can reach a destination arbitrarily close to the goal state prescribed earlier along the admissible path resulting from the algorithm. Several variations of the fundamental motion planning problem were also considered in this work, including but not limited to control affine system with drift, holonomic constraints, state and input constraints, indefinite boundary conditions, free terminal time, etc.

In terms of stability analysis, the author has studied several approaches related to non-monotonic Lyapunov functions. The author has first proposed the concept of almost Lyapunov functions – which do not have negative time derivative everywhere but rather on the complement of some "bad sets" – for autonomous nonlinear systems. Local and global stability results have been shown in this case, provided that the "bad sets" are sufficiently small. The definition of almost Lyapunov functions was then generalized to nonlinear systems with inputs, in which case the well known ISS can be guaranteed again when the "bad sets" are sufficiently small. On the other hand, the known approach of showing asymptotic stability for autonomous nonlinear systems via studying the higher order derivatives of the

Lyapunov functions was also generalized to study ISS for time-varying systems with inputs. By properly defining the higher order derivatives of Lyapunov functions in the presence of inputs, it was proven that as long as there is a negative definite linear combination of those higher order derivatives with non-negative coefficients, the system is ISS.

During the study of stability of nonlinear systems, it was realized that a nonlinear system being ISS is equivalent to the fact that its auxiliary system is GUAS. Inspired by this connection, we also tried to answer the question of equivalence between several stability-related properties for switched systems. In particular, the gap between GS plus AG and ISS for the state-dependent switched system has been researched. Several regularity assumptions were proposed to draw the equivalence of the two sets of stability properties. It was proven that when the solution trajectories of the switched system with sufficiently small inputs are always transversal to the switch guards – which was called the transversality condition – then ISS is equivalent to GS plus AG. The key step in the proof was to show that under the transversality condition, GAS is equivalent to GUAS. As a byproduct, the property of continuous dependence of solutions on initial conditions for state-dependent switched systems under the same assumptions was concluded.

REFERENCES

[1] S. M. LaValle and S. A. Hutchinson, "Optimal motion planning for multiple robots having independent goals," *IEEE Transactions on Robotics and Automation*, vol. 14, no. 6, pp. 912–925, 1998.

[2] J. Laumond, *Robot Motion Planning and Control*, ser. Lecture notes in control and information sciences. Springer, 1998. [Online]. Available: https://books.google.co.kr/books?id=qTdSAAAAMAAJ

[3] H. Choset, K. M. Lynch, S. Hutchinson, G. A. Kantor, W. Burgard, L. E. Kavraki, and S. Thrun, *Principles of Robot Motion: Theory, Algorithms, and Implementation*. MIT Press, 2005.

[4] S. M. LaValle, *Planning Algorithms*. Cambridge, U.K.: Cambridge University Press, 2006, available at http://planning.cs.uiuc.edu/.

[5] T. D. Murphey, "Motion planning for kinematically overconstrained vehicles using feedback primitives," in *Robotics and Automation, 2006. ICRA 2006. Proceedings 2006 IEEE International Conference on*. IEEE, 2006, pp. 1643–1648.

[6] R. Tedrake, I. R. Manchester, M. Tobenkin, and J. W. Roberts, "LQR-trees: Feedback motion planning via sums-of-squares verification," *The International Journal of Robotics Research*, vol. 29, no. 8, pp. 1038–1052, 2010.

[7] S. Karaman and E. Frazzoli, "Sampling-based algorithms for optimal motion planning," *The International Journal of Robotics Research*, vol. 30, no. 7, pp. 846–894, 2011. [Online]. Available: http://dx.doi.org/10.1177/0278364911406761

[8] H. Dai, A. Valenzuela, and R. Tedrake, "Whole-body motion planning with centroidal dynamics and full kinematics," in *2014 IEEE-RAS International Conference on Humanoid Robots*, Nov 2014, pp. 295–302.

[9] B. Paden, M. Čáp, S. Z. Yong, D. Yershov, and E. Frazzoli, "A survey of motion planning and control techniques for self-driving urban vehicles," *IEEE Transactions on Intelligent Vehicles*, vol. 1, no. 1, pp. 33–55, 2016.

[10] J. Z. Woodruff and K. M. Lynch, "Planning and control for dynamic, nonprehensile, and hybrid manipulation tasks," in *IEEE International Conference on Robotics and Automation*, Singapore, 05/2017 2017.

[11] R. W. Brockett, *Control Theory and Singular Riemannian Geometry.* New York: Springer, 1982, pp. 11–27.

[12] F. Jean, *Control of Nonholonomic Systems: From Sub-Riemannian Geometry to Motion Planning.* Springer, 2014.

[13] Z. Li and J. Canny, *Nonholonomic Motion Planning*, ser. The Springer International Series in Engineering and Computer Science. Springer US, 1993.

[14] M.-A. Belabbas and S. Liu, "New method for motion planning for non-holonomic systems using partial differential equations," *2017 American Control Conference (ACC)*, pp. 4189–4194, 2017.

[15] S. Liu and M.-A. Belabbas, "A homotopy method for motion planning," *Arxiv 1901.10094*, 2019. [Online]. Available: http://arxiv.org/abs/1901.10094

[16] S. Liu, Y. Fan, and M.-A. Belabbas, "Affine geometric heat flow and motion planning for dynamic systems," in *11th IFAC Symposium on Nonlinear Control Systems NOLCOS 2019*, vol. 52, no. 16, 2019, pp. 168 – 173.

[17] Y. Fan, S. Liu, and M.-A. Belabbas, "Mid-air motion planning of floating robot using heat flow method," in *1st IFAC Workshop on Robot Control WROCO 2019*, vol. 52, no. 22, 2019, pp. 19 – 24.

[18] S. Liu, Y. Fan, and M.-A. Belabbas, "Geometric motion planning for affine control systems with indefinite boundary conditions and free terminal time," *arXiv e-prints*, p. arXiv:2001.04540, Jan 2020.

[19] H. Khalil, *Nonlinear Systems, 3rd ed.* Prentice Hall, 2002.

[20] D. Aeyels and J. Peuteman, "A new asymptotic stability criterion for nonlinear time-variant differential equations," *IEEE Transactions on Automatic Control*, vol. 43, no. 7, pp. 968–971, July 1998.

[21] A. A. Ahmadi and P. A. Parrilo, "Non-monotonic Lyapunov functions for stability of discrete time nonlinear and switched systems," in *2008 47th IEEE Conference on Decision and Control*, Dec 2008, pp. 614–621.

[22] I. Karafyllis, "Can we prove stability by using a positive definite function with non sign-definite derivative?" *IMA Journal of Mathematical Control and Information*, vol. 29, no. 2, pp. 147–170, 11 2011.

[23] V. Meigoli and S. K. Y. Nikravesh, "Stability analysis of nonlinear systems using higher order derivatives of Lyapunov function candidates," *Systems & Control Letters*, vol. 61, no. 10, pp. 973 – 979, 2012.

[24] S. Liu, D. Liberzon, and V. Zharnitsky, "On almost Lyapunov functions for non-vanishing vector fields," in *2016 IEEE 55th Conference on Decision and Control (CDC)*, Dec 2016, pp. 5557–5562.

[25] S. Liu and D. Liberzon, "On almost Lyapunov functions for systems with inputs," in *2019 IEEE 58th Conference on Decision and Control (CDC)*, Dec 2019, pp. 468 – 473.

[26] S. Liu and D. Liberzon, "Higher order derivatives of Lyapunov functions for stability of systems with inputs," in *2019 IEEE 58th Conference on Decision and Control (CDC)*, Dec 2019, pp. 6146 – 6151.

[27] S. Liu, D. Liberzon, and V. Zharnitsky, "Almost Lyapunov functions for nonlinear systems," *Automatica*, vol. 113, p. 108758, 2020. [Online]. Available: http://www.sciencedirect.com/science/article/pii/S0005109819306211

[28] D. Liberzon, *Switching in Systems and Control*. Boston, MA: Birkhäuser, 2003.

[29] E. D. Sontag and Y. Wang, "New characterizations of input-to-state stability," *IEEE Transactions on Automatic Control*, vol. 41, no. 9, pp. 1283–1294, Sep 1996.

[30] S. Liu and D. Liberzon, "Global stability and asymptotic gain imply input-to-state stability for state-dependent switched systems," in *2018 IEEE 57th Conference on Decision and Control (CDC)*, Dec 2018, pp. 2360–2365.

[31] M. do Carmo, *Riemannian Geometry*, ser. Mathematics (Boston, Mass.). Birkhäuser, 1992. [Online]. Available: https://books.google.com/books?id=uXJQQgAACAAJ

[32] S. Wang, J. B. Hoagg, and T. M. Seigler, "Orientation control on so(3) with piecewise sinusoids," *Automatica*, vol. 100, pp. 114 – 122, 2019.

[33] H.-B. Dürr, M. S. Stanković, C. Ebenbauer, and K. H. Johansson, "Lie bracket approximation of extremum seeking systems," *Automatica*, vol. 49, no. 6, pp. 1538–1552, 2013.

[34] S. Michalowsky, B. Gharesifard, and C. Ebenbauer, "Distributed extremum seeking over directed graphs," in *Decision and Control (CDC), 2017 IEEE 56th Annual Conference on*. IEEE, 2017, pp. 2095–2101.

[35] R. W. Brockett, "On the rectification of vibratory motion," *Sensors and Actuators*, vol. 20, no. 1-2, pp. 91–96, 1989.

[36] R. M. Murray, Z. Li, S. S. Sastry, and S. S. Sastry, *A Mathematical Introduction to Robotic Manipulation*. CRC press, 1994.

[37] G. Lafferriere and H. J. Sussmann, "A differential geometric approach to motion planning," in *Nonholonomic Motion Planning*. Springer, 1993, pp. 235–270.

[38] J.-P. Gauthier and M. Kawskiz, "Minimal complexity sinusoidal controls for path planning," in *Decision and Control (CDC), 2014 IEEE 53rd Annual Conference on*. IEEE, 2014, pp. 3731–3736.

[39] A. Majumdar and R. Tedrake, "Robust online motion planning with regions of finite time invariance," in *Algorithmic Foundations of Robotics X*. Springer, 2013, pp. 543–558.

[40] C. J. Tomlin, I. Mitchell, A. M. Bayen, and M. Oishi, "Computational techniques for the verification of hybrid systems," *Proceedings of the IEEE*, vol. 91, no. 7, pp. 986–1001, 2003.

[41] M. Posa, "Optimization for control and planning of multi-contact dynamic motion," Ph.D. dissertation, Massachusetts Institute of Technology, 2017.

[42] J. Kuffner, S. Kagami, K. Nishiwaki, M. Inaba, and H. Inoue, "Online footstep planning for humanoid robots," in *2003 IEEE International Conference on Robotics and Automation*, vol. 1, Sept 2003, pp. 932–937 vol.1.

[43] A. D. Luca and G. Oriolo, *Modelling and Control of Nonholonomic Mechanical Systems*. Springer, 1995, pp. 277–342.

[44] J. . Godhavn, A. Balluchi, L. Crawford, and S. Sastry, "Path planning for nonholonomic systems with drift," in *Proceedings of the 1997 American Control Conference*, vol. 1, June 1997, pp. 532–536.

[45] M. Reyhanoglu, A. van der Schaft, N. H. Mcclamroch, and I. Kolmanovsky, "Dynamics and control of a class of underactuated mechanical systems," *IEEE Transactions on Automatic Control*, vol. 44, no. 9, pp. 1663–1671, Sep 1999.

[46] K.-S. Chou and X.-P. Zhu, *The Curve Shortening Problem*. CRC Press book, 2001.

[47] H. J. Sussmann, "A general theorem on local controllability," *SIAM Journal on Control and Optimization*, vol. 25, no. 1, pp. 158–194, 1987. [Online]. Available: http://dx.doi.org/10.1137/0325011

[48] C. O. Aguilar and A. D. Lewis, "Small-time local controllability for a class of homogeneous systems," *SIAM Journal on Control and Optimization*, vol. 50, no. 3, pp. 1502–1517, 01 2012.

[49] J. Jost, *Riemannian Geometry and Geometric Analysis*, ser. Universitext. Berlin: Springer, 1995.

[50] R. S. Strichartz, "Sub-Riemannian geometry," *J. Differential Geom.*, vol. 24, no. 2, pp. 221–263, 1986. [Online]. Available: https://doi.org/10.4310/jdg/1214440436

[51] L. E. Dubins, "On curves of minimal length with a constraint on average curvature, and with prescribed initial and terminal positions and tangents," *American Journal of Mathematics*, vol. 79, no. 3, p. 497, Jul 1957.

[52] J. Nocedal and S. J. Wright, *Numerical Optimization*. New York : Springer, 1999.

[53] G. Leitmann, "Guaranteed avoidance strategies," *Journal of Optimization Theory and Applications*, vol. 32, no. 4, pp. 569–576, Dec 1980.

[54] E. Papadopoulos, I. Fragkos, and I. Tortopidis, "On robot gymnastics planning with non-zero angular momentum," in *Proceedings 2007 IEEE International Conference on Robotics and Automation*, April 2007, pp. 1443–1448.

[55] R. Shu, A. Siravuru, A. Rai, T. Dear, K. Sreenath, and H. Choset, "Optimal control for geometric motion planning of a robot diver," in *2016 IEEE/RSJ International Conference on Intelligent Robots and Systems (IROS)*, Oct 2016, pp. 4780–4785.

[56] D. Liberzon, *Calculus of Variations and Optimal Control Theory: A Concise Introduction*. Princeton University Press, 2012.

[57] E. T. Whittaker and G. N. Watson, *A Course of Modern Analysis*, 4th ed., ser. Cambridge Mathematical Library. Cambridge University Press, 1996.

[58] R. D. Driver, "Methods of A. M. Lyapunov and their application (V.I.Zubov)," *SIAM Review*, vol. 7, no. 4, pp. 570–571, 1965.

[59] F. Camilli, L. Grüne, and F. Wirth, "A generalization of Zubov's method to perturbed systems," *SIAM Journal on Control and Optimization*, vol. 40, no. 2, pp. 496–515, 2001.

[60] S. Dubljevi and N. Kazantzis, "A new Lyapunov design approach for nonlinear systems based on Zubov's method," *Automatica*, vol. 38, no. 11, pp. 1999 – 2007, 2002.

[61] B. Reznick, "Some concrete aspects of Hilbert's 17th problem," *Contemporary Mathematics*, pp. 251–272, 2000.

[62] G. Chesi, *Domain of Attraction: Analysis and Control via SOS Programming*. London:Springer, 2011.

[63] G. Blekherman, P. A. Parrilo, and R. R. Thomas, *Semidefinite Optimization and Convex Algebraic Geometry*. Society for Industrial and Applied Mathematics : Mathematical Optimization Society, 2012.

[64] R. Tempo, G. Calafiore, and F. Dabbene, *Randomized Algorithms for Analysis and Control of Uncertain Systems, 2nd ed.* London: Springer, 2012.

[65] M. Vidyasagar, *A Theory of Learning and Generalization: With Applications to Neural Networks and Control Systems*. Secaucus, NJ, USA: Springer-Verlag New York, Inc., 1997.

[66] J. Kenanian, A. Balkan, R. M. Jungers, and P. Tabuada, "Data driven stability analysis of black-box switched linear systems," *arXiv e-prints*, Mar. 2018.

[67] A. Butz, "Higher order derivatives of Liapunov functions," *IEEE Transactions on Automatic Control*, vol. 14, no. 1, pp. 111–112, February 1969.

[68] R. Bellman, "Vector lyanpunov functions," *SIAM Journal on Control*, vol. 1, no. 1, pp. 32–3, 1962, copyright - Copyright] Society for Industrial and Applied Mathematics; Last updated - 2012-03-04.

[69] S. G. Nersesov and W. M. Haddad, "On the stability and control of nonlinear dynamical systems via vector Lyapunov functions," *IEEE Transactions on Automatic Control*, vol. 51, no. 2, pp. 203–215, Feb 2006.

[70] S. Fakhimi derakhshan and A. Fatehi, "Non-monotonic Lyapunov functions for stability analysis and stabilization of discrete time Takagi-Sugeno fuzzy systems," *International Journal of Innovative Computing, Information and Control*, vol. 10, pp. 1567–1586, 01 2014.

[71] V. Meigoli and S. K. Y. Nikravesh, "A new theorem on higher order derivatives of Lyapunov functions," *ISA Transactions*, vol. 48, no. 2, pp. 173 – 179, 2009.

[72] D. Liberzon, C. Ying, and V. Zharnitsky, "On almost Lyapunov functions," in *2014 IEEE 53th Conference on Decision and Control (CDC)*, Dec 2014, pp. 3083–3088.

[73] R. Courant and F. John, *Introduction to Calculus and Analysis, Volume II.* Springer New York, 1989.

[74] E. D. Sontag, "Smooth stabilization implies coprime factorization," *IEEE Transactions on Automatic Control*, vol. 34, no. 4, pp. 435–443, Apr 1989.

[75] R. Foote, "The volume swept out by a moving planar region," in *Mathematics Magazine*. Mathematical Association of America, Oct 2006, vol. 79, no. 4.

[76] J. M. Sullivan, "Curves of finite total curvature," in *Discrete Differential Geometry*, A. I. Bobenko, J. M. Sullivan, P. Schröder, and G. M. Ziegler, Eds. Basel: Birkhäuser Basel, 2008.

[77] A. Teel and L. Praly, "On assigning the derivative of a disturbance attenuation control Lyapunov function," *Mathematics of Control, Signals, and Systems*, vol. 13, pp. 95–124, 05 2000.

[78] A. Papachristodoulou, J. Anderson, G. Valmorbida, S. Prajna, P. Seiler, and P. Parrilo, "SOSTOOLS version 3.00 sum of squares optimization toolbox for MATLAB," *arXiv e-prints*, p. arXiv:1310.4716, Oct 2013.

[79] A. A. Ahmadi and P. A. Parrilo, "On higher order derivatives of Lyapunov functions," in *Proceedings of the 2011 American Control Conference*, June 2011, pp. 1313–1314.

[80] E. D. Sontag and Y. Wang, "On characterizations of the input-to-state stability property," *Systems and Control Letters*, vol. 24, no. 5, pp. 351 – 359, 1995.

[81] D. Liberzon and D. Nesic, "Input-to-state stabilization of linear systems with quantized state measurements," *IEEE Transactions on Automatic Control*, vol. 52, no. 5, pp. 767–781, May 2007.

[82] G. Yang and D. Liberzon, "Feedback stabilization of switched linear systems with unknown disturbances under data-rate constraints," *IEEE Transactions on Automatic Control*, vol. 63, no. 7, pp. 2107–2122, July 2018.

[83] Y. Sharon and D. Liberzon, "Input to state stabilizing controller for systems with coarse quantization," *IEEE Transactions on Automatic Control*, vol. 57, no. 4, pp. 830–844, April 2012.

[84] W. P. M. H. Heemels, K. H. Johansson, and P. Tabuada, "An introduction to event-triggered and self-triggered control," in *2012 IEEE 51st IEEE Conference on Decision and Control (CDC)*, Dec 2012, pp. 3270–3285.

[85] L. I. Allerhand and U. Shaked, "Robust state-dependent switching of linear systems with dwell time," *IEEE Transactions on Automatic Control*, vol. 58, no. 4, pp. 994–1001, April 2013.

[86] Z. Wu, M. Cui, P. Shi, and H. R. Karimi, "Stability of stochastic nonlinear systems with state-dependent switching," *IEEE Transactions on Automatic Control*, vol. 58, no. 8, pp. 1904–1918, Aug 2013.

[87] R. Goebel, R. G. Sanfelice, and A. R. Teel, *Hybrid Dynamical Systems: Modeling, Stability, and Robustness*. Princeton University Press, 2012.

[88] C. Cai and A. Teel, "Robust input-to-state stability for hybrid systems," *SIAM Journal on Control and Optimization*, vol. 51, no. 2, pp. 1651–1678, 2013.

[89] M. Broucke and A. Arapostathis, "Continuous selections of trajectories of hybrid systems," *Systems and Control Letters*, vol. 47, no. 2, pp. 149 – 157, 2002.

[90] L. Tavernini, "Differential automata and their discrete simulators," *Non-Linear Anal.*, vol. 11, no. 6, pp. 665–683, June 1987.

[91] I. A. Hiskens and M. A. Pai, "Trajectory sensitivity analysis of hybrid systems," *IEEE Transactions on Circuits and Systems I: Fundamental Theory and Applications*, vol. 47, no. 2, pp. 204–220, Feb 2000.

[92] Y. Lin, E. D. Sontag, and Y. Wang, "A smooth converse Lyapunov theorem for robust stability," *SIAM Journal on Control and Optimization*, vol. 34, no. 1, pp. 124–160, 1996.

[93] A. F. Filippov, *Differential Equations with Discontinuous Righthand Sides*. Springer, Dordrecht, 1988.

[94] B. Ingalls, E. D. Sontag, and Y. Wang, "An infinite-time relaxation theorem for differential inclusions," in *Proceedings of the American Mathmatical Society*, 2000.